Ontario

Ontario Geological Survey
Open File Report 6175

Geochemistry and Radiogenic Isotope Characteristics of the Sills of the Nipigon Embayment: Lake Nipigon Region Geoscience Initiative

2005

Ontario

ONTARIO GEOLOGICAL SURVEY

Open File Report 6175

Geochemistry and Radiogenic Isotope Characteristics of the Sills of the Nipigon Embayment: Lake Nipigon Region Geoscience Initiative

by

A.J. Richardson, P. Hollings and J.M. Franklin

2005

Parts of this publication may be quoted if credit is given. It is recommended that reference to this publication be made in the following form:

Richardson, A.J., Hollings, P. and Franklin, J.M. 2005. Geochemistry and radiogenic isotope characteristics of the sills of the Nipigon Embayment: Lake Nipigon Region Geoscience Initiative; Ontario Geological Survey, Open File Report 6175, 88p.

Ontario Prospectors Association

Ontario
Northern Ontario
Heritage Fund
Fonds du patrimoine
du Nord de l'Ontario

The Lake Nipigon Region Geoscience Initiative is a two-year program of geoscience studies in the Lake Nipigon region operated by the Ontario Prospectors' Association (OPA) and funded through an agreement with the Northern Ontario Heritage Fund Corporation (NOHFC). Projects of this initiative are planned in collaboration with the Ontario Geological Survey (OGS), Lakehead University, mineral industry and government partners.

© Queen's Printer for Ontario, 2005

106-01524/

© Queen's Printer for Ontario, 2005.

Open File Reports of the Ontario Geological Survey are available for viewing at the Mines Library in Sudbury, at the Mines and Minerals Information Centre in Toronto, and at the regional Mines and Minerals office whose district includes the area covered by the report (see below).

Copies can be purchased at Publication Sales and the office whose district includes the area covered by the report. Although a particular report may not be in stock at locations other than the Publication Sales office in Sudbury, they can generally be obtained within 3 working days. All telephone, fax, mail and e-mail orders should be directed to the Publication Sales office in Sudbury. Use of VISA or MasterCard ensures the fastest possible service. Cheques or money orders should be made payable to the *Minister of Finance*.

Mines and Minerals Information Centre (MMIC) Macdonald Block, Room M2-17 900 Bay St. Toronto, Ontario M7A 1C3	Tel:	(416) 314-3800
Mines Library 933 Ramsey Lake Road, Level A3 Sudbury, Ontario P3E 6B5	Tel:	(705) 670-5615
Publication Sales 933 Ramsey Lake Rd., Level A3 Sudbury, Ontario P3E 6B5	Tel:	(705) 670-5691(local) 1-888-415-9845(toll-free)
	Fax:	(705) 670-5770
	E-mail:	pubsales@ndm.gov.on.ca

Regional Mines and Minerals Offices:

Kenora - Suite 104, 810 Robertson St., Kenora P9N 4J2

Kirkland Lake - 10 Government Rd. E., Kirkland Lake P2N 1A8

Red Lake - Box 324, Ontario Government Building, Red Lake P0V 2M0

Sault Ste. Marie - 70 Foster Dr., Ste. 200, Sault Ste. Marie P6A 6V8

Southern Ontario - P.O. Bag Service 43, 126 Old Troy Rd., Tweed K0K 3J0

Sudbury - Level B3, 933 Ramsey Lake Rd., Sudbury P3E 6B5

Thunder Bay - Suite B002, 435 James St. S., Thunder Bay P7E 6S7

Timmins - Ontario Government Complex, P.O. Bag 3060, Hwy. 101 East, South Porcupine P0N 1H0

Toronto - MMIC, Macdonald Block, Room M2-17, 900 Bay St., Toronto M7A 1C3

This report has not received a technical edit. Discrepancies may occur for which the Ontario Ministry of Northern Development and Mines does not assume any liability. Source references are included in the report and users are urged to verify critical information. Recommendations and statements of opinions expressed are those of the author or authors and are not to be construed as statements of government policy.

If you wish to reproduce any of the text, tables or illustrations in this report, please write for permission to the Team Leader, Publication Services, Ministry of Northern Development and Mines, 933 Ramsey Lake Road, Level B4, Sudbury, Ontario P3E 6B5.

Cette publication est disponible en anglais seulement.

Parts of this report may be quoted if credit is given. It is recommended that reference be made in the following form:

Richardson, A.J., Hollings, P. and Franklin, J.M. 2005. Geochemistry and radiogenic isotope characteristics of the sills of the Nipigon Embayment: Lake Nipigon Region Geoscience Initiative; Ontario Geological Survey, Open File Report 6175, 88p.

Contents

Abstract xi

Introduction 1

Previous Geological Work 1

Regional Geology 2
  Archean 2
    The Superior Province 2
      The Quetico Subprovince 3
      The Wabigoon Subprovince 4
        Economic Mineralization of the Wabigoon Subprovince 5
  Proterozoic 5
    The Southern Province 5
      Animikie Group Sediments 6
      Paleoproterozoic Anorogenic Granite Complexes 7
      The Sibley Group Sediments 7
    Rocks of the Keweenawan Midcontinent Rift 9
      Osler Group 9
      Mamainse Point Formation 9
      Duluth Complex 10
      North Shore Volcanic Group 10
      Logan Igneous Suite 10

Methodology 11
  Field Work 11
  Analytical Techniques 11
    Samarium–Neodymium (Sm/Nd), Rubidium–Strontium (Rb/Sr) and Lead–Lead (Pb/Pb) Isotope Methodology 13
    Scanning Electron Microscopy Electron Dispersion System Methodology 15

General Sill Characteristics 15

Sill Emplacement Mechanisms and Regional Correlation 21
  Introduction 21
  Petrography 21
    Summary of Optical Petrology 27
  Mineral Chemistry 27
  Magnetic Susceptibility 27

Isotope Geochemistry 28

Discussion 39
  Emplacement Mechanisms 39
  Geochemistry 41
  Radiogenic Isotopes 43
    Rubidium–Strontium (Rb/Sr) and Neodymium–Samarium (Nd/Sm) 43
    Lead–Lead (Pb/Pb) 45

Discussion of Lead Isotope Data 51
  - Jackfish Island Sills 51
  - McIntyre Sills 51
  - Nipigon Sills 53
  - Pillar Lake Volcanics 55
  - Other Units 56
  - Summary of Lead Isotope Data 56

Conclusions 57

Acknowledgments 57

References 58

Appendix 1. Major, Trace and Rare Earth Element Geochemical Data for the Nipigon Sills 67

Appendix 2. Major, Trace and Rare Earth Element Geochemical Data for the McIntyre Sills 82

Appendix 3. Major, Trace and Rare Earth Element Geochemical Data for the Shillabeer Sills 84

Appendix 4. Rb/Sr, Sm/Nd and Pb/Pb Isotope Data for All Sills 86

Metric Conversion Table 88

FIGURES

1. Regional geology map showing study area location 2
2. Map of the Superior Province showing the location of the principal subprovinces 3
3. Map showing location of gravity anomaly associated with the Midcontinent Rift 8
4. Map showing sample locations and the regional geology of the Nipigon Embayment 12
5. Regional geology map showing the location of the Nipigon, Inspiration, Jackfish Island and McIntyre sills in the Nipigon Embayment 14
6. Bivariant plots for the diabase sills of the Nipigon Embayment: a) MgO versus TiO_2 showing the development of a high TiO_2 group (Logan, Shillabeer, Jackfish Island and McIntyre sills) and a low TiO_2 group (Nipigon and Inspiration sills); b) MgO versus Al_2O_3; and c) MgO versus P_2O_5 17
7. Primitive mantle-normalized plots of the sills identified in the Nipigon Embayment: a) Jackfish Island and McIntyre sills, Shillabeer sill, Disraeli intrusion and Hawaiian oceanic island basalt; and b) Nipigon sills, Inspiration sills and Parana–Etendeka continental flood basalts 18
8. Primitive mantle-normalized plots of the Jackfish Island and McIntyre sills 19
9. Summary logs of diamond-drill holes DDH 3, DDH 5 and DDH 6 showing sample locations within the drill holes and lithologies observed 22
10. a) Plot of $^{87}Sr/^{86}Sr$ versus ε_{Nd} for the sills of the Nipigon Embayment. b) Detail of Figure 10a, arrows point toward Sibley and Quetico data on Figure 10a. 34
11. a) Plot of MgO versus ε_{Nd} for all diabase sills. b) Plot of chondrite-normalized La/Yb versus ε_{Nd} 35
12. Plot of K_2O versus ε_{Nd} values for the diabase sills of the Nipigon Embayment 36
13. Plots of a) $^{206}Pb/^{204}Pb$ versus $^{207}Pb/^{204}Pb$; and b) $^{206}Pb/^{204}Pb$ versus $^{208}Pb/^{204}Pb$ for the sills of the Nipigon Embayment 37
14. Plot of $^{207}Pb/^{204}Pb$ versus $^{208}Pb/^{204}Pb$ for the sills of the Nipigon Embayment 36
15. Map showing the locations of U/Pb ages from the Nipigon Embayment 40

16. Map showing the locations of samples analyzed for radiogenic isotopes and measured ε_{Nd} values for each sample 42

17. Location of samples for isotopic studies of Proterozoic mafic igneous suites in the Lake Nipigon area, Ontario 46

18. Petrochemistry plots: Plots A and C are for immobile elements; and B is a Jensen plot. Plots D and F combine Mg number, chondrite-normalized La/Yb ratio and TiO_2 to illustrate the separation of lithogroups, and Plot E is a probability plot, illustrating the coherence of each of the suites 48

19. a) Uranogenic lead (^{206}Pb/^{204}Pb versus ^{207}Pb/^{204}Pb) isotope plot. b) Thorogenic lead (^{206}Pb/^{204}Pb versus ^{208}Pb/^{204}Pb) isotope plot 49

20. ^{206}Pb/^{204}Pb versus ^{207}Pb/^{204}Pb diagram of the Jackfish Island sill lead isotopic data 50

21. Histograms showing the anomalous content in sample 03CAM228 (Jackfish Island sill) of elements that are commonly associated with crustal contamination of a melt 50

22. Uranogenic lead isotopic (^{206}Pb/^{204}Pb versus ^{207}Pb/^{204}Pb) diagram with isochron age and slope data for the McIntyre sills sample suite 52

23. Plots for the McIntyre sills sample suite showing relationship between radiogenicity of the lead isotope determinations and various elements of isotopic ratios that are commonly indicators of melt contamination 52

24. Lead isotopic (^{206}Pb/^{204}Pb versus ^{207}Pb/^{204}Pb) diagram of Nipigon sills sample suite 53

25. Plots for the Nipigon sills sample suite showing the relationship between radiogenicity of the lead isotope determinations and various elements of isotopic ratios that are commonly indicators of melt contamination 54

26. Lead isotopic (^{206}Pb/^{204}Pb versus ^{207}Pb/^{204}Pb) diagram for a subset of the Nipigon suite that forms a distinct linear array 54

27. Lead isotopic (^{206}Pb/^{204}Pb versus ^{207}Pb/^{204}Pb) diagram of the Pillar Lake volcanics 55

28. Lead isotopic (^{206}Pb/^{204}Pb versus ^{207}Pb/^{204}Pb) diagram of samples from the Inspiration and Shillabeer suites 56

PHOTOS

1. Photograph of sill tops observed: a) tortoise-shell texture in McIntyre Bay, sample LN70; and b) vesicular sill top in McIntyre Bay near sample LN98 16

2. Diabase sill at Kama Hill showing lower contact with Kama Hill Formation: a) diabase sill with lower contact; and b) close-up view of Kama Hill Formations metasedimentary rocks 20

3. Photomicrograph of a) typical "complete" alteration; and b) typical "minor" alteration 23

4. Photomicrograph of typical ophitic textured diabase found in the Nipigon Embayment 24

5. Photomicrograph of a) typical "moderate" alteration, and b) typical unaltered diabase 26

6. Diabase sill relationships with country rock: a) diabase sill intruding Rove Formation metasedimentary rocks and b) diabase sill assimilating Sibley Group metasedimentary rocks in core from DDH 6 38

TABLES

1. Terminology of the rocks of the Nipigon Embayment 6

2. Geochemical data for samples from mafic and ultramafic units in the Nipigon Embayment 29

3. Derived isotopic variables for the Lake Nipigon radiogenic isotope study 55

Abstract

The Nipigon sills are part of the Mesoproterozoic Keweenawan Midcontinent Rift event. The igneous activity, interpreted to be the result of a mantle plume, extends from Kansas to southern Ontario. The Midcontinent Rift was active for approximately 25 million years producing in excess of 1.5 million km^3 of intrusive and extrusive rocks. The diabase sills of the Nipigon embayment (Nipigon, McIntyre and Inspiration sills) are thick, relatively flat-lying hypabyssal, medium-grained subophitic to ophitic olivine gabbronorite with U/Pb ages ranging from 1107 to 1112 Ma. Also present within the region are a number of thinner mafic to ultramafic sills (Jackfish Island and Shillabeer sills) that may be related to the larger mafic to ultramafic intrusions (e.g., the Seagull and Kitto intrusions).

This project was undertaken to evaluate geochemical variations within the Nipigon sills. Selected samples were analyzed for major, trace and rare earth elements with a representative subset analyzed for Rb/Sr, Sm/Nd and Pb/Pb isotopes. Three distinct sill suites were identified: the Nipigon, Shillabeer and McIntyre suites. One additional suite was identified by T.R. Hart and C.A. MacDonald (OGS) using geochemical data generated as part of their mapping projects in the Nipigon Embayment (Inspiration sills) and they also better characterized the Jackfish Island sills originally identified by Sutcliffe (1986) on Jackfish Island. The Nipigon suite crops out over much of the Nipigon embayment and is characterized by TiO_2 values of 0.7 to 2.7 and La/Yb_{cn} ratios of 2 to 5. The spatially restricted McIntyre suite comprises 10 surface samples and is characterized by higher TiO_2 (2.7 to 3.1 weight %) and La/Yb_{cn} (6.4 to 7.2) than the Nipigon suite. The Shillabeer suite is represented by only a small number of samples and is characterized by elevated TiO_2 (2.6 to 2.8 weight %), generally higher MgO values and the highest La/Yb_{cn} ratios (12.3 to 14.9) of the three suites. The McIntyre suite is geochemically similar to the Jackfish Island suite located to the north, whereas the Shillabeer suite resembles samples from the ultramafic Disraeli intrusion.

Geochemically, the 5 sill suites all broadly resemble plume-related basalts comparable to modern oceanic island basalt, however, the majority of samples are characterized by negative Nb anomalies that are not typical of oceanic island basalt, but are found in continental flood basalts. The negative Nb anomalies and elevated Th contents of the sills are consistent with contamination by an older light rare earth element (LREE) enriched source comparable to Archean granites. All the diabase samples have negative ε_{Nd} values consistent with contamination by an older source. Variations in the trace element and isotope systematics suggest that sills underwent a pervasive contamination by an Archean source deep in the crust followed by limited and spatially restricted contamination by both Archean and Proterozoic sources during emplacement.

Geochemistry and Radiogenic Isotope Characteristics of the Sills of the Nipigon Embayment: Lake Nipigon Region Geoscience Initiative

A.J. Richardson[1], P. Hollings[1] and J.M. Franklin[2]

Ontario Geological Survey
Open File Report 6175
2005

---

[1]Department of Geology, Lakehead University, Thunder Bay, Ontario P7B 5E1
[2]Franklin Geosciences Ltd., 24 Commanche Drive, Nepean, Ontario K2E 6E9

Introduction

This project was undertaken as part of the Lake Nipigon Region Geoscience Initiative (LNRGI): a project operated by the Ontario Prospectors Association and funded through the Northern Ontario Heritage Fund Corporation (NOHFC) with partnerships involving Lakehead University (LU), the Ontario Geological Survey (OGS) and local communities. The LNRGI is an effort to better understand the geology of the Nipigon Embayment with the goals of attracting mineral exploration and economic development to the Lake Nipigon region, providing the foundation for informed future land use decisions and to contribute to the geological understanding of the Nipigon Embayment. The purpose of this project was to study the mafic sills of the basin using whole rock geochemistry, radiogenic isotopes and mineral chemistry with the goal of understanding how these rocks compare with other similar rocks of major rift basins, as well as investigating their emplacement histories and determining the source magma characteristics leading to a better understanding of the formation of the Nipigon sills. Terminology of the rocks of the Nipigon Embayment used in this report is based on a revised classification proposed by P. Hollings, T.R. Hart, R.M. Easton and M.C. Smyk arising from the wealth of geochemical data collected as part of the LNRGI. This terminology has yet to be fully published, although portions of it can be found in Richardson and Hollings (2004) and Hart and MacDonald (2005). This work forms the core of a M.Sc. thesis by the senior author. The interpretation of the lead isotope data is primarily the work of J.M. Franklin.

Previous Geological Work

The geology of the Lake Nipigon basin was first studied in the mid 1800s when Sir William Logan surveyed the area as part of a regional mapping program, designed to catalogue the natural resource wealth of the Dominion of Canada, with emphasis on coal exploration. His efforts concluded with the first reconnaissance scale (1 inch to 25 miles) map of the geology and geography of Canada as far west as Manitoba and as far north as lakes Timiskaming and Nipigon (Logan 1863). This was followed by geological surveys undertaken by Robert Bell between 1866 and 1869 (Bell 1870). In the first decade of the twentieth century, Alfred Wilson completed a mapping program in the Nipigon Basin resulting in the first detailed geological map of the area (Wilson 1910). More recently, Coates (1972) completed a 1:63 360 scale map of the region and Sutcliffe (1982, 1986) completed 1:50 000 scale maps of the southern Lake Nipigon basin with a detailed examination of the diabase sills and a brief study of the ultramafic rocks of the Disraeli and Seagull–Leckie lakes area. Regional studies of the Sibley Group have also been undertaken (e.g., Franklin et al. 1980; Cheadle 1986; Rogala 2003). Much of the regional work was stimulated by exploration for iron in the early 1900s, copper and other base metals in the 1960s (Coates 1972), uranium in the 1970s and 1980s (Scott 1987) with the most recent work (1990s to present) focussing on the nickel–platinum group element (Ni-PGE) potential of the mafic to ultramafic intrusive bodies of the region (Osmani and Rees 1998; Heggie 2005).

As part of the contributions of the OGS to the LNRGI, a series of 1:50 000 scale maps of the Nipigon Embayment were completed (MacDonald et al. 2004a, 2004b; Hart and Préfontaine 2004a, 2004b; MacDonald, Tremblay and ter Meer 2005a, 2005b; MacDonald et al. 2005; Hart, Whaley and Pace 2005), along with several reports (MacDonald 2004; Hart and Magyarosi 2004a; MacDonald, Tremblay and Easton 2005; Hart 2005a). Also as part of the regional study gravity, airborne magnetic (total field) and airborne gamma-ray spectrometer surveys were undertaken (OGS 2004a-l, 2005). Precision uranium–lead (U/Pb) ages were obtained for several rock suites of the Nipigon Embayment by L.M. Heaman, and preliminary results were discussed by Heaman and Easton (2005). Detailed petrographic studies of the rock suites of the Nipigon Embayment were completed by GeoConsult for the LNRGI (Schandl 2004, 2005).

Regional Geology

ARCHEAN

The Superior Province

The Superior Province is the world's largest Archean craton covering an area of 1 572 000 km^2. Approximately 565 000 km^2 is located within the boundaries of Ontario. The Superior Province represents an accumulation of granite-greenstone, metasedimentary, plutonic and high-grade gneissic terranes spanning approximately 400 million years with ages ranging from 3.1 to 2.7 Ga (Thurston 1991). The granite-greenstone terranes consist of low-grade metavolcanic rocks surrounded and intruded by granitic rocks. The metasedimentary subprovinces are predominantly clastic metasedimentary rocks with low-grade margins and amphibolite to granulite facies interiors. The plutonic subprovinces are characterized by tonalite gneiss, with both intrusive and extrusive mafic rocks occurring as a minor component, and as large sodic and potassic plutons. The high-grade gneiss subprovinces consist of amphibolite to granulite facies meta-igneous and supracrustal gneisses cut by tonalite and syenitic intrusions (Thurston 1991). Of the subprovinces of the Superior Province, the Quetico and Wabigoon underlie the rocks of the Nipigon Embayment (Figure 1).

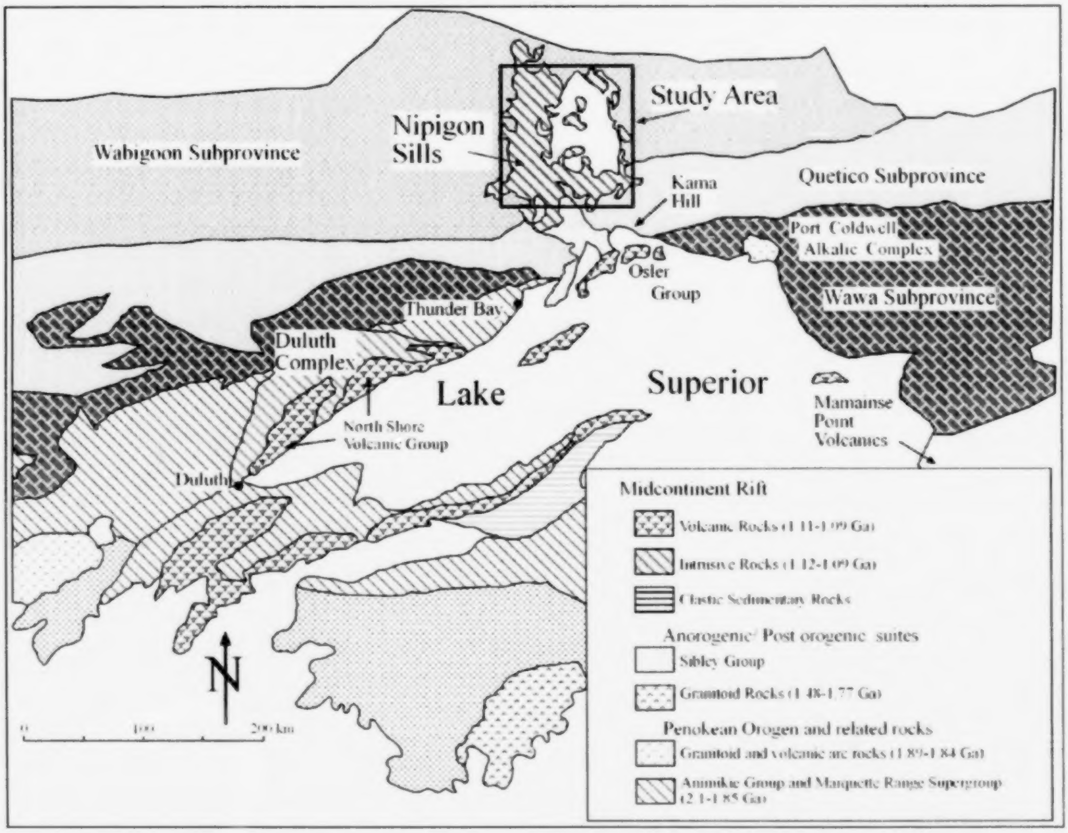
Study Area
Nipigon
Sills
Wabigoon Subprovince
Quetico Subprovince
Kama
Hill
Port Coldwell
Alkalic Complex
Osler
Group
Wawa Subprovince
Thunder Bay
Duluth
Complex
Lake
Superior
North Shore
Volcanic Group
Mamainse
Point
Volcanics
Duluth
Midcontinent Rift
Volcanic Rocks (1.11-1.09 Ga)
Intrusive Rocks (1.12-1.09 Ga)
Clastic Sedimentary Rocks
Anorogenic/ Post orogenic suites
Sibley Group
Granitoid Rocks (1.48-1.77 Ga)
Penokean Orogen and related rocks
Granitoid and volcanic arc rocks (1.89-1.84 Ga)
Animikie Group and Marquette Range Supergroup (2.1-1.85 Ga)
N
0
100
200 km

Figure 1. Regional geology map showing study area location (*modified after* Sutcliffe 1986).

THE QUETICO SUBPROVINCE

The Quetico Subprovince extends from northern Minnesota to the Opatica Subprovince, the continuation of the Quetico Subprovince in Quebec, spanning nearly 1000 km in a roughly east to west oriented belt approximately 70 km wide (Figure 2). The Quetico Subprovince underlies the southern portion of the Nipigon Embayment and, where exposed, is composed of metamorphosed turbiditic wackes interpreted to be largely derived from the neighbouring Wawa, Wabigoon and Abitibi subprovinces during the period from 2.70 to 2.69 Ga (Williams 1991).

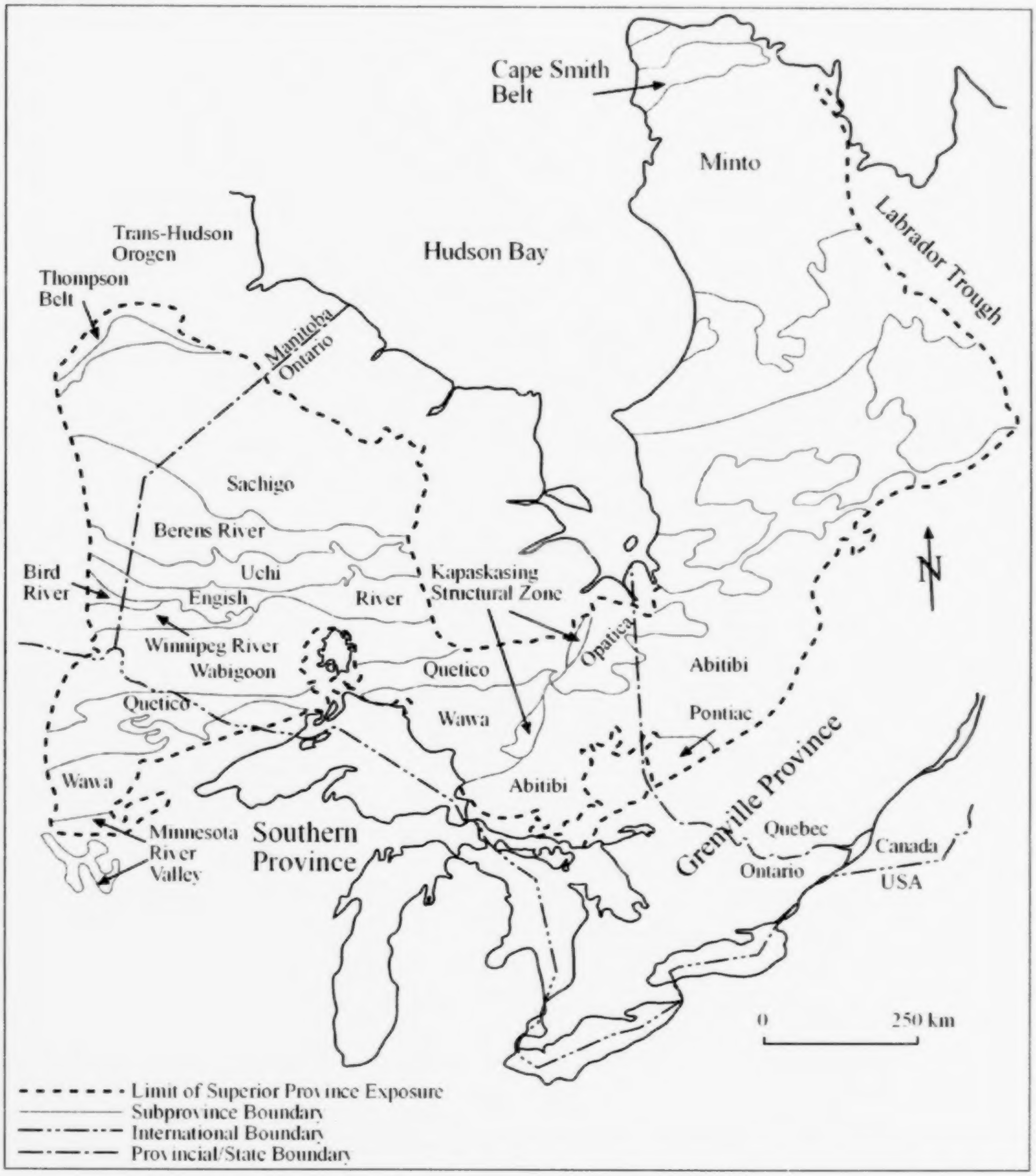
Cape Smith Belt
Minto
Labrador Trough
Hudson Bay
Trans-Hudson Orogen
Thompson Belt
Manitoba
Ontario
Sachigo
Berens River
Bird River
Uchi
English
River
Kapaskasing Structural Zone
Winnipeg River
Wabigoon
Quetico
Opatica
Abitibi
Quetico
Wawa
Pontiac
Wawa
Abitibi
Grenville Province
Minnesota River Valley
Southern Province
Quebec
Ontario
Canada
USA
N
0
250 km
Limit of Superior Province Exposure
Subprovince Boundary
International Boundary
Provincial/State Boundary

Figure 2. Map of the Superior Province showing the location of the principal subprovinces (*modified after* Card and Ciesielski 1986).

Four lithologies of sedimentary derived rocks have been described in the Quetico Subprovince (Williams 1991). 1) The first is a sequence of sandy to silty, grey to buff coloured metre, to decimetre-scale bedded graded and non-graded wackes. Loading and dewatering structures are present as well as scours, grain-size grading, ripple marks and cross-stratification. These sedimentary derived rocks young regionally northward, though reversals are common on metre to kilometre scales (Williams 1991).
2) Iron formations are present, though rare, in the Quetico Subprovince and consist of thin layers of quartz-magnetite. These are present in wackes throughout the Quetico, are typically only centimetres thick and generally are not laterally continuous, although some layers appear to form discontinuously traceable layers for up to hundreds of kilometres in the north-central Quetico Subprovince (Williams 1991). 3) Polymictic, volcanically derived, matrix- and clast-supported conglomerate units occur intermittently within wackes of the Quetico Subprovince. These can be up to several metres thick and have no preferred distribution. It has been inferred that these are resedimented volcanically derived detritus from the bordering greenstone terranes (Williams 1991). 4) Ultramafic wackes, siltstones and breccias occur sporadically within the Quetico Subprovince. These are chlorite- and amphibole-rich sedimentary rocks interpreted to be derived from the erosion of nearby ultramafic bodies (Williams 1991).

The depositional environment, as recorded by the metasedimentary rocks of the Quetico Subprovince, indicates a submarine basin of great lateral extent dominated by turbidite fans. The lack of volcanic detritus interbedded in the metasedimentary rocks has been interpreted to indicate that sedimentation was rapid (<10 million years; Williams 1991). The Quetico Subprovince has been interpreted to be the fore-arc accretionary prism of the Wabigoon Subprovince (Percival and Williams 1989; Williams 1990), whereas the relationship between the Quetico and Wawa subprovinces is one of a greenstone terrane underthrusting a fore-arc accretionary prism (Williams 1991).

Within the Quetico Subprovince, abundant felsic and intermediate intrusions can be found as well rare, widely scattered gabbroic and ultramafic rocks. Felsic volcanic rocks occur along the southern margin of the Quetico Subprovince and are interpreted to have been derived from volcanic rocks of the Wawa Subprovince as a result of melting during burial and metamorphism (Williams 1988). Ultramafic pods, plutons and layers occur at many locations within the Quetico Subprovince. These bodies are usually a few metres across and are difficult to classify definitively as intrusive, as their contacts are obscured by metasomatization characterized by zones of platy and fibrous chlorite, actinolite and biotite (Williams 1991). Intermediate and felsic intrusive igneous rocks include tonalite, granodiorite, granite, peraluminous granitic rocks, diorite and rare nepheline syenites (Williams 1991).

The Quetico Subprovince has been subjected to 4 episodes of deformation from soft sediment slumping and recumbent folding (D_1), followed by layer-parallel shearing, folding and regional-scale fabric formation (D_2). Both bedding and planar anisotropy were subject to upright folding (D_3) and localized shearing (D_4) (Williams 1991).

THE WABIGOON SUBPROVINCE

The Wabigoon Subprovince is a 900 km long, 150 km wide granite-greenstone terrane in the northwestern Superior Province (Blackburn et al. 1991; *see* Figure 2). It is composed of metamorphosed volcanic and volcanically derived sedimentary rocks ranging in age from 3.0 to 2.71 Ga, which are cut by granitic batholiths, gabbroic sills and stocks, which range in age from 3.0 to 2.69 Ga. The Wabigoon Subprovince has been extensively mapped as the subject of studies by Lawson (1885, 1888, 1913) and Pettijohn (1935), among others, with more extensive geological, geochemical and geochronological studies in recent years (e.g., Blackburn et al. 1991; Tomlinson et al. 2001; Hart, ter Meer and Jolette 2002). The Wabigoon Subprovince is divided into 3 regions: the western Wabigoon, the central Wabigoon and the eastern Wabigoon.

The western Wabigoon is a series of interconnected greenstone belts surrounding large granitoid batholiths. Volcanic sequences include ultramafic (komatiitic), mafic (tholeiitic, calc-alkaline and minor alkalic) and felsic (calk-alkaline) rocks. Metasedimentary sequences are mostly turbidites, fan-fluvial and rare platformal clastic rocks. Iron formations are only rarely found (Blackburn et al. 1991). Felsic volcanic sequences within the western Wabigoon have had an age determined of circa 2.7 Ga (Tomlinson et al. 2004, and references therein).

The central Wabigoon is dominated by large areas of granitoid and gneissic rocks. Schwerdtner (1984) has proposed that the domal plutonic structures in the central Wabigoon are the result of cross-folding. Uranium-lead geochronology and isotopic studies have shown that the central Wabigoon is dominated by several generations of tonalite and tonalite gneiss which both act as basement to and intrude small greenstone belts (cf. Tomlinson et al. 2003, and references therein). Data from Davis and Jackson (1988) indicate some gneiss bodies are older than 3075 Ma and several are 2.75 billion years old. More recently, Tomlinson et al. (2003) have recognized volcanic sequences with ages of 3.00 to 2.90, 2.83 and 2.7 Ga within the central Wabigoon.

The eastern Wabigoon consists largely of isolated greenstone belts surrounded by granitoid units. The greenstone belts of this region can be traced using geophysics underneath the overlying Proterozoic Nipigon diabase on the western side of Lake Nipigon (e.g., Blackburn et al. 1991; Hart, ter Meer and Jolette 2002). Clastic metasedimentary rocks are rare except in areas transitional to the Quetico and English River subprovinces. The metavolcanic units are centered concentrically around volcanic centres. Geochronological work has yielded an age of 2769 $^{+6}/_{-5}$ Ma (Anglin et al. 1988) from a rhyolite unit, whereas more recent studies have yielded ages for supracrustal rocks of 3.06 and 2.92 Ga (Stott and Davis 1999) and Neoarchean ages of 2.74 to 2.72 Ga (Davis 1999).

Economic Mineralization of the Wabigoon Subprovince

The greenstone belts of the Wabigoon Subprovince have historically been an important source of metallic and non-metallic elements for Ontario. Volcanogenic massive sulphide (VMS) deposits provided base metals (e.g., Sturgeon Lake Cu-Zn deposit; Morton and Franklin 1987). The Steep Rock Algoma-type iron formation near Atikokan, Ontario, contained approximately 700 Mt of iron ore (Blackburn et al. 1991). North American Palladium Ltd. currently operates its Lac des Iles Mine located approximately 100 km north of Thunder Bay. The mine is Canada's only primary producer of palladium and platinum with ore reserves of 88 Mt at a grade of 1.51g/t Pd (Hinchey, Hattori and Lavigne 2005). High-grade, low-tonnage iron formation-hosted gold mines in the Beardmore–Geraldton area were also once important sources of economic activity (Mason and White 1986; Anglin and Franklin 1985).

PROTEROZOIC

The Southern Province

The Southern Province is composed of rocks of the Penokean Orogen. The southern margin of the Southern Province consists of siliceous, continental margin metasedimentary rocks of the Huronian Supergroup formed 2.2 to 2.4 billion years ago. South of Lake Superior, the southern margin of the Superior Province is overlain by rocks of the Marquette Range Supergroup (2.2 to 1.7 Ga), a deformed, rifted passive margin sequence, which is, in turn, overlain by the Animikie Group (Thurston 1991; *see* Figure 1). Mesoproterozoic rocks of the Southern Province are represented by the 1546.5±10 Ma (Heaman and Easton 2005) English Bay complex (MacDonald 2004; Hollings, Fralick and Kissin 2004)

Table 1. Terminology of the rocks of the Nipigon Embayment. The classification used in this report is based on a revised classification proposed by P. Hollings, T.R. Hart, R.M. Easton and M.C. Smyk arising from the wealth of geochemical data collected as part of the LNRGI. This terminology has yet to be fully published, although portions of it can be found in Richardson and Hollings (2004) and in Hart and MacDonald (2005).

Logan Igneous Suite	
Diabase to Gabbro Sills	**Mafic to Ultramafic Intrusions and/or Sills**
Logan sills *(geographically south of Thunder Bay)*	Disraeli intrusion
	Hele intrusion
Nipigon sills *(geographically centred on Lake Nipigon and north of Thunder Bay)*	Kitto intrusion
McIntyre sills *(geographically located in the west-central Nipigon Embayment)*	Seagull intrusion
	Jackfish Island sill
Inspiration sills *(geographically located in the northwest of the Nipigon Embayment)*	Shillabeer sill
Other Igneous Intrusions	
Badwater Creek gabbro *(previously known as the Pillar Lake gabbro)*	
Badwater Creek syenite *(previously known as the Pillar Lake syenite or Pillar Lake sanukitoid)*	

located on the western shore of Lake Nipigon, and the recently recognized Badwater Creek gabbro (1598 Ma: Heaman and Easton 2005; MacDonald 2004; Table 1) and the Badwater Creek syenite cropping out in the same region (1590 Ma: Heaman and Easton 2005; MacDonald 2004). The Sibley Group sediments overlie Animikie Group and Archean basement rocks and are themselves overlain by, and are intercalated with, rocks associated with the Keweenawan Rift (1.1 Ga; Sutcliffe 1991).

ANIMIKIE GROUP SEDIMENTS

The Paleoproterozoic Animikie Group metasedimentary rocks form a homoclinal sequence southwest of Thunder Bay (*see* Figure 1). The Animikie basin occupies parts of Ontario, Minnesota, Wisconsin and Michigan and has been divided into 2 segments by the Midcontinent Rift (*see* Figure 1). In the northern part of the Animikie basin, the Group has been divided into 2 formations. The Gunflint Formation consists of a lower gravelly, basal conglomerate and argillaceous hematite-magnetite iron formation up to 15 m thick, a central unit up to 35 m thick sequence of argillite tuff, argillite, carbonate and chert and an upper unit up to 80 m thick consisting of thin-bedded chert, ferruginous carbonate, chert and hematite iron formation (Sutcliffe 1991). The overlying Rove Formation consists of a lower black, locally pyritic shale, which grades upward into shales interbedded with arkosic greywacke of turbidite origin. An age of 1836±5 Ma has been obtained from zircons from a tuffaceous layer by Addison et al. (2005). Evidence from diamond-drill holes indicates the Rove Formation is up to 1000 m thick (Sutcliffe 1991).

PALEOPROTEROZOIC ANOROGENIC GRANITE COMPLEXES

An anorogenic magmatic event in the northern Lake Nipigon region near English Bay predates the deposition of the Sibley Group (*see also* Hollings, Fralick and Kissin 2004, Figure 5; MacDonald 2004). The English Bay complex consists primarily of subvolcanic quartz alkali feldspar porphyry to alkali granite, with minor fragmental dacite to rhyolite (Hollings, Fralick and Kissin 2004; MacDonald 2004). The quartz feldspar porphyry has a U/Pb age of 1537 $^{+10}/_{-4.2}$ Ma (Davis and Sutcliffe 1985), whereas a rhyolitic tuff has a U/Pb age of 1547.5±10 Ma (Heaman and Easton 2005). These ages are comparable with a series of widely separated anorogenic igneous plutons emplaced in a wide belt from California to Labrador between 1.4 and 1.5 Ga (Sutcliffe 1991). Hollings, Fralick and Kissin (2004) suggest, from geochemical evidence, that the English Bay granite-rhyolite complex is of a mantle plume origin and the coincident emplacement of the complex in the same region as later rift volcanics suggests the English Bay complex may have been intruded along a major crustal weakness, which later facilitated the development of the Nipigon basin and the possible failed arm of the Midcontinent Rift.

THE SIBLEY GROUP SEDIMENTS

The Sibley Group (*see* Figure 1) consists of 5 formations. Franklin et al. (1980) described the lower 3 units of the Sibley Group: the Pass Lake, Rossport and the Kama Hill formations. The upper 2 units, the Outan Island and Nipigon Bay formations were recognized and described by Rogala (2003). The lowest unit, the Pass Lake Formation, consists of a lower conglomerate (Loon Lake Member) with overlying parallel-laminated and cross-bedded arenitic sandstones (Fork Bay Member). The Rossport Formation unconformably overlies the Pass Lake and consists of 3 members. The lowest stratigraphic unit is the Channel Island Member consisting of massive siltstone, sandstone, dolomitic sandstone and cyclic siltstone dolomite (Sutcliffe 1991). The Middlebrun Bay Member is dominated by alternating purple stromatolitic and sandstone layers. The Fire Hill Member is characterized by a mud-chip conglomerate unit (Sutcliffe 1991). The Kama Hill Formation overlies the Fire Hill Member and is dominated by horizontally laminated fine sandstone/siltstone, mud-cracked fine sandstone/siltstone and laminated mudstone (Franklin et al. 1980; Sutcliffe 1991). The Outan Island Formation is divided into a lower unit, the Lyon Member, dominated by fine-grained sandstones and mudstones thought to represent a deltaic environment, and an upper unit, the Hele Member, dominated by fine- to coarse-grained sandstone thought to represent a fluvial environment (Cheadle 1986). The Nipigon Bay Formation is dominated by cross-stratified sandstone and horizontally laminated sandstone interpreted to represent an eolian environment (Rogala 2003). The overall environment in which the Sibley Group was deposited represents a lacustrine system (Pass Lake Formation) gradually evolving to a saline playa lake environment (Rossport Formation). As the climate progressively became drier, a sabkha-type environment evolved (Kama Hill Formation). The Outan Island Formation represents the transition from subaqueous to subaerial conditions and the Nipigon Bay Formation represents a wholly eolian environment (Rogala 2003).

Previous geochronological work by Franklin et al. (1980) on clays from the Rossport and Kama Hill formations yielded a Rb/Sr age of 1339±33 Ma. This has been interpreted to be a diagenetic age representing a minimum possible age for this part of the Sibley Group. Detrital zircon ages from the Pass Lake Formation (Fork Bay Member) range from 3034 to 1602 Ma with the latter being a maximum possible depositional age for the Pass Lake Formation (Heaman and Easton 2005). Ages of detrital zircons from the Outan Island and Nipigon Bay formations were also obtained. Maximum possible ages of deposition were 1450 and 1670 Ma, respectively (Heaman and Easton 2005); however, stratigraphic relationships require the Nipigon Bay Formation to be the younger of the two. Of interest may be the facts that the dominant zircon population age of the Pass Lake Formation is largely absent in the upper 2 units of the Sibley Group, and also that circa 1530 Ma English Bay complex zircons (L.M. Heaman, University of Alberta, personal communication, 2005) are lacking in the Pass Lake and Nipigon Bay formations. Richardson (2003) suggested the English Bay complex to be a sediment source for the Fork Bay Member of the Pass Lake Formation based on zircon mineral chemistry, however, the U/Pb ages do not support this conclusion.

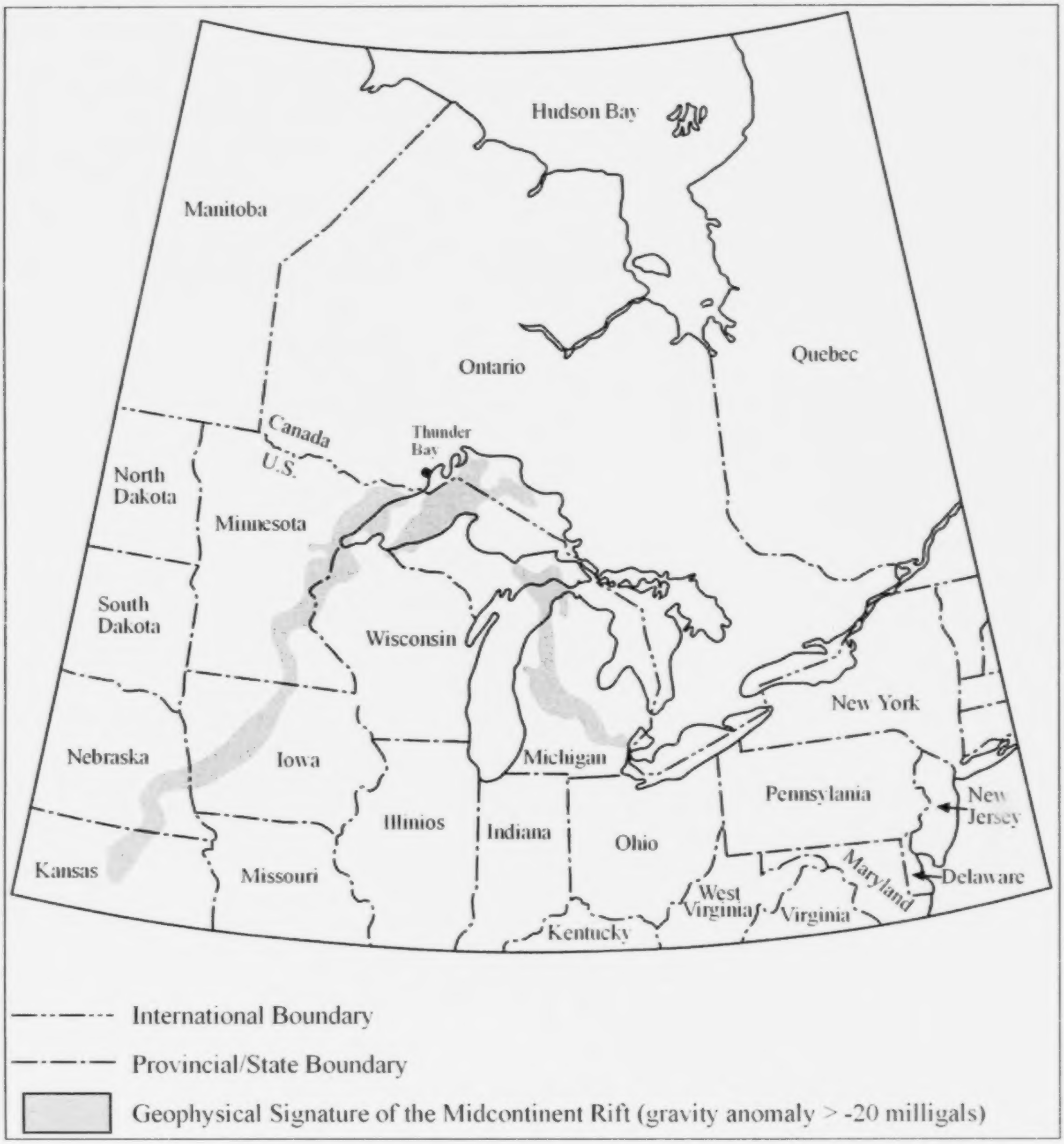
Hudson Bay
Manitoba
Ontario
Quebec
Canada
U.S.
Thunder Bay
North Dakota
Minnesota
South Dakota
Wisconsin
Nebraska
Iowa
Michigan
New York
Pennsylvania
New Jersey
Kansas
Missouri
Illinios
Indiana
Ohio
Maryland
Delaware
West Virginia
Virginia
Kentucky
International Boundary
Provincial/State Boundary
Geophysical Signature of the Midcontinent Rift (gravity anomaly > -20 milligals)

Figure 3. Map showing location of gravity anomaly associated with the Midcontinent Rift (*from* Klasner, Cannon and van Schmus 1982).

Rocks of the Keweenawan Midcontinent Rift

Approximately 1.1 billion years ago, in excess of 1 500 000 km^3 of basaltic sheets, flows and intrusive diabase sills were emplaced in the Lake Superior region (Klewin and Shirey 1992). The source of the magma has been interpreted to be of mantle-plume origin, which subsequently initiated the formation of a continental rift (Nicholson and Shirey 1990). An approximate time period for crustal extension associated with the rift can be estimated from U/Pb ages of 1124.3±4.8 Ma (Seagull intrusion; Heaman and Easton 2005) to 1097.7±1 Ma (Devil's Kettle Rhyolite, North Shore Volcanic Group; Davis and Green 1997) during which time volcanic and sedimentary rocks filled the rift basin to an estimated depth of 30 km (Cannon et al. 1989; Heaman and Easton 2005). The geophysical signature of igneous activity associated with the rift event can be traced as far to the southwest as Kansas (USA) and to the southeast as the Grenville Front in southern Ontario (Figure 3; Klasner, Cannon and Van Schmus 1982; Davis and Green 1997).

OSLER GROUP

To the south of the Nipigon basin, rift-related rocks include the Osler Group, the North Shore Volcanic Group, the Mamainse Point Formation, the Portage Lake volcanics and the Duluth Complex. The Osler Group volcanic rocks (*see* Figure 1) are a series of pillowed, massive and columnar jointed basaltic amygdaloidal, ropy and locally pahoehoe textured flows that crop out along the north shore of Lake Superior on the Black Bay peninsula, and on Simpson, Ignace and Wilson islands (Lightfoot, Sutcliffe and Doherty 1991). Seismic reflection data interpreted by Cannon et al. (1989) indicate that the Osler Group basalts are up to 3 km thick. A rhyolite unit at the base of the Osler Group has an age of 1107 Ma (Davis and Sutcliffe 1985), whereas the Agate Point rhyolite, toward the top of the sequence, has a U/Pb age of 1105.3±2.1 Ma (Davis and Green 1997). The Osler Group can be divided into 2 geophysically distinct units: one with normal magnetic polarity, and the other reversed (Halls 1974). The contact between the two is marked by the presence of the Puff Island conglomerate with a disconformity between the lower and upper flows. This has been interpreted to represent a break in eruption history. The Osler Group is overlain and intruded by the St. Ignace Island complex—an intercalated sequence of basalt and rhyolite flows (Sutcliffe and Smith 1988).

MAMAINSE POINT FORMATION

The Mamainse Point Formation is a 6 km thick mafic extrusive sequence overlying Precambrian basement rocks located northwest of Sault Ste. Marie, Ontario (Lightfoot et al. 1999; *see* Figure 1). The flows dip approximately 30° to the west-southwest at the top of the sequence, increasing to 55° at the base. The flows are interbedded with coarse conglomerate and rhyolite and intruded by felsite bodies (Lightfoot et al. 1999). The sequence has undergone low-grade hydrothermal metamorphism. Approximately 300 flows make up the sequence, many of which have upper and lower vesicular zones and some of which have ropy pahoehoe surfaces. Phenocrysts of plagioclase and pseudomorphed olivine are common and rarely plagioclase crystals concentrate into radial clusters of glomeroporphyritic plagioclase (e.g., the "Daisystone flow"; Lightfoot et al. 1999). The felsic bodies are quartz porphyry, felsite and flow-banded rhyolite. All but the quartz porphyry are phenocryst poor and were reported by Green (1971) to be compositionally similar to the quartz latites of the Minnesota North Shore Volcanic Group (Lightfoot et al. 1999).

DULUTH COMPLEX

The Duluth Complex and the North Shore Volcanic Group are major portions of the intrusive and extrusive igneous activity associated with the rift system (*see* Figure 1). The Duluth Complex is a layered mafic intrusive body approximately 3 to 4.5 km thick (Miller et al. 2002). The complex is emplaced in extrusive basalts of the North Shore Volcanic Group, with the basalts under the complex being reversely polarized, whereas the upper basalts are normally polarized (Weiblen and Morey 1980). At the basal contact, troctolitic rocks of the Duluth Complex intruded basalts of the North Shore Volcanic Group as well as the Rove and Virginia formations and the Bibawik iron formation. Rocks of the upper Duluth Complex form the anorthositic series. This series was later intruded by the troctolitic series as indicated by inclusions of anorthosite series rocks within the troctolite rocks. The anorthositic series rocks form the cap of the Duluth Complex. Felsic rocks occur as small irregular bodies principally along the upper boundary between the anorthosite series and the troctolitic rocks. Troctolite series rocks are medium to coarse grained and generally exhibit textures associated with flow (Weiblen and Morey 1980). The geochronology of the Duluth Complex is discussed by Paces and Miller (1993).

NORTH SHORE VOLCANIC GROUP

The North Shore Volcanic Group represents a significant period of extrusive volcanism associated with the rift event. The North Shore Volcanic Group is a thick sequence of plateau lavas dominated by basaltic compositions, but ranging from basalt through to rhyolite (Green 1989). The rhyolitic flows fall into 2 categories: icelandites and rhyolites, with the majority of rhyolites being ignimbrites, and both containing approximately 72 to 73% SiO_2. The majority of flows are porphyritic and contain no vertical compositional zoning with respect to phenocryst abundance or mineralogy (Green and Fitz 1993). The North Shore Volcanic Group rocks consists of 2 series of eruptive plateaus separated by a change in magnetic polarity. The stratigraphically higher unit is normally polarized with up to 7 km of preserved flows, whereas the reversely polarized lower unit contains up to 320 m of flows (Green 1989). A subaerial eruption environment is indicated by the general lack of pillows, the presence of pahoehoe and ropy surface morphology and individual flow thicknesses ranging from a few metres to a few hundred metres (Green 1989). Comprising up to 25% of the flows of the North Shore Volcanic Group, rhyolites tend to form large cliffs and other impressive geomorphological features (e.g., Palisade rhyolite near Silver Bay, Minnesota).

LOGAN IGNEOUS SUITE

The Nipigon and Logan sills represent the remnants of the northern expression of the Midcontinent Rift (*see* Table 1). The Logan sills generally refer to diabase features found south of Thunder Bay, Ontario, whereas Nipigon sills refer to the same type of rocks found to the north (*see* Table 1 for proposed nomenclature). Hart, MacDonald et al. (2005) suggests a geochemical separation of the two. They report that the Logan sills contain a higher concentration of TiO_2 (3 to 4 weight %) than sills of the Nipigon suite (1 to 2.5 weight %).

The first comprehensive mapping program which focussed on the diabase sills around Lake Nipigon was undertaken by R.H. Sutcliffe as part of a PhD thesis (Sutcliffe 1986). He separated the dominant rock types of the sills into a picritic rock derived from olivine fractionation at shallow levels and a diabase unit. The diabase sills were suggested to have crystallized under a lithostatic load of less than 0.4 kbar and crystallized over a temperature range from 1100 to 800°C (Sutcliffe 1986). Chemical variation within the sills was attributed to multiple magma pulses, crystal accumulation and movement of volatiles (Sutcliffe 1986).

Work by MacDonald, Tremblay and Easton (2005) suggests that the sills in the western Lake Nipigon basin can be divided, based on geochemical differences, into 3 additional sill types. The first and most volumetrically abundant is the Nipigon diabase sills, estimated to represent 70 to 80% of the rocks within the map area. This sill type can be described as generally brown to grey brown, massive, medium grained, intergranular textured and gabbroic (MacDonald, Tremblay and Easton 2005). Local variation included fine- and coarse-grained textures with medium- to coarse-grained varieties commonly displaying ophitic and poikilitic textures. The Inspiration sills were recognized by MacDonald and Tremblay (2004b, 2004c) and are located in the northern part of the Nipigon Embayment. The Inspiration sills in outcrop are similar to the Nipigon sills with medium-grained subophitic textures (MacDonald, Tremblay and Easton 2005). Local variations include fine- and coarse-grained diabase, potassium-bearing monzogabbro and leucocratic diabase pods (MacDonald, Tremblay and Easton 2005). The Jackfish Island sill is a 50 to 60 m thick olivine gabbro to peridotite sill that intrudes the English Bay complex (MacDonald, Tremblay and Easton 2005) and was first recognized by Sutcliffe (1986) on Jackfish Island (referred to in this report as Jackfish Island sill).

Methodology

FIELD WORK

As part of this study, a detailed sampling program was undertaken in the summers of 2003 and 2004 involving both existing diamond-drill core, available through the OGS core library located in Conmee Township, Ontario, and surface samples from the shoreline of Lake Nipigon and the diabase cliffs at Kama Hill, approximately 20 km east of the town of Nipigon on Highway 17. Target sample mass was approximately 500 g and was taken from below the waterline (where possible) in order to minimize damage to the shoreline environment. Permission was obtained to sample within the protected boundaries of the Lake Nipigon basin waterways from the Ministry of Natural Resources (MNR) before the program commenced. Sampling in the areas of Lake Nipigon identified as caribou calving grounds was avoided during the period of time specified by the MNR. Logging roads, local highways and waterways were used to access sample areas. A total of 250 surface samples from the Lake Nipigon shoreline (Figure 4), 531 samples from diamond-drill core and 30 surface samples from the Kama Hill diabase cliffs were collected.

ANALYTICAL TECHNIQUES

Samples selected for analysis were cut, crushed and milled at the rock laboratory at Lakehead University. Samples were trimmed and cut using a diamond cut-off saw and coarse crushed between tungsten carbide plates with the sample between paper to minimize contamination by transition and rare earth elements (REE). Samples were milled to –200 mesh in an agate ring mill so as to reduce risk of contamination of trace elements that occurs with tungsten carbide and some other materials (Jenner 1996). Tools and working surfaces were cleaned with acetone between each sample.

Samples were analyzed for major elements by X-ray fluorescence (XRF) and for trace and rare earth elements by inductively coupled plasma mass spectrometry (ICP–MS) at the University of Saskatchewan located in Saskatoon, Saskatchewan, and at the Geoscience Laboratories (Geo Labs) of the Ministry of Northern Development and Mines in Sudbury, Ontario. Analytical methodology used by Geo Labs is the same as the procedures used by the University of Saskatchewan laboratory.

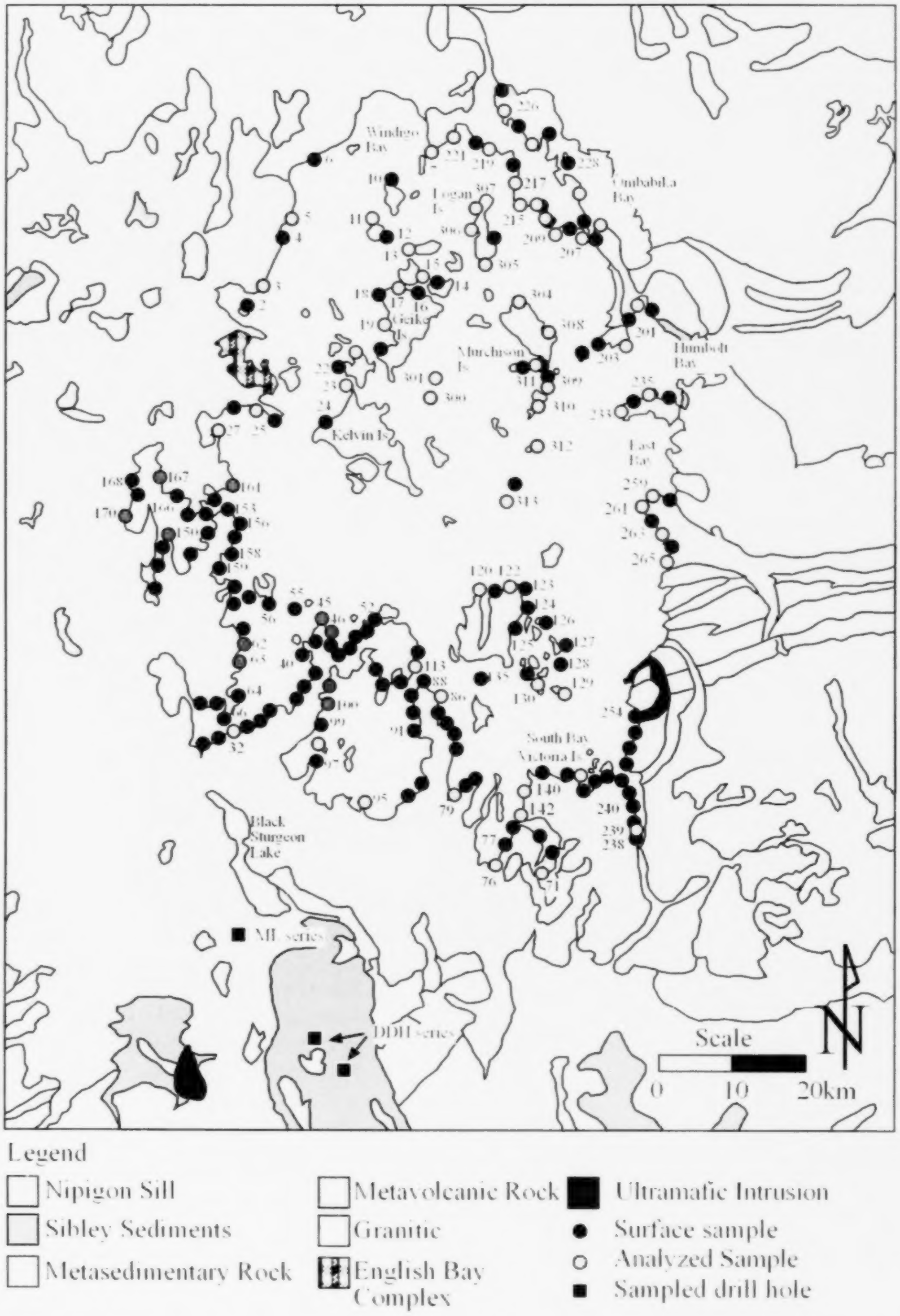
Windigo Bay
Logan Is
Umbabika Bay
Geikie Is
Murchison Is
Humbolt Bay
Kelvin Is
East Bay
South Bay
Victoria Is
Black Sturgeon Lake
ML series
DDH series
Scale
0
10
20km
N
Legend
Nipigon Sill
Sibley Sediments
Metasedimentary Rock
Metavolcanic Rock
Granitic
English Bay Complex
Ultramafic Intrusion
● Surface sample
○ Analyzed Sample
■ Sampled drill hole

Figure 4. Map showing sample locations and the regional geology of the Nipigon Embayment (*modified after* Sutcliffe 1986).

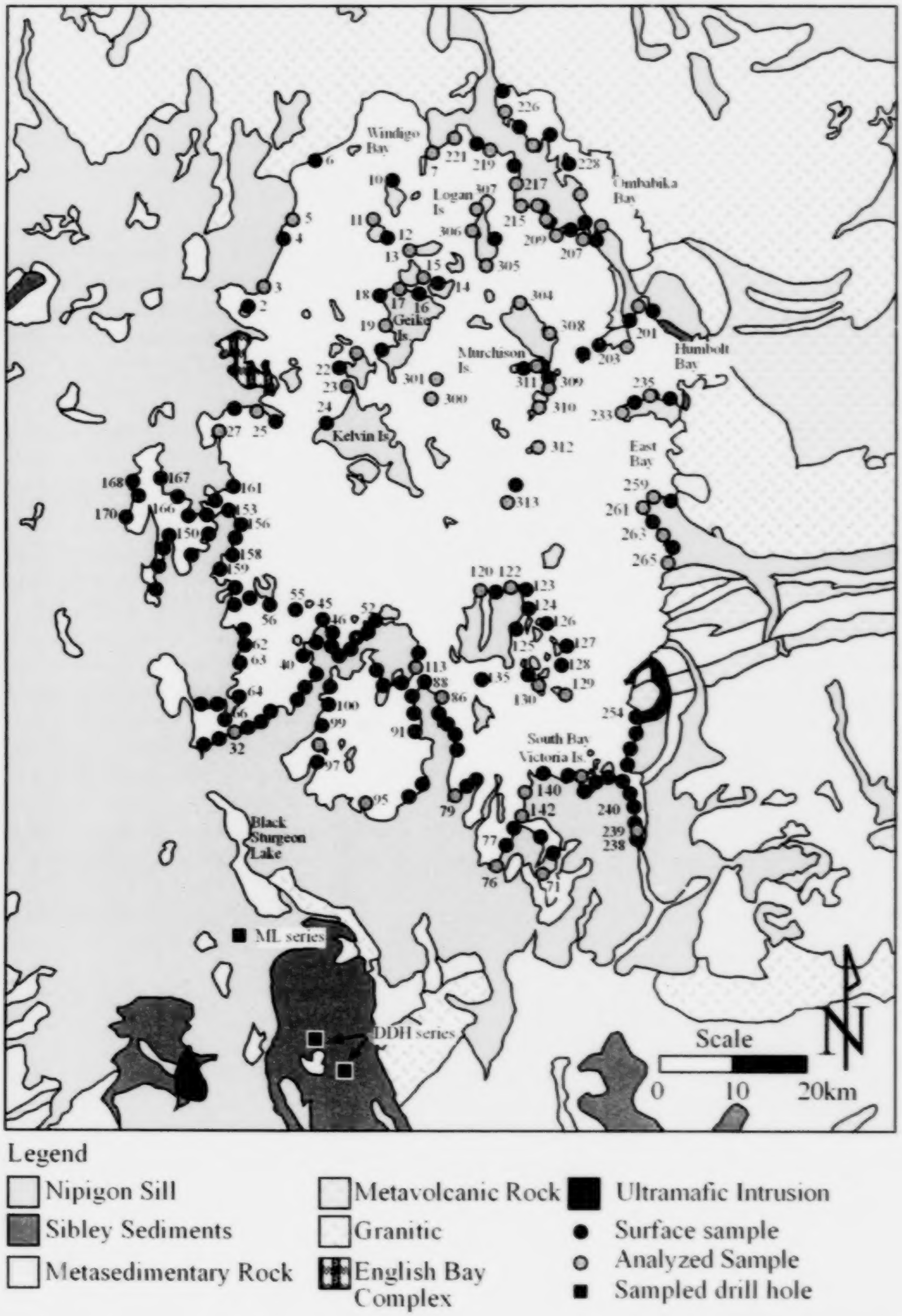
Windigo Bay
Logan Is
Ombabika Bay
Geike Is.
Murchison Is.
Humbolt Bay
Kelvin Is.
East Bay
South Bay
Victoria Is.
Black Sturgeon Lake
ML series
DDH series
Scale
0
10
20km
N
Legend
Nipigon Sill
Sibley Sediments
Metasedimentary Rock
Metavolcanic Rock
Granitic
English Bay Complex
Ultramafic Intrusion
● Surface sample
○ Analyzed Sample
■ Sampled drill hole

Figure 4. Map showing sample locations and the regional geology of the Nipigon Embayment (*modified after* Sutcliffe 1986).

Major elements were also determined using XRF at X-Ray Assay Laboratories (XRAL) (SGS Canada Inc.), in Don Mills, Ontario, using 2 g of sample prepared as a fused disk. In addition, selected trace elements (e.g., Zr and Y) were analyzed using a pressed pellet to allow comparison with data generated by ICP–MS. Totals for major element oxide data were generally within 2% of 100% and have been recalculated to a 100% volatile-free basis. Detection limits for major elements are 0.01 weight % and relative standard deviations of duplicate analyses are within 5%.

Trace elements, including the rare earth elements (REE) and high field strength elements (HFSE), were analyzed at the University of Saskatchewan, using a Perkin-Elmer Elan 5000 ICP–MS following the protocol of Jenner et al. (1990) and Longerich et al. (1990). Data reduction followed the procedure of Jenner et al. (1990). Thirty-one trace elements were determined using a $HF–HNO_3$ dissolution on 100 mg aliquots of powder. Thorium, Nb, Hf, Zr and REEs were also analyzed using the Na_2O_2 sinter technique of Longerich et al. (1990) on 200 mg aliquots of powder to circumvent potential problems associated with incomplete dissolution of refractory minerals hosting HFSE and REE and/or their instability in analytes. Analysis of acids, distilled deionized water and procedural blanks yielded levels of <10 ppb for Hf, Zr, Nb and REEs. Detection limits for some critical elements, defined as 3σ of the procedural blank, are as follows: Th (0.01 ppm), Nb (0.006 ppm), Hf (0.008 ppm), Zr (0.004 ppm), La (0.01 ppm) and Ce (0.009 ppm).

Chondrite-normalized (e.g., La/Sm_{cn}) and primitive mantle-normalized ratios (e.g., Th/Nb_{pm}) are calculated from the values of Sun and McDonough (1989) as are the primitive mantle-normalized diagrams. Ratios of HFSE/HFSE* are calculated following the logarithmic method of McCuaig, Kerrich and Xie (1994), except that Gd is used in place of Eu for Zr/Zr* and Hf/Hf*. All analyses performed during the course of this study utilized standards, duplicate samples and blanks, both in-house as part of the normal procedures of the analytical facilities, as well as standards submitted for replicate analyses by Lakehead University researchers.

Samarium–Neodymium (Sm/Nd), Rubidium–Strontium (Rb/Sr) and Lead–Lead (Pb/Pb) Isotope Methodology

Samples were analyzed for Sm and Nd isotopes at the analytical facility at the University of Alberta. Rock powders were accurately weighed and totally spiked with a known amount of mixed $^{150}Nd–^{149}Sm$ tracer solution. Dissolution occurs in mixed 24N HF + 16N HNO_3 media in sealed PFA Teflon™ vessels at 160°C for 5 days. The fluoride residue is converted to chloride with HCl, and Nd and Sm are separated by conventional cation and HDEHP-based chromatography. Chemical processing blanks are <40 pg of either Sm or Nd, and are insignificant relative to the amount of Sm or Nd analyzed for any rock sample. The isotopic composition of Nd is determined in static mode by multi-collector inductively coupled plasma mass spectrometry (MC-ICP–MS). All isotope ratios are normalized for variable mass fractionation to a value of $^{146}Nd/^{144}Nd = 0.7219$ using the exponential fractionation law. The $^{143}Nd/^{144}Nd$ ratio of samples is presented relative to a value of 0.511850 for the La Jolla Nd isotopic standard, monitored by use of an Alfa Nd isotopic standard for each analytical session. Samarium isotopic abundances are measured in static mode by MC-ICP–MS, and are normalized for variable mass fractionation to a value of 1.17537 for $^{152}Sm/^{154}Sm$ also using the exponential law. Rubidium-strontium isotope analyses were performed following the analytical procedures of Holmden et al. (1996) and Creaser et al. (1997). Lead-lead isotope analyses were conducted following the analytical procedures of Cumming and Krstic (1991) and Lugmair and Galer (1992).

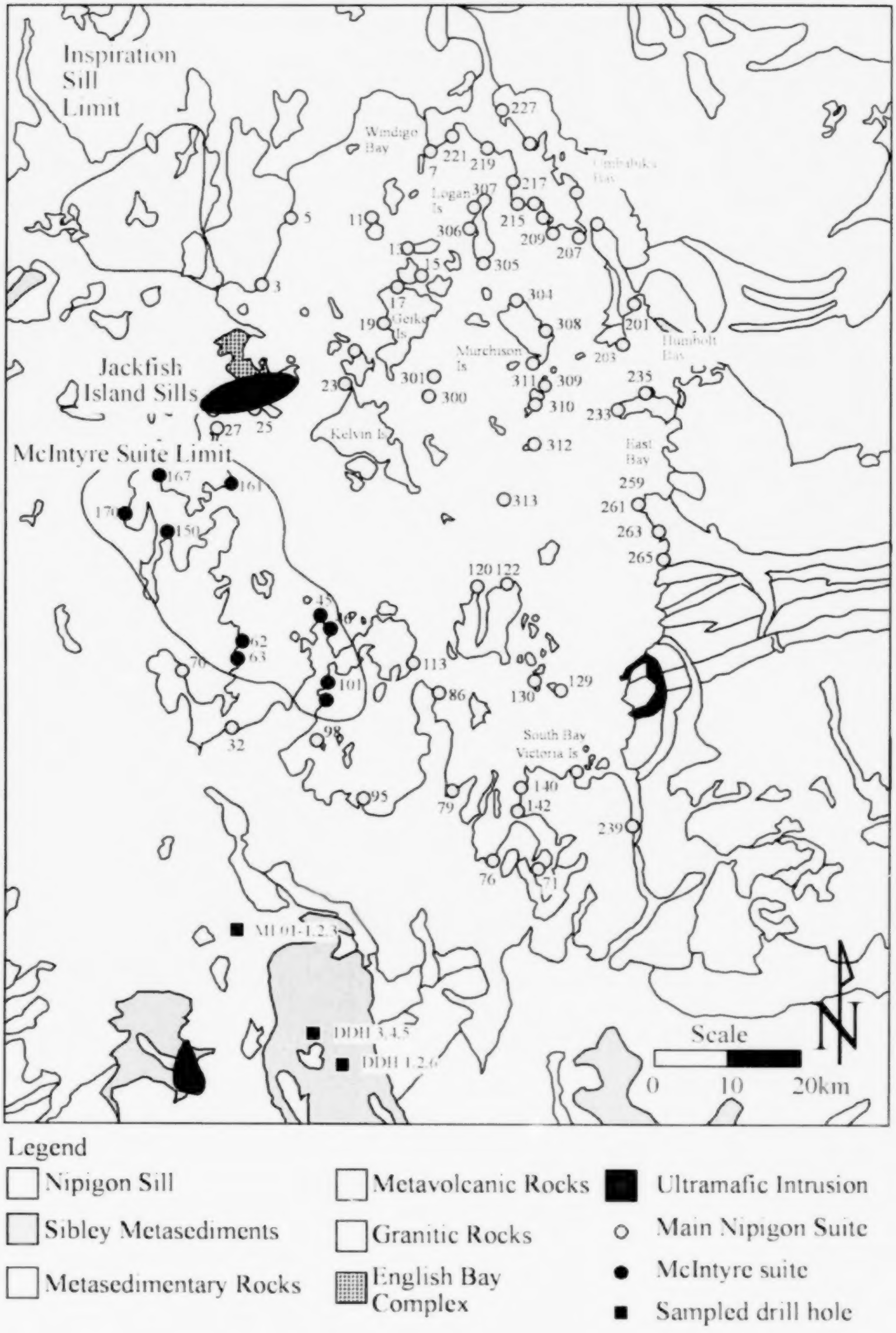
Inspiration Sill Limit
Jackfish Island Sills
McIntyre Suite Limit
Windigo Bay
Logan Is
Ombabika Bay
Geike Is
Murchison Is
Humbolt Bay
Kelvin Is
East Bay
South Bay
Victoria Is
227
221
219
7
217
307
215
11
306
209
207
13
15
305
304
17
19
308
201
203
301
300
311
309
235
23
310
233
27
25
312
167
161
259
170
150
313
261
263
265
120
122
45
62
63
70
113
101
86
129
130
32
98
140
142
95
79
239
76
71
MI 01-1,2,3
DDH 3,4,5
DDH 1,2,6
Scale
0
10
20km
N
Legend
Nipigon Sill
Metavolcanic Rocks
Ultramafic Intrusion
Sibley Metasediments
Granitic Rocks
Main Nipigon Suite
Metasedimentary Rocks
English Bay Complex
McIntyre suite
Sampled drill hole

Figure 5. Regional geology map showing the location of the Nipigon, Inspiration, Jackfish Island and McIntyre sills in the Nipigon Embayment (*modified after* Sutcliffe 1986).

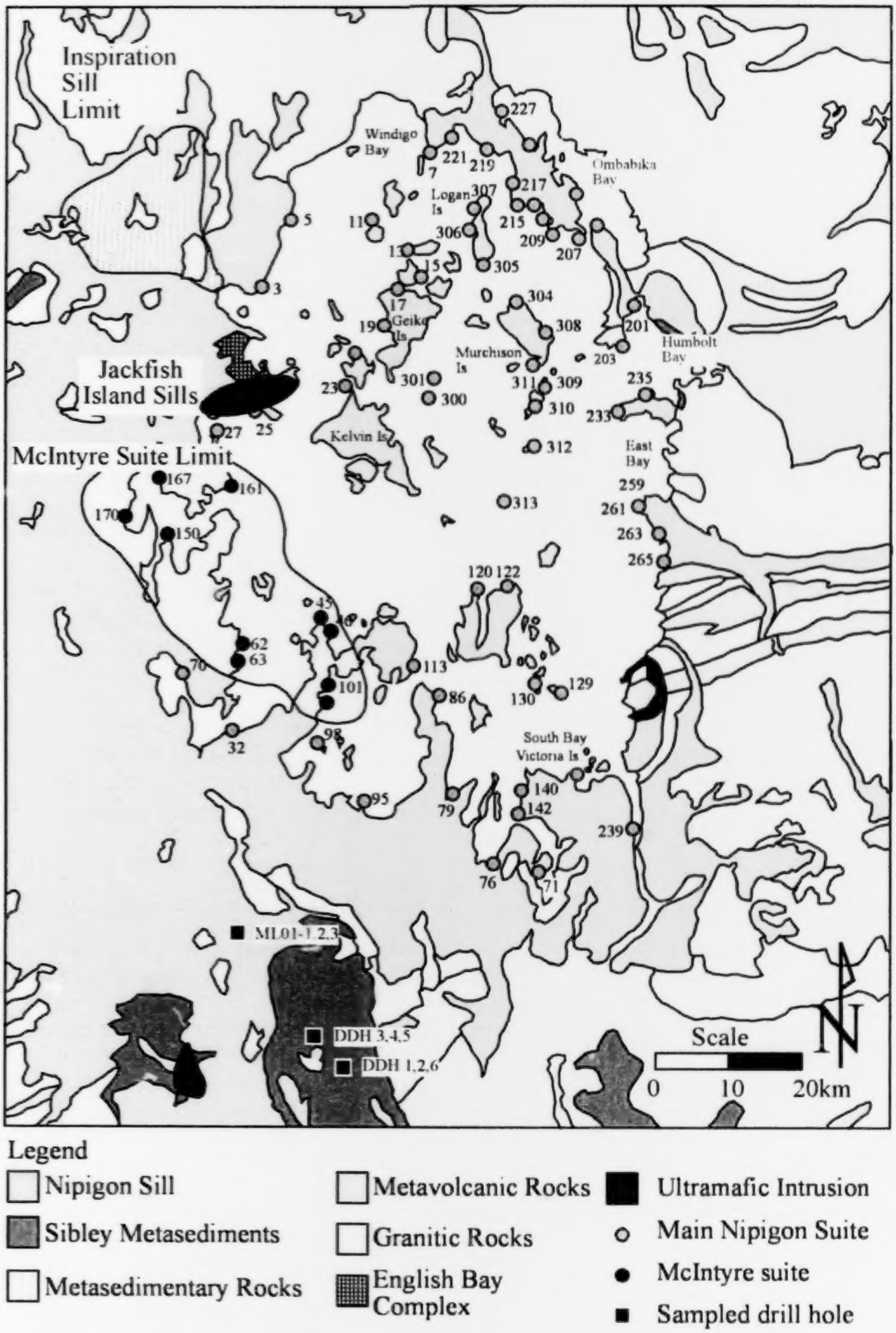
Inspiration Sill Limit
Jackfish Island Sills
McIntyre Suite Limit
Windigo Bay
Logan Is
Geike Is
Murchison Is
Kelvin Is
Ombabika Bay
Humbolt Bay
East Bay
South Bay
Victoria Is
227
221
219
7
217
307
215
306
209
207
305
304
308
201
203
235
233
311
309
310
312
313
301
300
11
13
15
17
19
23
27
25
5
3
167
161
170
150
45
62
63
70
101
32
98
95
113
86
120
122
129
130
79
140
142
239
259
261
263
265
76
71
ML01-1,2,3
DDH 3,4,5
DDH 1,2,6
Scale
0
10
20km
N
Legend
Nipigon Sill
Sibley Metasediments
Metasedimentary Rocks
Metavolcanic Rocks
Granitic Rocks
English Bay Complex
Ultramafic Intrusion
Main Nipigon Suite
McIntyre suite
Sampled drill hole

Figure 5. Regional geology map showing the location of the Nipigon, Inspiration, Jackfish Island and McIntyre sills in the Nipigon Embayment (*modified after* Sutcliffe 1986).

Scanning Electron Microscopy Electron Dispersion System Methodology

Samples analyzed for mineral chemistry data were prepared into 30 µm thin sections and carbon coated to prevent charge build-up. The samples were then analyzed using the Lakehead University Instrument Laboratories JEOL 5700 scanning electron microscope (SEM) equipped with an Oxford energy dispersion system (EDS). The system has a resolution of 139 eV. Samples were analyzed for 50 seconds at a beam current of 0.475 nA, spot size of 0.2 µm and a count rate of 2000 cps (for nickel metal). Full ZAF algorithm matrix-correction software was applied automatically to raw acquired data via a LINK ISIS analytical system. During use, the instrument was calibrated hourly using pure nickel metal and standardized using geological standards before each session.

General Sill Characteristics

The previously described Nipigon sills have been subdivided into 2 diabase sill suites and an ultramafic sill suite (*see* Table 1) based on geochemical data generated by this study, in addition to the suites identified by Sutcliffe (1986) and MacDonald, Tremblay and Easton (2005). These subdivisions do not include the Logan sills, which historically have been considered to be the circa 1.1 billion years old diabase sills to the south of Thunder Bay, Ontario, whereas the Nipigon sills represent those sills in the north. The diabase sills from this study can be divided into 3 suites: the Nipigon, the McIntyre and the Shillabeer (*see* Table 1). The geomorphology of the sills is common to all suites—competent, massive though occasionally columnar jointed, erosion resistant outcrops commonly forming cliffs, hills and ridges.

The Nipigon suite crops out throughout the Nipigon basin with observable sill thicknesses estimated at 120 to 150 m (Inner Barn Island located in English Bay, Lake Nipigon). Diamond-drill core from the southern Black Sturgeon Lake area (ML series drill holes, Figure 5) indicate sill thickness to be in excess of 250 m. The McIntyre sills are found only in outcrop and their geographic distribution is shown in Figure 5. The majority of outcrop within the area of the McIntyre suite is generally flat lying with two examples of sill tops identified by surface textures ("tortoise shell") and vesicles (some large, up to 3 cm) in the Chief Bay (sample LN 66) and McIntyre Bay (sample LN 98) areas of Lake Nipigon (Photo 1; *see* Figure 4). The Shillabeer suite is seen in drill core from a series of holes north of Shillabeer Lake (this study; *see* Figure 5) and drill hole NI-92-7 to the west of Disraeli Lake (T.R. Hart, OGS, personal communication, 2005). Identified in the top sill of DDH 3 and DDH 5, the Shillabeer suite is up to 60 m thick in DDH 3, but is only represented by one sample from the top of DDH 5 where it must be <30 m thick as the drill hole is collared in the Shillabeer suite sill.

Petrographically, these 3 suites are broadly similar, lacking any distinctive variations that can be correlated with geochemical variations. The Nipigon suite can be broadly characterized as having approximately 50 to 60 modal % plagioclase as randomly oriented laths ranging from 0.5 to 1.5 mm in length. Plagioclase alteration is typically mild sericite with more rare zeolite. Mafic mineralogy is dominated by pyroxene (40 to 50 modal %) typically forming equant oikocrysts from 1 to 3 mm in size. Pyroxene alteration is typically mild to moderate chlorite. Olivine is present in some samples and generally forms equant fresh to moderately altered grains in comprising up to 1 modal %. Identified trace minerals (<1 modal %) are biotite and hornblende. The McIntyre suite samples studied show little variation from the Nipigon suite in terms of mineralogy, grain size or alteration.

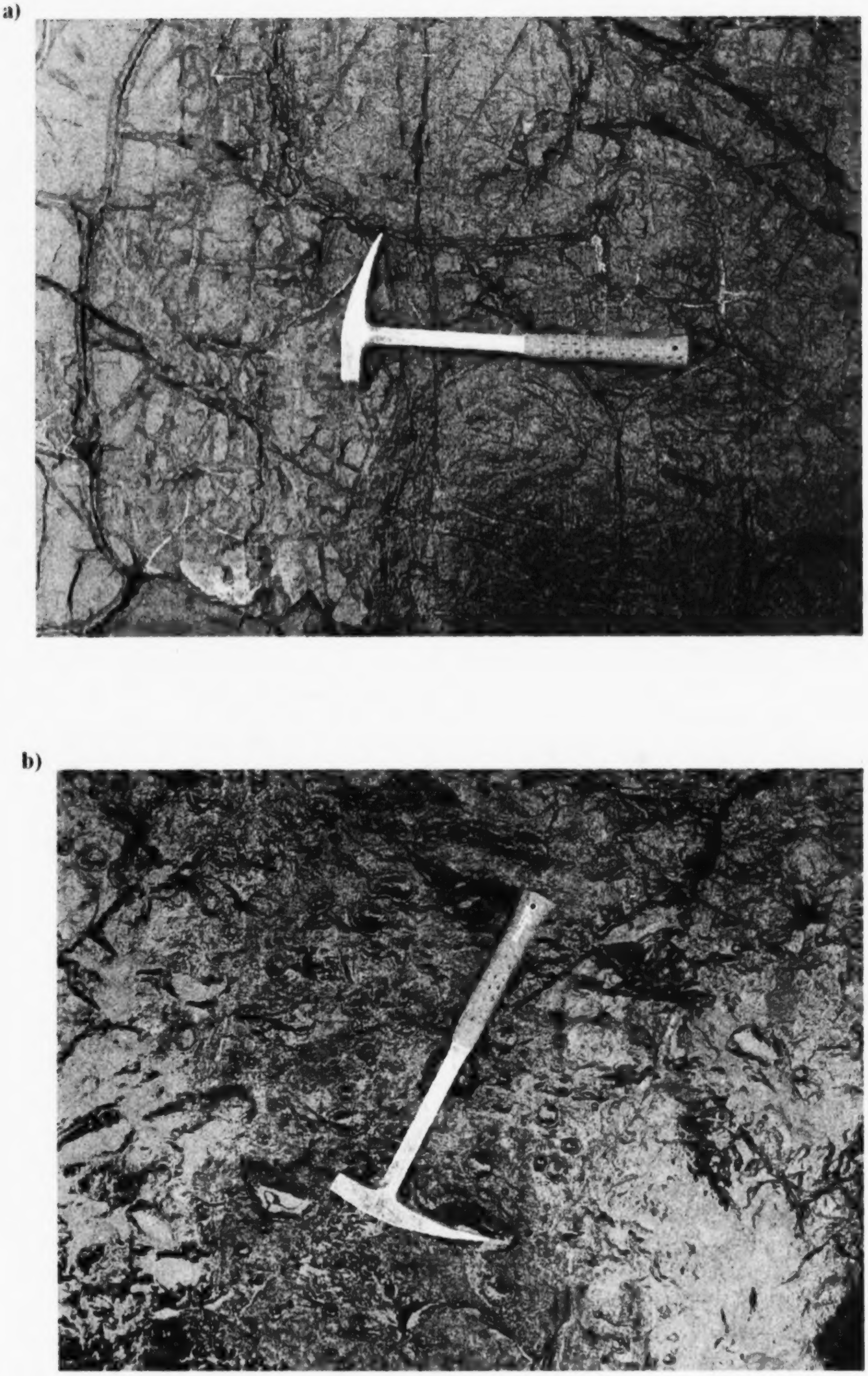

Photo 1. Photograph of sill tops observed: a) tortoise-shell texture in McIntyre Bay, sample LN70; and b) vesicular sill top in McIntyre Bay near sample LN98.

Of the 250 samples collected from the shoreline of Lake Nipigon, 85 were analyzed for major, trace and rare earth elements (*see* Figure 4). The Nipigon sills can be broken into 2 broad categories: a high TiO_2 subset and a low TiO_2 subset (Figure 6a). The high TiO_2 subset consists of the Logan, Jackfish, McIntyre and Shillabeer suites. The low TiO_2 subset comprises the Nipigon and the Inspiration sills. The trend exhibited by TiO_2 is roughly mirrored by P_2O_5 with the same broad classification with the exception of the McIntyre suite, which falls out of the high subset trending toward the low.

The Nipigon suite is represented by 115 (43 drill core and 72 surface) samples from a total of 138 samples analyzed (Appendix 1). This suite is characterized by TiO_2 values of 0.7 to 2.7 weight %, MgO values of 2.3 to 11.4 weight %, Mg# of 21 to 63 and La/Yb_{cn} ratio of 1.3 to 6.5. Primitive mantle-normalized REE plots show the Nipigon with the shallowest REE slope with La/Yb_{cn} ratios of 2 to 5 and negative Nb, Ti and Y anomalies (Figure 7). The McIntyre suite is represented by 10 surface samples and is characterized by higher TiO_2 (2.7 to 3.1 weight %) and La/Yb_{cn} (6.4 to 7.2; Figure 8; Appendix 2) than the Nipigon, but comparable MgO (4.7 to 7.1 weight %) and Mg# (38 to 51). The Shillabeer suite is

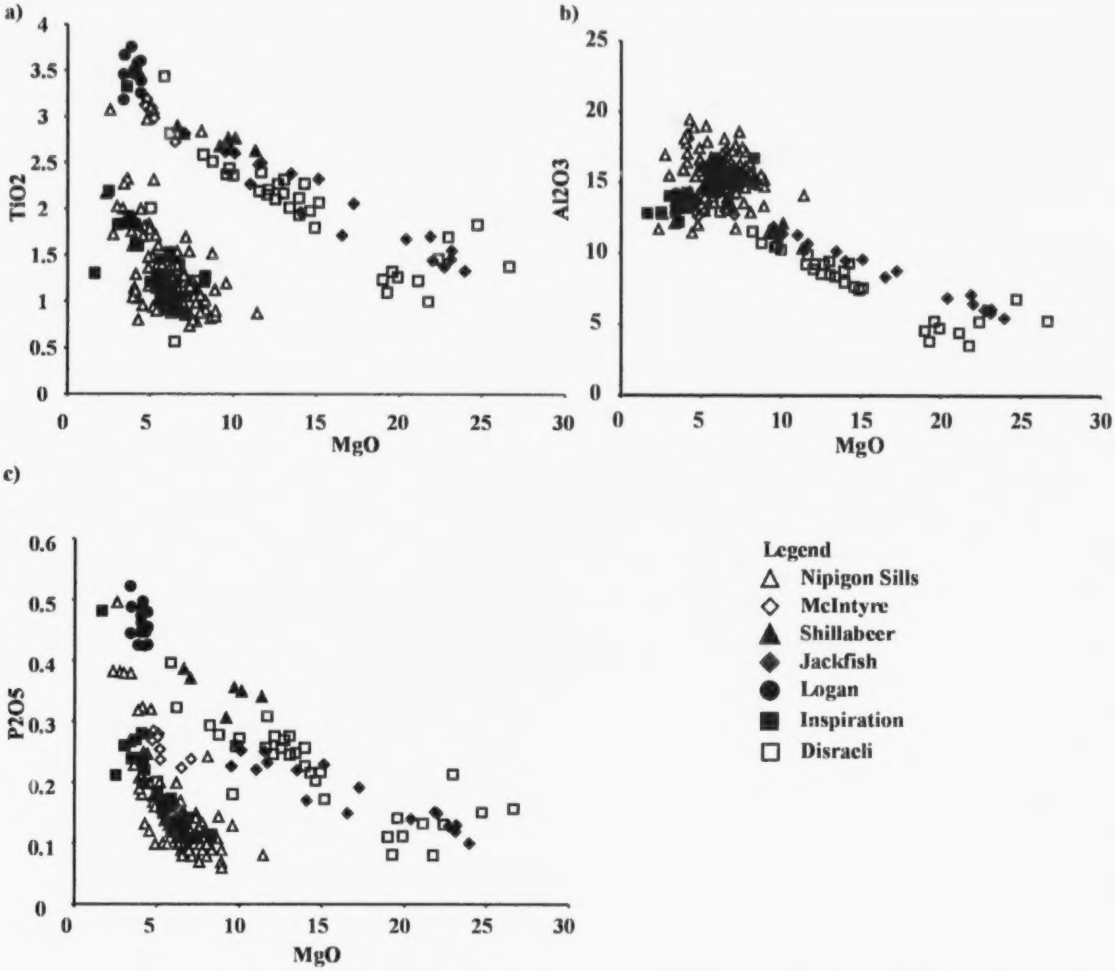

Figure 6. Bivariant plots for the diabase sills of the Nipigon Embayment: a) MgO versus TiO_2 showing the development of a high TiO_2 group (Logan, Shillabeer, Jackfish Island and McIntyre sills) and a low TiO_2 group (Nipigon and Inspiration sills); b) MgO versus Al_2O_3; and c) MgO versus P_2O_5. Jackfish Island and Inspiration data *from* MacDonald (2004); Logan sills and Disraeli intrusion data *from* Franklin (unpublished data, 2004).

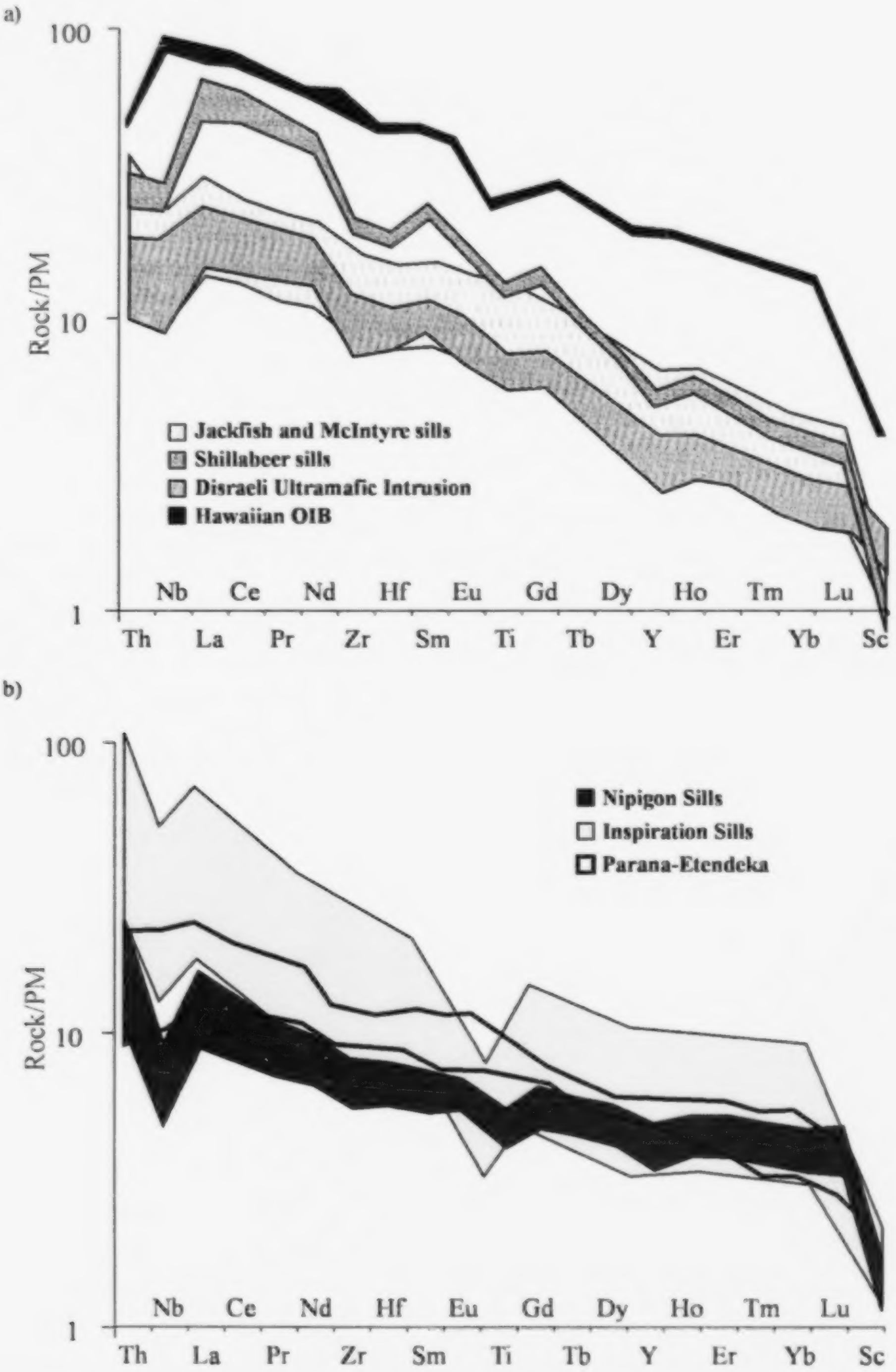

Figure 7. Primitive mantle-normalized plots of the sill suites identified in the Nipigon Embayment: a) Jackfish Island and McIntyre sills, Shillabeer sills, Disraeli intrusion and Hawaiian oceanic island basalt (OIB); and b) Nipigon sills, Inspiration sills and Parana–Etendeka continental flood basalts. Primitive mantle-normalizing values *from* Sun and McDonough (1989). Jackfish Island and Inspiration data *from* MacDonald (2004). Hawaiian OIB and Parana-Etendeka values *from* Gibson, Thompson and Dickin (2000).

represented by 6 drill core samples from DDH 3 (5 samples) and DDH 5 (1 sample). The Shillabeer suite is characterized by elevated TiO_2 (2.6 to 2.8 weight %), but comparable MgO (6.6 to 11.3 weight %) and Mg# (52 to 74) and displays the highest La/Yb_{cn} ratios (12.3 to 14.9) of the 3 suites (*see* Figures 6, 7 and 8; Appendix 3). The Shillabeer suite has a steep REE slope with La/Yb_{cn} ratios of 12 to 14 and negative Nb, Zr, Hf, Ti and Y anomalies (*see* Figure 7). When compared to data from other sill suites recognized within the Nipigon basin, it can be seen that the Inspiration sills are characterized by major element characteristics similar to the Nipigon suite (*see* Figure 6), but have higher $LaYb_{cn}$ ratios (*see* Figure 7), whereas the McIntyre and Shillabeer sills are characterized by elevated TiO_2 comparable to the Logan and Jackfish sills (*see* Figure 6).

Five diamond-drill holes were selected for detailed sampling and analysis along with a portion of the surface samples: drill holes DDH 3 (9 samples over 89 m), DDH 5 (4 samples over 84 m) and DDH 6 (5 samples over 268 m), ML01-01 (26 samples over 404 m) and ML01-03 (5 samples over 425 m). Locations of sampled drill holes are shown in Figure 5. In addition T.R. Hart (OGS) undertook additional analyses of samples from drill hole ML01-01.

Major element variation within DDH 3 is limited to TiO_2, K_2O and P_2O_5 concentrations and is divisible into 2 sills: an upper sill, which is part of the Shillabeer suite (5 samples; *see* Appendix 3), and a lower sill, which is part of the Nipigon suite (4 samples; *see* Appendix 1). Values for TiO_2, MgO, K_2O and P_2O_5 for the 2 suites are presented in Appendixes 1 and 3. Differences in Cr and Ni concentrations between the Shillabeer and Nipigon suites exist (upper: 30.6 to 427 ppm Cr, 47.0 to 219 ppm Ni; lower: 40.4 to 164 ppm Cr, 41.4 to 101 ppm Ni). Variations are also present in Rb, Sr, Cs, Ta, Nb, Zr, and Hf contents with values presented in Appendixes 1, 2 and 3. Primitive mantle-normalized REE values are also different for the Shillabeer and Nipigon suites (*see* Figure 7).

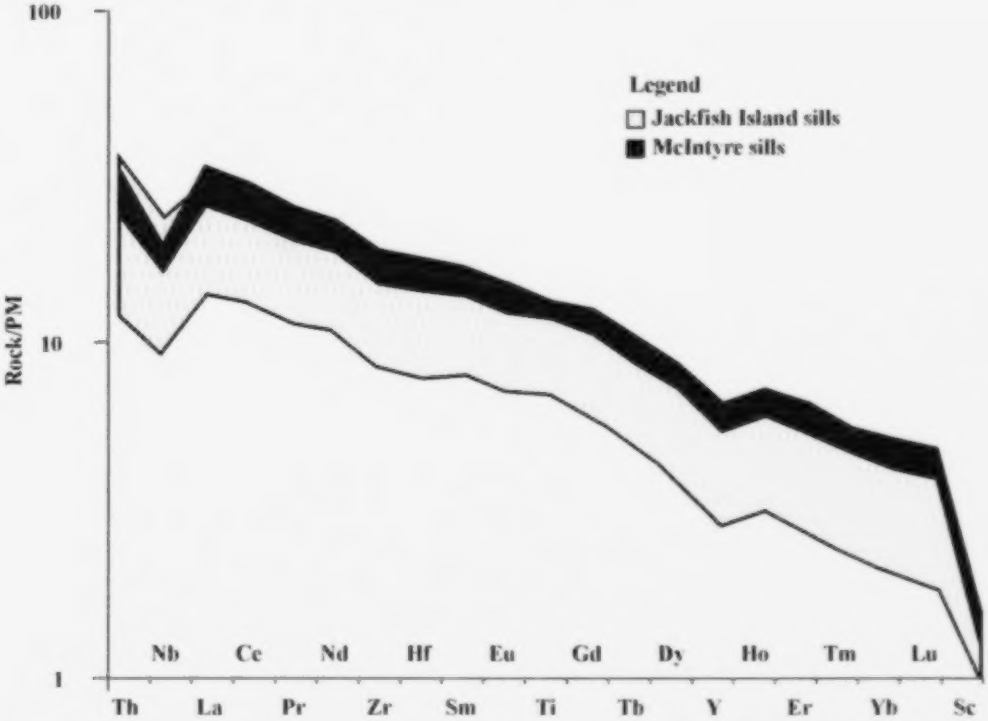

Figure 8. Primitive mantle-normalized plots of the Jackfish Island and McIntyre sills illustrating the similarities between the 2 units. Normalizing values *from* Sun and McDonough (1989). Jackfish Island sill data *from* MacDonald (2004).

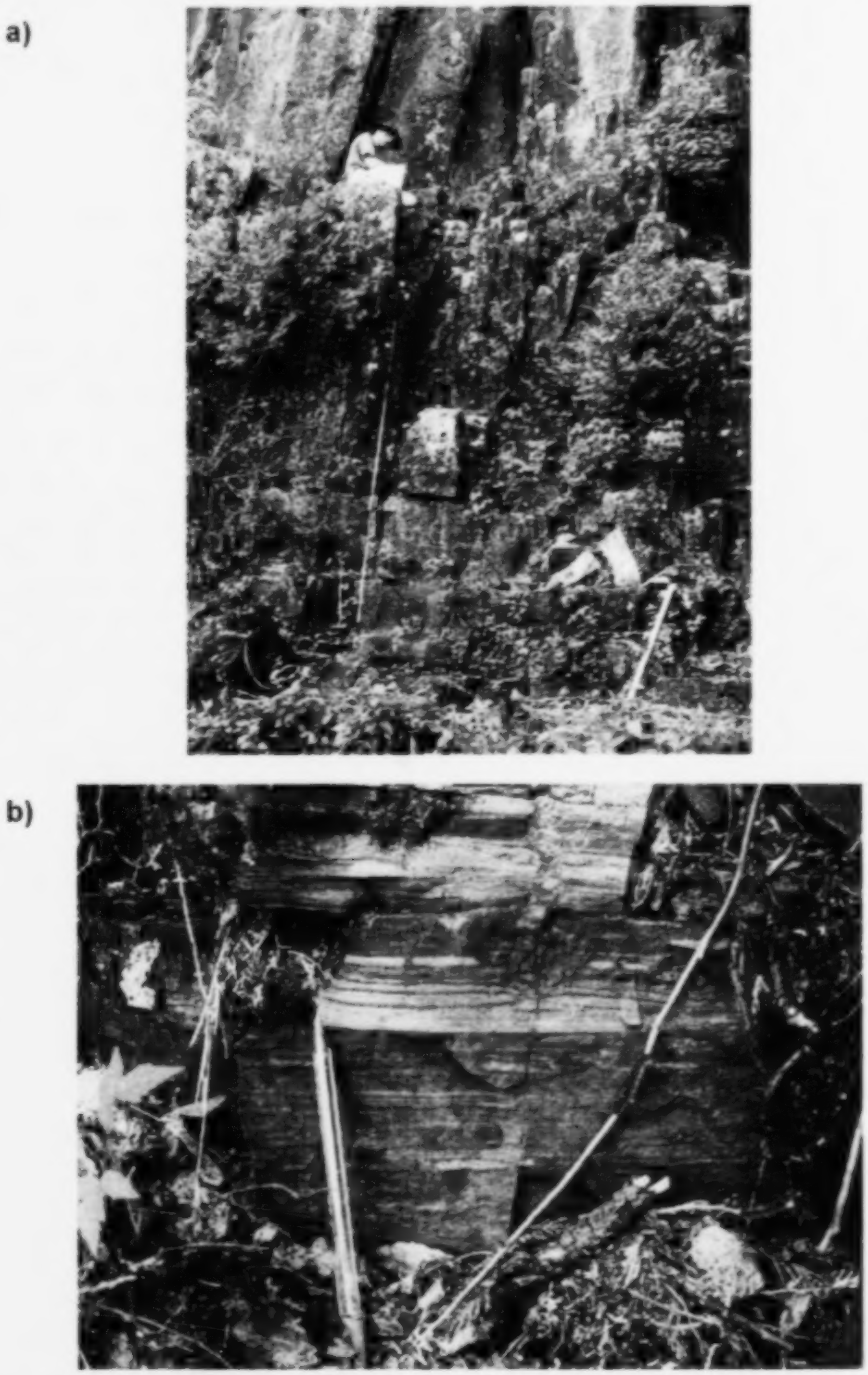

Photo 2. Diabase sill at Kama Hill showing lower contact with Kama Hill Formation (KH samples 1 through 10): a) diabase sill with lower contact; and b) close-up view of Kama Hill Formations metasedimentary rocks.

Similar to DDH 3, samples from DDH 5 can be separated into 2 suites: an upper suite (Shillabeer) represented by one sample at 54.5 m, and a lower suite (Nipigon) represented by the remainder. The upper suite sample from DDH 5 is geochemically similar to corresponding samples from DDH 3 with values shown in Appendix 3.

Analyzed samples from DDH 6 were taken at 62, 152, 200, 264 and 300 m. Geochemically, samples from DDH 6 fall within the characteristics of the Nipigon suite observed in DDH 3 and DDH 5 with variations of TiO_2 (0.98 weight % at 264 m) and K_2O (0.34 weight % at 264 m, *see* Appendix 1).

In addition to the five drill holes sampled, a detailed sample traverse was undertaken at the base of a thick diabase sill at Kama Hill (*see* Figure 1). Of the 10 samples collected, 3 were analyzed. No significant variations were observed between the 3 samples even though they were close to the basal contact between the sill and Kama Hill Formation metasediments (Photo 2).

Sill Emplacement Mechanisms and Regional Correlation

INTRODUCTION

One of the objectives of this study was to investigate the emplacement mechanisms of the up to 250 m thick diabase sills. Because of difficulties accessing cliff exposures, diamond-drill core was selected for the detailed study. A detailed petrographic investigation of DDH 6 (Figure 9) was undertaken in order to look for evidence of mineralogical (cryptic) layering or multiple magma injections so as to investigate emplacement mechanisms. Recognition of either of these features would provide insights into how these approximately 250 m thick sills formed: cryptic layering, which would indicate a single pulse of magma, or multiple pulses, which would suggest incremental growth. This drill hole (DDH 6) was selected as it is geochemically uniform and presents a large cross-sectional thickness of what is thought to be a single Nipigon suite sill in the Shillabeer Lake area (*see* Figure 5).

PETROGRAPHY

This work was undertaken after a preliminary visual and petrographic analysis of surface samples yielded no obvious trends or suggestive mineralogical correlations. A total of 28 thin sections were prepared and examined from DDH 6. Variation within examined samples of DDH 6 appears to be random with no consistent distribution of mineral species or alteration throughout the sill. The following section contains a detailed description of the drill hole.

- The interval 34 to 36 m is represented by 2 samples in which the plagioclase chadacrysts (60 modal %) occurring as randomly oriented laths approximately 0.5 mm along the long axis and nearly completely altered (Photo 3a) to sericite, epidote and zeolite minerals. Pyroxene (40 modal %) occurs as large 1 to 1.25 mm oikocrysts nearly completely altered to chlorite with small, fresh pyroxene crystals up to 0.25 mm in size. Textures remain preserved and can be described as subophitic (Photo 4).
- The sampled interval from 36 to 38 m is represented by 1 sample in which the plagioclase (60 modal %) shows only minor alteration (Photo 3b). Grain size is 0.25 to 0.5 mm with the laths randomly oriented. Pyroxenes (40 modal %) occur as large, moderate to highly altered oikocrysts and as small (<0.25 mm), fresh grains. Textures remain subophitic.

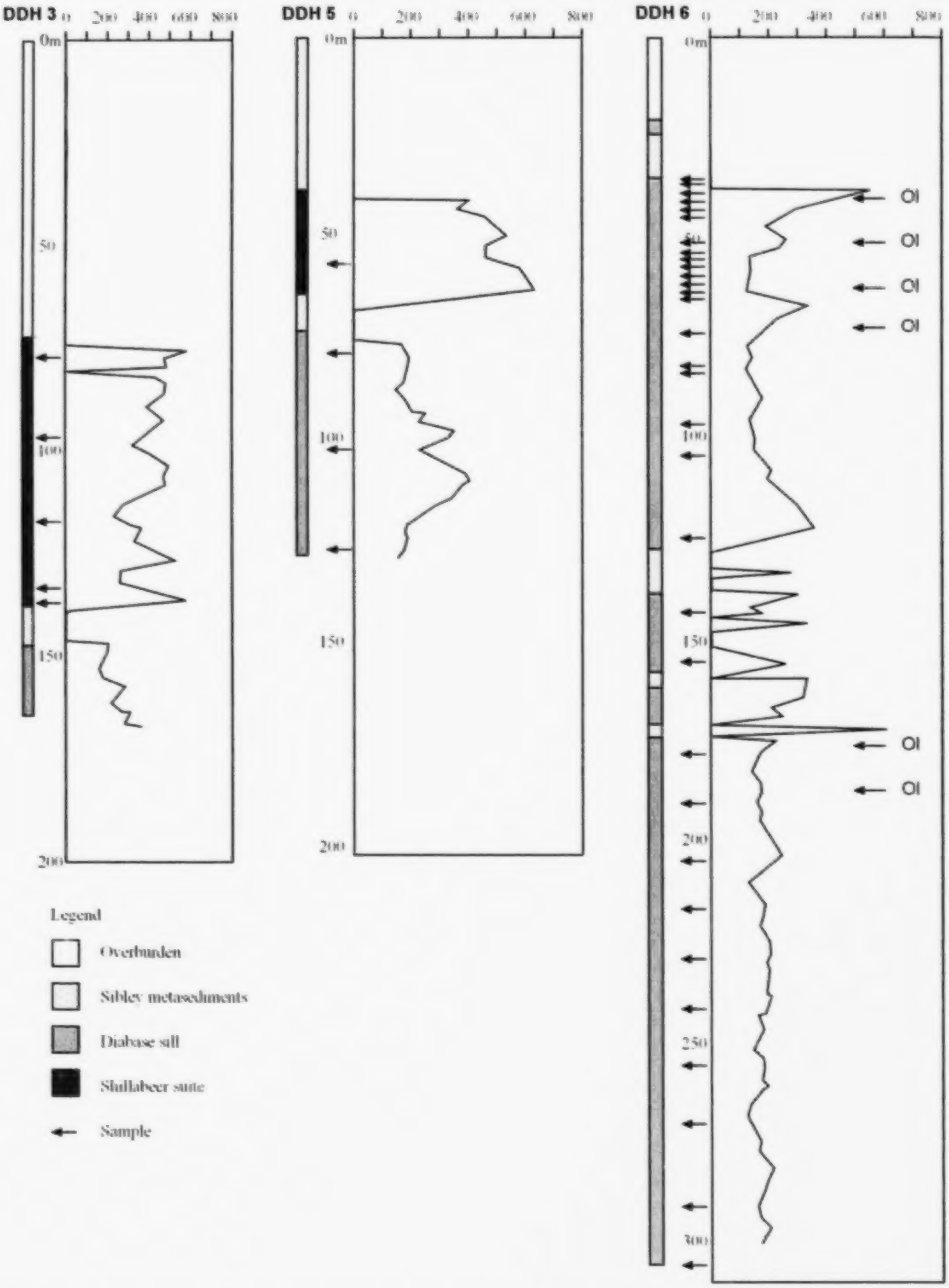

Figure 9. Summary logs of diamond-drill holes DDH 3, DDH 5 and DDH 6 showing sample locations within the drill holes and lithologies observed. Magnetic susceptibility measurements (10^{-5} standard SI) taken at 2 m intervals along the core are also shown.

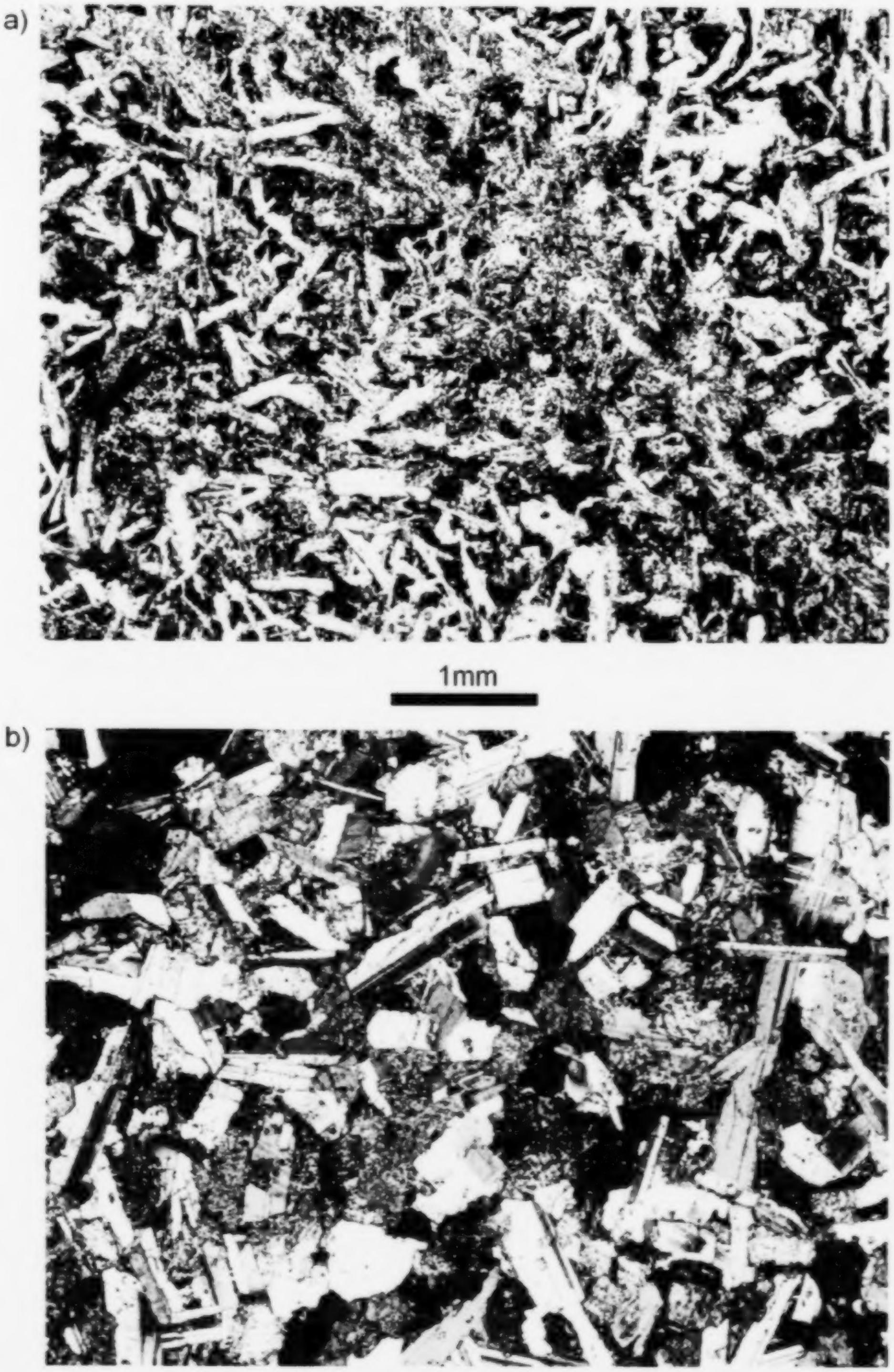

Photo 3. Photomicrograph of a) typical "complete" alteration; and b) typical "minor" alteration.

- The interval from 38 to 40 m is represented by 1 sample in which plagioclase occurs as 0.2 to 0.4 mm randomly oriented laths highly altered to epidote and sericite. Pyroxene occurs as 0.5 to 1.0 mm oikocrysts and has experienced only slight alteration. Textures remain subophitic.
- The interval at 42 m is represented by 1 sample. Plagioclase (50 modal %) occurs as up to 1 mm randomly oriented laths, with the degree of alteration varying from zero to moderate (Photo 5a). Zeolite and carbonate alteration sometimes occurs with one twin of a crystal being unaltered and the other twin being moderately altered. Pyroxene (30–40 modal %) oikocrysts have experienced weak to strong alteration. Fresh, unaltered olivine occurs (up to 1 modal %).
- The interval 42 to 50 m is represented by 1 sample at 43.6 m. Plagioclase (60 modal %) occurs as fresh to moderately carbonate-altered laths of random orientation. Pyroxenes (40 modal %) occur as oikocrysts with weak to strong alteration. The igneous texture is subophitic.
- The interval at 50 m is distinguished by an increase in grain size. Plagioclase (60 modal %) occurs as randomly oriented unaltered laths up to 1.5 mm along the long axis. Pyroxene (40 modal %) is typically suboikocrystic to intergranular with weak to moderate chlorite alteration.
- The interval 52 to 56 m is represented by 3 samples at 52, 54 and 56 m. Grain size decreases to 0.25 to 0.5 mm randomly oriented plagioclase laths (60 modal %). Pyroxene is slightly to highly altered (chlorite) forming large ($\leq$1 mm) suboikolitic phenocrysts. An intergranular texture is dominant. Trace biotite was also observed.
- The interval 68 to 78 m is represented by 1 sample at 72 m. Plagioclase (60 modal %) occurs as 0.5 mm randomly oriented laths with zero to minor alteration (Photo 5b). Pyroxenes (40 modal %) occur as large ($\leq$1 mm) oikocrysts with minor to moderate chlorite alteration. Olivine ($\leq$1 modal %) occurs as small, unaltered phenocrysts.

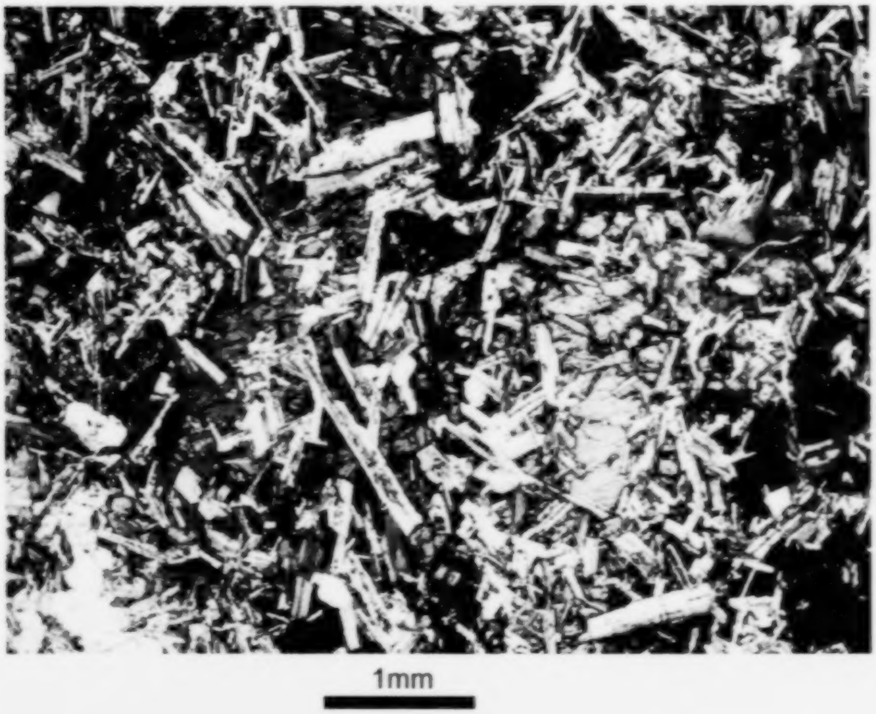

Photo 4. Photomicrograph of typical ophitic textured diabase found in the Nipigon Embayment.

- The interval 74 to 80 m is represented by 2 samples at 80 and 82 m. Plagioclase (60 modal %) occurs as 0.25 to 1 mm randomly oriented laths with little to no alteration. Pyroxene (40 modal %) occurs as large (≤5 mm) oikocrysts exhibiting zero to moderate alteration.
- The interval 82 to 94 m is represented by 1 sample. Plagioclase (60 modal %) occurs as fresh to weakly sericite-altered randomly oriented laths up to 1 mm along the long axis. Pyroxene (≤40 modal %) occurs as fresh to weakly chlorite altered oikocrysts up to 5 mm. The igneous texture is subophitic.
- The interval 94 to 102 m is represented by 1 sample. Plagioclase (50 modal %) occurs as fresh to weakly sericitized randomly oriented laths up to 1.5 mm. Pyroxene occurs as fresh to moderately chlorite-altered oikocrysts up to 4 mm. Minor (<1 modal %) hornblende was observed as small equant grains 0.5 to 1.0 mm. Textures are subophitic.
- The interval 102 to 122 m is represented by 1 sample. Plagioclase occurs as moderate to highly sericite-altered 0.5 to 1.0 mm randomly oriented laths with some grains exhibiting near complete replacement by alteration minerals. Pyroxene occurs as highly chlorite-altered, some relict, grains up to 3 mm. Trace weakly chlorite-altered olivine was observed as well as minor (<1 modal %) hornblende.
- The interval 124 to 140 m is Sibley Group metasediments and was not sampled.
- The interval 140 to 151.6 m is represented by 1 sample. Plagioclase occurs as fresh (rare) to totally altered zeolite and sericite-altered laths (or relict plagioclase laths). Pyroxene is moderately to totally chlorite and carbonate altered with some relict grains. The sample is pervasively altered by chlorite, carbonate and zeolite minerals.
- The interval 151.6 to 174 m is represented by 1 sample at 151.6 m. Plagioclase occurs as fresh to weakly sericitized randomly oriented laths 1.0 to 1.5 mm. Pyroxene occurs as weak to moderately chlorite-altered oikocrysts up to 4 mm. Trace fresh and weakly iddingsite-altered olivine was observed.
- The following sample was from 174 m. Plagioclase (60 modal %) occurs as randomly oriented weakly to moderately sericitized laths up to 0.5 mm along the long axis. Pyroxenes (30–40 modal %) occur as 0.25 to 0.5 mm equant grains with weak to moderate alteration (chlorite). Olivine (≤1 modal %) occurs as small <0.25 mm grains with weak alteration. Overall alteration masks the intergranular to subophitic igneous texture.
- The interval from 174 to 186 m is represented by 1 sample. Plagioclase (50 modal %) occurs as large randomly oriented laths (up to 2 mm) exhibiting zero to slight sericite alteration. Pyroxene (~50 modal %) occurs as large (≤3 mm) phenocrysts, which are generally unaltered to weakly chlorite altered. Up to 1 modal % anhedral unaltered olivine was observed. The overall igneous texture can be described as subophitic.
- The interval from 186 to 212 m is nearly identical to the preceding interval, but did not contain olivine.
- The interval 212 to 236 m is represented by 2 samples at 224 and 236 m. Plagioclase (50 modal %) is unaltered to slightly sericite-altered laths up to 1.5 mm along the long axis. Pyroxene (50 modal %) phenocrysts are equant, slightly chlorite altered. Overall igneous texture is intergranular to subophitic.
- The interval 236 to 250 m is represented by 1 sample at 250 m. Plagioclase (60 modal %) occurs as 1 to 1.25 mm randomly oriented laths with minor sericite alteration. Equant oikocrysts of pyroxene (40 modal %) are generally fresh to minor chlorite altered and are dominantly 1 to 1.5 mm across. Plagioclase laths form local aggregates (glomeroporphyritic) with the overall igneous texture described as subophitic.

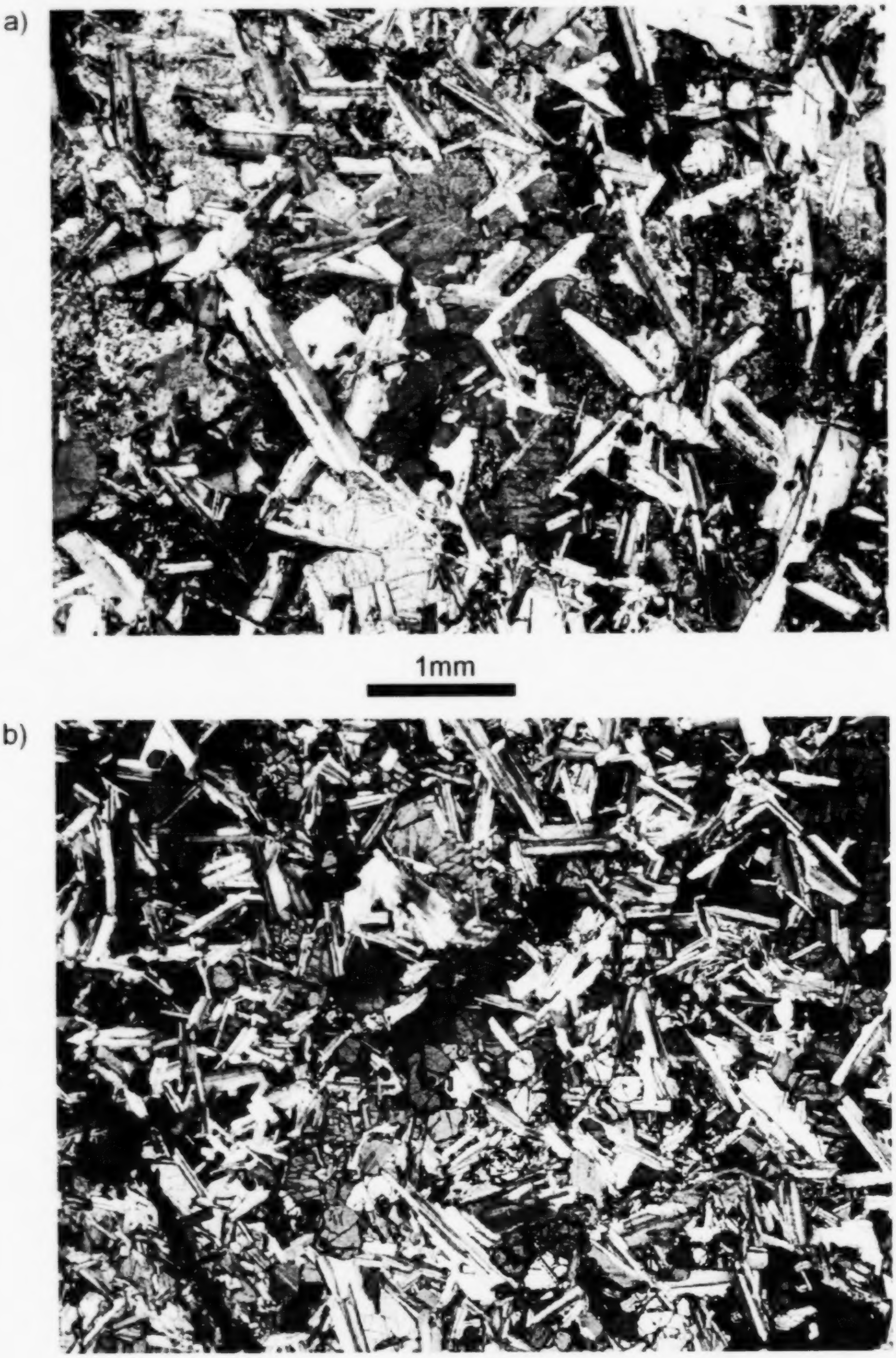

Photo 5. Photomicrograph of a) typical "moderate" alteration, and b) typical unaltered diabase.

- The interval 250 to 264 m is represented by 1 sample at 264 m. Plagioclase occurs as large (1–3 mm) randomly oriented laths of trace to zero alteration. Pyroxene occurs as large (≤5 mm) equant oikocrysts of zero to trace alteration (chlorite). The overall igneous texture is subophitic to ophitic.
- The interval 264 to 284 m is represented by 1 sample at 284 m. Plagioclase (60 modal %) are weak to moderately sericite-altered laths up to 1 mm along the long axis. Pyroxene (40 modal %) are small (<1 mm) equant grains with weak to strong chlorite alteration.
- The interval 284 to 300 m is represented by 1 sample at 300 m. The sample is moderately altered with relict pyroxene identifiable (possibly up to 3 mm equant grains).

Summary of Optical Petrology

The mineralogy of these rocks are dominantly bimodal with plagioclase forming 0.25 to 1.5 mm chadacrysts and larger, up to 5 mm, pyroxene as oikocrysts. Alteration is generally weak to moderate with alteration minerals predominantly sericite, epidote and chlorite. Alteration does not appear to be associated with proximity to Sibley Group metasediments within the hole. Olivine is rare and never accounts for more than 1 modal % of a sample. Common to nearly all samples is the occurrence of up to 1 modal % opaque minerals. Samples containing olivine also generally contain small, secondary, unaltered pyroxenes, which were not commonly found in samples with no olivine.

Initial petrographic study of samples from the Nipigon suite available from the Shillabeer Lake area drill holes suggest the sills are mineralogically homogeneous with minor variations in modal percentages of plagioclase and pyroxene.

MINERAL CHEMISTRY

The mineral chemistry of 4 samples from DDH 6 were analyzed by SEM. The principal minerals pyroxene and plagioclase were analyzed along with olivine, when it was found. Oxide minerals found in analyzed samples are magnetite and ilmenite. Compositionally, plagioclase was found to range from oligoclase to anorthite though the majority of samples (55 of 72 analyzed grains) were bytownite (39) to labradorite (16). Olivine was not observed. Pyroxene compositions ranged from 23 to 47 weight % En, 16 to 54 weight % Wo and 2.6 to 44 weight % Fs.

Five surface samples from the Nipigon suite were also analyzed by SEM–EDS for their mineral chemistry. Olivine compositions range from Fo_{48} to Fo_{63}. Pyroxene compositions range from $En_{3.73}$ to $En_{61.0}$, $Fs_{2.64}$ to Fs_{94} and $Wo_{2.21}$ to $Wo_{58.0}$. Plagioclase compositions range from bytownite (18 grains), labradorite (8 grains) to albite (1 grain). While this preliminary study does not reveal obvious trends, additional work is planned to investigate this in more detail.

MAGNETIC SUSCEPTIBILITY

Magnetic susceptibility data were gathered while relogging the drill holes and were measured using a portable magnetic susceptibility meter. Magnetic susceptibility is a useful tool for measuring the volume of magnetic minerals present in a sample. This was undertaken to determine if a correlation between magnetic mineral content and silicate minerals could be made. Readings were taken at 2 m intervals and are summarized in graphical form in Figure 9. A weak correlation between the presence of olivine in the sample and a high magnetic susceptibility value can be observed. However, not all high values correlate with olivine content.

Isotope Geochemistry

A representative selection of samples were analyzed for rubidium, strontium, neodymium, samarium and lead isotopes with the goal of understanding the processes, mantle sources and potential contaminants, both within the crust and the mantle, which have affected the diabase sills of the Nipigon Embayment during and prior to emplacement. The 3 sills identified by major, trace and rare earth element geochemistry are the Nipigon, McIntyre and Shillabeer suites. Sutcliffe (1986) identified the ultramafic Jackfish Island suite. MacDonald, Tremblay and Easton (2005) identified an additional 2 suites in the western Lake Nipigon basin. Termed the Inspiration, and Jackfish-like suites, they possess unique geochemical characteristics not observed in the rest of the basin. The Jackfish-like suite is now recognized to be analogous to the McIntyre suite of this study and that terminology will be used for the remainder of this report (*see* Table 1). Also identified by MacDonald, Tremblay and Easton (2005) was a fourth suite, which is geochemically consistent with the Nipigon suite and is interpreted to be a continuation of this suite. Samples from the suites recognized by MacDonald, Tremblay and Easton (2005) were also analyzed for the above listed isotopes as part of this study (Figure 10). In addition, volcanic rocks from the Pillar Lake area —"Pillar Lake volcanics"—, which predate the Midcontinent Rift event, were also analyzed. Geochemical variations characterizing the western Lake Nipigon suites are presented in Figures 6, 7 and 8.

A range of isotope values for the 5 sill suites is summarized in Table 2 with the full data set given in Appendix 4. Nipigon suite samples form 2 distinct trends when $^{87}Sr/^{86}Sr$ is plotted against ε_{Nd}, as shown in Figure 10. The first is a steeply dipping curve where as ε_{Nd} becomes increasingly negative as $^{87}Sr/^{86}Sr$ value increases slightly. The second trend is a nearly horizontal trend as $^{87}Sr/^{86}Sr$ value increases. The first, nearly vertical, trend is exhibited also by the Jackfish Island and McIntyre suites. The Inspiration suite does not show a pronounced trend, but simply plots as a group (Figure 10). The Pillar Lake volcanics generally behave similarly to the Inspiration sills, which trend towards Sibley Group, as shown in Figure 10b.

On a plot of La/Yb$_{cn}$ versus ε_{Nd}, the Nipigon suite develops a weak trend toward increased La/Yb$_{cn}$ with a corresponding decrease in ε_{Nd} (Figure 11b). The Jackfish Island and McIntyre suites do not appear to have the same trend with La/Yb$_{cn}$ remaining nearly constant with a decrease in ε_{Nd} (Figure 11b). The Pillar Lake volcanics exhibit a weak positive correlation between crustal contamination and MgO value (Figure 11a). In Figures 11b and 12, the Pillar Lake samples plot as a horizontal trend toward increased LREE slope and higher K_2O content, respectively, without a corresponding increase in ε_{Nd}.

The 5 suites of rocks form a linear trend on a plot of $^{206}Pb/^{204}Pb$ versus $^{207}Pb/^{204}Pb$ (Figure 13a). The Shillabeer suite does not plot on the trend. A plot of $^{207}Pb/^{204}Pb$ versus $^{208}Pb/^{204}Pb$ (Figure 14) generates more scatter than is seen on plots of either $^{206}Pb/^{204}Pb$ versus $^{207}Pb/^{204}Pb$ or $^{206}Pb/^{204}Pb$ versus $^{208}Pb/^{204}Pb$ (Figures 13a or 13b, respectively) with the Jackfish Island and McIntyre suites developing a trend separate from the Nipigon and Inspiration suites. The Pillar Lake volcanics do not fall on either trend, but has higher $^{208}Pb/^{204}Pb$ values than the other suites. In Figure 14, all suites plotted except the Pillar Lake volcanics form a linear trend.

Table 2. Geochemical data for samples from mafic and ultramafic units in the Nipigon Embayment

				Lead Isotope Data and Derived Ratios													
Sample	**Suite**	**Easting (m. NAD27)**	**Northing (m. NAD27)**	**^{206}Pb/^{204}Pb**	**^{207}Pb/^{204}Pb**	**^{208}Pb/^{204}Pb**	**Model Age Ga[1]**	**^{238}U/^{204}Pb**	**^{232}Th/^{204}Pb**	**^{232}Th/^{238}Pb**	**^{87}Rb/^{86}Sr**	**^{87}Sr/^{86}Sr corrected**	**Initial ^{87}Sr/^{86}Sr**	**^{147}Sm/^{144}Nd**	**^{143}Nd/^{144}Nd**	**εNd**
03CAM033	**Inspiration**	353054	5551498	19.367	15.915	39.707	0.1075	10.8309	43.3479	3.8734	0.2827	0.7104	0.7060	0.1269	0.5118	-6.5937
03CAM128	**Inspiration**	349169	5564683	18.989	15.890	39.376	0.3189	10.8153	44.0380	3.9407	0.2837	0.7102	0.7057	0.1267	0.5118	-6.1971
03CAM265	**Inspiration**	360424	5545318	19.084	15.777	39.342	0.0331	10.2989	40.7129	3.8259	0.2099	0.7092	0.7059	0.1279	0.5118	-6.0936
03CAM300	**Inspiration**	355953	5559674	18.895	15.885	39.324	0.3729	10.8178	44.4062	3.9728	0.3308	0.7106	0.7054	0.1255	0.5118	-6.3606
03CAM122	**Jackfish Island**	370235	5534964	17.660	15.424	38.638	0.3719	9.0909	40.6314	4.3256	0.1166	0.7060	0.7042	0.1482	0.5122	-0.8067
03CAM227	**Jackfish Island**	367504.34	5533118.88	17.937	15.497	38.487	0.3081	9.3413	39.1181	4.0528	0.1030	0.7056	0.7040	0.1506	0.5123	-1.0608
03CAM228	**Jackfish Island**	367504.34	5533118.88	20.067	15.970	39.128	-0.2629	10.9356	36.9421	3.2694	0.0951	0.7057	0.7042	0.1506	0.5123	-0.5473
ADH3-33	**Nipigon**	376299	5446449	19.935	15.818	39.481	-0.5007	10.3331	36.6138	3.4293	0.4539	0.7137	0.7065	0.1623	0.5123	-2.4010
ADH5-17	**Nipigon**	373679	5444646	21.220	15.887	40.721	-1.3141	10.4906	35.9742	3.3188	0.6703	0.7174	0.7068	0.1591	0.5122	-2.2848
ADH6-13	**Nipigon**	376663	5437496	19.368	15.929	37.531	0.1341	10.8922	32.4399	2.8824	0.3401	0.7114	0.7060	0.1754	0.5123	-2.6868
ADH6-98	**Nipigon**	376663	5437496	19.134	15.760	38.913	-0.0393	10.2148	37.8779	3.5888	0.1397	0.7069	0.7047	0.1725	0.5124	-1.1458
AML-01-44	**Nipigon**	359505	5458026	19.575	15.790	39.173	-0.2983	10.2659	36.8538	3.4744	0.2458	0.7083	0.7045	0.1722	0.5124	-1.0923
AML03-08	**Nipigon**	361090	5458097	19.354	15.785	39.048	-0.1471	10.2804	37.5635	3.5363	0.2208	0.7086	0.7051	0.1670	0.5123	-2.4874
AML03-56	**Nipigon**	361090	5458097	18.905	15.718	38.674	0.0387	10.0790	37.4142	3.5926	0.0964	0.7059	0.7043	0.1708	0.5124	-0.7600
LN - 120	**Nipigon**	394781	5503064	19.515	15.763	39.173	-0.3138	10.1644	36.7240	3.4967	0.2633	0.7082	0.7040	0.1715	0.5124	-1.0184
LN - 129	**Nipigon**	406356	5491671	19.046	15.729	38.808	-0.0408	10.0995	37.3500	3.5791	0.1471	0.7066	0.7043	0.1797	0.5125	-0.9273
LN - 76	**Nipigon**	398211	5468311	19.989	15.889	39.581	-0.3799	10.6144	38.0451	3.4689	0.2720	0.7083	0.7041	0.1684	0.5124	-1.4667
LN 70	**Nipigon**	355536	5493869	20.306	15.855	40.067	-0.6917	10.4377	37.6823	3.4940	0.2571	0.7091	0.7051	0.1721	0.5124	-1.0746
LN 203	**Nipigon**	415974	5541109	20.945	15.923	40.598	-1.0049	10.6486	37.5643	3.4141	0.1644	0.7081	0.7056	0.1687	0.5124	-1.2199
LN 221	**Nipigon**	392832	5563478	20.062	15.814	39.779	-0.6051	10.3017	37.1095	3.4863	0.3519	0.7104	0.7049	0.1570	0.5123	-1.2877
LN 229	**Nipigon**	409197	5559243	20.275	15.812	39.577	-0.7733	10.2699	35.0094	3.2992	0.1483	0.7068	0.7045	0.1577	0.5123	-1.0104
LN 231	**Nipigon**	409778	5536087	20.117	15.835	39.845	-0.5962	10.3806	37.4656	3.4930	0.2420	0.7093	0.7055	0.1597	0.5122	-2.6078
LN 233	**Nipigon**	415032	5529128	20.017	15.910	39.832	-0.3543	10.6961	39.4114	3.5660	0.3983	0.7106	0.7043	0.1454	0.5119	-6.4198
LN 239	**Nipigon**	416391	5572872	18.684	15.738	38.376	0.2420	10.2190	37.8429	3.5840	0.1035	0.7062	0.7046	0.1767	0.5124	-1.6190
LN 259	**Nipigon**	419054	5516774	19.482	15.787	39.172	-0.2366	10.2675	37.3700	3.5225	0.3380	0.7105	0.7052	0.1625	0.5123	-2.3506
LN 301	**Nipigon**	391576	5533653	18.140	15.578	38.214	0.3208	9.6487	37.7741	3.7889	0.2186	0.7086	0.7052	0.1581	0.5122	-2.7681
LN 306	**Nipigon**	395021	5551701	20.848	15.985	40.522	-0.7813	10.9018	38.9118	3.4544	0.3990	0.7122	0.7059	0.1407	0.5119	-6.2913
LN 311	**Nipigon**	402264	5536935	18.989	15.751	38.703	0.0484	10.2074	37.6485	3.5696	0.1787	0.7077	0.7049	0.1613	0.5123	-2.4792
LN 313	**Nipigon**	400038	5518293	19.727	15.783	39.535	-0.4258	10.2177	37.4565	3.5478	0.2590	0.7082	0.7042	0.1593	0.5123	-1.0169
LN - 101	**McIntyre**	375141	5490615	24.388	16.125	43.124	-3.2644	11.2876	33.9810	2.9136	0.1087	0.7067	0.7050	0.1453	0.5121	-3.2060
LN - 45	**McIntyre**	374584	5500167	24.410	16.126	42.203	-3.2843	11.2887	31.2752	2.6813	0.1515	0.7075	0.7051	0.1455	0.5121	-3.1277
LN 161	**McIntyre**	360677	5517422	18.428	15.530	39.318	-0.0074	9.3710	40.1908	4.1508	0.1108	0.7063	0.7045	0.1461	0.5121	-2.5474
LN 167	**McIntyre**	352634	5519762	17.824	15.536	38.589	0.4755	9.5482	41.5550	4.2120	0.1319	0.7066	0.7045	0.1459	0.5122	-2.2694
LN 170	**McIntyre**	347622	5513969	17.748	15.553	38.628	0.5663	9.6513	42.8933	4.3012	0.1134	0.7064	0.7046	0.1455	0.5121	-2.5789
03CAM030	**Pillar Lake Volcanics**	350660	5566356	25.337	16.334	51.441	-3.3228	12.0414	57.3395	4.6086	0.0948	0.7102	0.7087	0.1377	0.5119	-6.7971
03CAM044	**Pillar Lake Volcanics**	346629	5563694	26.536	16.367	49.715	-4.3530	12.1494	46.8412	3.7313	0.2886	0.7105	0.7060	0.1396	0.5119	-7.1621
03CAM123	**Pillar Lake Volcanics**	346320	5563473	30.938	16.830	52.994	-6.8925	13.8172	44.4323	3.1122	0.3201	0.7112	0.7062	0.1175	0.5117	-6.8799
03CAM126	**Pillar Lake Volcanics**	349169	5564683	21.862	15.975	50.732	-1.5766	10.7941	70.6808	6.3373	0.1603	0.7121	0.7096	0.1359	0.5118	-7.6766
03CAM142	**Pillar Lake Volcanics**	345918	5562546	25.800	16.365	51.100	-3.6282	12.1487	54.4081	4.3343	0.1175	0.7088	0.7069	0.1168	0.5117	-6.6935
ADH3-28	**Shillabeer**	376299	5446449	21.280	15.727	42.022	-1.8529	9.8797	37.4106	3.6647	0.0287	0.7039	0.7035	0.1248	0.5118	-5.5895
ADH5-2	**Shillabeer**	373679	5444646	21.267	15.636	40.971	-2.1601	9.5421	32.2281	3.2687	0.1043	0.7048	0.7032	0.1269	0.5119	-5.5232

[1] Stacy and Kramers (1975)

Table 2. continued

		Major Elements (weight %)										Trace Elements (ppm)									
Sample	Suite	SiO_2	TiO_2	Al_2O_3	Fe_2O_3	MnO	MgO	CaO	K_2O	Na_2O	P_2O_5	Cr	Ni	Rb	Sr	Cs	Sc	V	Ta	Nb	Zr
03CAM033	**Inspiration**	51.66	1.05	14.86	11.67	0.19	6.30	10.28	1.07	2.79	0.14	150	68	26	255	0			1	15	131
03CAM128	**Inspiration**	51.53	1.08	15.75	11.57	0.19	5.99	9.83	1.08	2.85	0.14	126	66	28	268	1			1	17	137
03CAM265	**Inspiration**	51.10	1.53	14.82	12.44	0.19	6.19	10.01	0.62	2.94	0.15	136	67	21	284	1			1	14	117
03CAM300	**Inspiration**	51.68	1.16	15.18	11.98	0.18	5.85	9.80	1.13	2.86	0.16	72	33	32	278	1			1	17	145
03CAM122	**Jackfish Island**	41.68	1.62	6.52	19.41	0.22	22.69	5.73	0.40	1.57	0.15	1508	1308	10	223	0			0	7	97
03CAM227	**Jackfish Island**	43.12	1.38	6.06	18.81	0.22	22.71	5.94	0.35	1.30	0.13	1379	1271	8	200	0			0	6	84
03CAM228	**Jackfish Island**	43.17	1.45	6.48	18.80	0.22	22.01	5.97	0.36	1.41	0.15	1316	1257	8	205	0			0	6	83
ADH3-33	**Nipigon**	49.24	1.52	14.50	14.84	0.21	6.29	9.15	1.28	2.81	0.16	151	102	32	200	1	29	314	0	7	127
ADH5-17	**Nipigon**	52.61	2.17	11.70	19.44	0.25	2.33	5.74	1.53	3.84	0.38	0	11	36	148	1	26	56	1	15	292
ADH6-13	**Nipigon**	49.76	1.38	13.71	13.64	0.19	6.68	11.36	0.71	2.46	0.10	323	62	90	182	0	46	423	1	7	88
ADH6-98	**Nipigon**	50.10	1.00	16.10	12.60	0.18	6.28	10.69	0.35	2.57	0.14	206	59	119	164	1	39	237	1	7	93
AML-01-44	**Nipigon**	49.55	1.39	13.60	16.19	0.26	5.79	10.20	0.47	2.42	0.15	103	63	13	140	0	35	285	0	6	112
AML03-08	**Nipigon**	50.87	1.40	14.02	14.32	0.21	5.71	10.06	0.56	2.73	0.13	129	59	51	167	0	43	359	1	8	99
AML03-56	**Nipigon**	49.31	0.95	16.47	12.96	0.19	6.55	10.62	0.35	2.51	0.08	203	69	123	188	0	34	311	1	4	49
LN - 120	**Nipigon**	49.34	1.84	13.63	16.68	0.24	4.93	10.01	0.50	2.66	0.18	51	50	13	145	0	36	320	0	7	127
LN - 129	**Nipigon**	49.96	1.05	13.55	12.86	0.22	7.66	12.13	0.27	2.20	0.10	322	82	7	129	0	40	320	0	3	67
LN - 76	**Nipigon**	49.54	1.61	13.75	15.74	0.24	5.49	10.43	0.51	2.56	0.14	67	53	15	154	1	35	320	0	7	110
LN 70	**Nipigon**	48.81	1.48	14.39	15.61	0.22	6.28	9.91	0.49	2.67	0.15	0	0	15	160	1	41	371	0	6	106
LN 203	**Nipigon**	47.90	1.54	14.93	15.49	0.18	6.63	9.65	0.58	2.95	0.15	106	142	11	209	1	39	334	0	6	123
LN 221	**Nipigon**	50.78	1.60	15.85	14.25	0.20	3.94	9.49	0.65	3.04	0.21	67	44	18	177	1	38	232	0	7	142
LN 229	**Nipigon**	49.33	0.97	18.99	10.97	0.15	5.30	10.67	0.41	3.04	0.17	125	101	10	190	0	29	185	0	4	89
LN 231	**Nipigon**	48.26	1.16	14.64	14.72	0.19	7.75	10.24	0.46	2.50	0.08	140	153	11	180	0	43	271	0	4	76
LN 233	**Nipigon**	50.27	1.31	15.23	13.87	0.20	5.68	9.60	0.87	2.81	0.16	102	105	22	212	1	41	264	0	8	114
LN 239	**Nipigon**	48.24	0.78	17.20	11.56	0.16	7.77	11.31	0.30	2.54	0.13	230	153	9	180	1	32	184	0	3	60
LN 259	**Nipigon**	52.18	0.94	14.89	13.25	0.20	5.18	9.36	0.87	2.93	0.20	59	56	23	176	1	42	168	0	7	130
LN 301	**Nipigon**	51.22	1.05	18.10	11.31	0.17	3.95	10.27	0.56	3.19	0.19		41	17	206	1	28	216	0	6	135
LN 306	**Nipigon**	50.75	1.44	14.41	13.63	0.19	6.18	9.87	0.87	2.45	0.20		93	23	185	1	35		1	8	118
LN 311	**Nipigon**	48.57	0.89	14.72	12.93	0.20	8.94	11.26	0.32	2.10	0.06		181	8	149	0	36	270	0	3	55
LN 313	**Nipigon**	49.67	1.48	15.82	13.95	0.20	4.89	10.67	0.45	2.72	0.16		57	12	156	0	37		0	6	112
LN - 101	**McIntyre**	49.77	3.10	13.62	14.90	0.13	5.08	8.50	0.61	4.01	0.28	59	83	16	419	0	21	313	1	14	219
LN - 45	**McIntyre**	49.52	3.12	13.63	15.01	0.16	4.75	8.94	0.68	3.91	0.28	59	73	21	390	0	21	293	1	14	220
LN 161	**McIntyre**	48.14	2.73	13.02	16.93	0.17	6.50	8.51	0.64	3.14	0.22			18	433	1	21	284	1	12	179
LN 167	**McIntyre**	48.91	3.03	12.98	15.96	0.16	5.19	9.25	0.76	3.51	0.25			21	438	1	26	362	1	15	215
LN 170	**McIntyre**	49.24	2.98	13.86	15.26	0.17	5.21	8.75	0.64	3.64	0.24			17	434	1	26	362	1	14	216
03CAM030	**Pillar Lake Volcanics**	53.80	1.24	15.39	6.62	0.12	6.12	9.62	0.42	5.37	0.12	104	42	9	261	0			1	18	158
03CAM044	**Pillar Lake Volcanics**	52.01	1.18	14.60	9.52	0.07	7.82	7.80	2.94	2.27	0.15	113	51	30	289	0			1	17	144
03CAM123	**Pillar Lake Volcanics**	52.73	1.18	14.86	7.89	0.08	8.24	8.35	3.03	2.30	0.16	124	56	31	275	0			1	18	148
03CAM126	**Pillar Lake Volcanics**	52.17	1.20	14.14	4.72	0.05	10.47	8.78	1.00	4.61	N D	127	43	13	229	0			1	24	150
03CAM142	**Pillar Lake Volcanics**	52.93	1.27	15.31	6.29	0.08	6.74	9.21	1.13	4.16	0.36	120	38	12	288	0			1	16	159
ADH3-28	**Shillabeer**	50.26	2.68	11.44	13.11	0.16	9.19	7.54	0.33	4.98	0.31	407	106	5	458	0	25	273	1	17	217
ADH5-2	**Shillabeer**	49.35	2.76	11.60	14.09	0.28	9.68	6.89	1.18	3.80	0.36	520	159	20	552	0	25	290	1	18	230

Table 2. continued

		Trace Elements (ppm)																	
Sample	**Suite**	**Hf**	**Th**	**U**	**Y**	**La**	**Ce**	**Pr**	**Nd**	**Sm**	**Eu**	**Gd**	**Tb**	**Dy**	**Ho**	**Er**	**Tm**	**Yb**	**Lu**
03CAM033	**Inspiration**	3.219	3.822	0.945	22.129	21.928	43.786	5.177	20.459	4.225	1.296	4.412	0.694	4.117	0.847	2.424	0.345	2.213	0.334
03CAM128	**Inspiration**	3.416	4.009	0.983	21.100	22.979	46.069	5.481	21.512	4.361	1.315	4.347	0.678	4.146	0.852	2.427	0.351	2.231	0.334
03CAM265	**Inspiration**	2.915	3.368	0.862	23.122	19.764	39.790	4.711	18.709	3.901	1.237	3.889	0.625	3.770	0.757	2.200	0.313	2.011	0.301
03CAM300	**Inspiration**	3.511	4.404	1.086	26.585	24.468	48.976	5.817	22.923	4.655	1.411	4.599	0.730	4.404	0.912	2.636	0.367	2.347	0.351
03CAM122	**Jackfish Island**	2.626	1.121	0.272	13.757	10.404	24.454	3.321	15.212	3.606	1.200	3.561	0.538	2.959	0.550	1.418	0.188	1.121	0.155
03CAM227	**Jackfish Island**	2.193	0.927	0.229	14.952	8.483	20.455	2.792	12.749	3.120	1.059	3.205	0.477	2.605	0.480	1.227	0.161	0.977	0.134
03CAM228	**Jackfish Island**	2.193	0.947	0.227	16.942	8.700	21.038	2.913	13.474	3.249	1.088	3.321	0.488	2.688	0.496	1.276	0.165	0.987	0.140
ADH3-33	**Nipigon**	3.330	2.381	0.706	30.010	12.714	28.335	3.749	16.629	4.450	1.404	5.248	0.884	5.494	1.141	3.312	0.470	2.987	0.446
ADH5-17	**Nipigon**	7.677	5.243	1.594	66.589	29.315	67.216	8.875	39.436	10.384	2.727	12.263	2.009	12.525	2.573	7.319	1.030	6.606	0.993
ADH6-13	**Nipigon**	2.198	1.449	0.373	23.534	7.711	18.510	2.480	11.109	3.217	1.095	4.044	0.649	4.375	0.895	2.697	0.364	2.397	0.335
ADH6-98	**Nipigon**	2.658	1.411	0.303	22.416	8.013	19.410	2.733	12.381	3.506	1.254	4.512	0.713	4.822	1.004	2.944	0.418	2.670	0.383
AML-01-44	**Nipigon**	3.100	1.570	0.431	31.560	10.130	23.280	3.172	15.070	4.220	1.449	5.249	0.902	5.774	1.223	3.612	0.517	3.340	0.502
AML03-08	**Nipigon**	2.881	1.937	0.508	23.095	9.750	22.972	3.117	13.517	3.828	1.332	4.861	0.767	5.124	1.032	3.142	0.427	2.880	0.397
AML03-56	**Nipigon**	1.628	0.776	0.202	13.984	4.899	11.668	1.640	7.705	2.268	0.926	2.834	0.481	3.252	0.660	2.004	0.276	1.888	0.268
LN - 120	**Nipigon**	3.500	1.710	0.477	34.580	11.160	26.030	3.625	17.220	4.700	1.631	5.936	1.019	6.483	1.368	4.044	0.568	3.630	0.545
LN - 129	**Nipigon**	1.900	0.850	0.241	21.480	5.860	13.720	1.964	9.410	2.720	0.993	3.485	0.609	3.940	0.843	2.483	0.347	2.190	0.338
LN - 76	**Nipigon**	3.004	1.672	0.465	29.584	10.576	23.985	3.244	14.892	4.046	1.353	4.931	0.851	5.347	1.148	3.369	0.479	3.034	0.462
LN 70	**Nipigon**	2.900	1.480	0.409	30.060	9.810	22.680	3.131	14.480	4.110	1.421	5.159	0.891	5.609	1.180	3.362	0.484	3.140	0.474
LN 203	**Nipigon**	3.134	1.517	0.469	27.513	9.848	22.872	3.150	14.166	3.913	1.302	4.733	0.799	5.048	1.052	3.069	0.437	2.760	0.411
LN 221	**Nipigon**	3.703	1.802	0.473	35.522	12.301	28.165	3.835	17.355	4.764	1.734	5.815	0.998	6.304	1.343	3.906	0.559	3.593	0.529
LN 229	**Nipigon**	2.204	1.182	0.337	23.690	9.025	20.485	2.803	12.782	3.436	1.272	4.142	0.668	4.231	0.879	2.554	0.356	2.214	0.321
LN 231	**Nipigon**	2.007	1.335	0.381	22.878	7.766	17.620	2.421	11.158	3.111	1.094	3.815	0.639	4.107	0.855	2.482	0.355	2.238	0.341
LN 233	**Nipigon**	2.902	2.612	0.760	26.721	14.562	30.664	3.832	16.513	3.973	1.308	4.558	0.750	4.807	0.993	2.896	0.413	2.612	0.393
LN 239	**Nipigon**	1.610	1.026	0.293	15.314	7.949	17.005	2.183	9.519	2.334	0.896	2.843	0.450	2.813	0.574	1.623	0.229	1.439	0.211
LN 259	**Nipigon**	3.326	2.388	0.682	32.945	14.411	31.746	4.139	18.987	4.918	1.625	5.871	0.968	5.921	1.234	3.571	0.504	3.235	0.477
LN 301	**Nipigon**	3.516	2.612	0.774	27.412	13.018	28.658	3.803	16.905	4.359	1.369	5.108	0.844	5.143	1.052	3.038	0.424	2.662	0.395
LN 306	**Nipigon**	3.110	3.040	0.821	28.737	16.746	35.198	4.478	19.285	4.515	1.232	5.411	0.873	5.365	1.101	3.174	0.450	2.870	0.434
LN 311	**Nipigon**	1.500	0.980	0.286	15.070	5.300	11.880	1.599	7.520	2.100	0.875	2.622	0.447	2.808	0.592	1.698	0.245	1.560	0.235
LN 313	**Nipigon**	3.004	1.442	0.403	28.643	9.634	22.093	3.076	14.291	3.996	1.393	4.945	0.837	5.240	1.121	3.206	0.456	2.924	0.438
LN - 101	**McIntyre**	5.732	2.977	0.883	30.473	23.081	54.247	7.361	32.826	7.814	2.433	7.802	1.168	6.489	1.217	3.224	0.425	2.554	0.360
LN - 45	**McIntyre**	5.836	3.019	1.102	31.546	23.838	56.089	7.656	34.414	8.211	2.635	8.222	1.228	6.811	1.282	3.373	0.441	2.646	0.358
LN 161	**McIntyre**	4.605	2.252	0.508	25.726	19.920	45.606	6.155	27.298	6.547	2.258	6.767	0.977	5.139	1.020	2.632	0.352	2.142	0.303
LN 167	**McIntyre**	5.618	2.688	0.645	29.392	22.691	53.368	7.138	32.442	7.634	2.566	7.786	1.141	6.322	1.176	3.086	0.406	2.458	0.348
LN 170	**McIntyre**	5.611	2.615	0.655	28.634	22.572	52.759	6.984	31.599	7.534	2.592	7.616	1.122	6.206	1.146	3.001	0.397	2.384	0.342
03CAM030	**Pillar Lake Volcanics**	3.900	4.600	0.772	24.500	16.300	37.300	4.838	20.610	4.580	1.260	4.784	0.767	4.590	0.950	2.736	0.391	2.520	0.381
03CAM044	**Pillar Lake Volcanics**	3.600	4.280	0.985	22.900	14.350	33.220	4.347	18.670	4.230	1.290	4.450	0.711	4.245	0.873	2.497	0.357	2.280	0.350
03CAM123	**Pillar Lake Volcanics**	3.700	4.300	1.274	25.540	30.430	60.440	6.630	24.940	4.700	1.365	4.693	0.755	4.589	0.946	2.698	0.390	2.470	0.375
03CAM126	**Pillar Lake Volcanics**	3.700	2.360	0.090	28.710	14.380	42.860	6.410	27.720	6.090	1.089	5.787	0.913	5.417	1.104	3.082	0.445	2.830	0.411
03CAM142	**Pillar Lake Volcanics**	3.900	5.670	0.662	26.470	33.320	68.160	8.193	31.770	6.140	1.403	5.737	0.864	5.076	1.025	2.881	0.409	2.640	0.389
ADH3-28	**Shillabeer**	5.550	2.220	0.522	24.223	33.473	82.814	11.303	48.694	10.010	2.828	8.378	1.089	5.620	0.972	2.441	0.314	1.912	0.256
ADH5-2	**Shillabeer**	5.747	2.207	0.659	25.914	33.807	84.609	11.738	50.792	10.602	3.038	8.663	1.135	5.891	1.037	2.559	0.325	1.971	0.266

Table 2. continued

			Normative Minerals (CIPW Norm)															
Sample	**Suite**	**% Anorthite**	**Quartz**	**Orthoclase**	**Albite**	**Anorthite**	**Nepheline**	**Diopside**	**Hypersthene**	**Olivine**	**Magnetite**	**Ilmenite**	**Hematite**	**Apatite**	**FeO total**	**Mg Number**	**La/Yb**	**Calculated Density**
03CAM033	**Inspiration**	49.87	0.47	6.40	25.45	25.32	0.00	20.51	17.38	0.00	2.71	1.48	0.00	0.30	10.50	51.70	9.91	2.64
03CAM128	**Inspiration**	51.38	0.57	6.45	25.98	27.46	0.00	16.97	18.02	0.00	2.74	1.52	0.00	0.30	10.41	50.66	10.30	2.64
03CAM265	**Inspiration**	49.01	1.36	3.72	26.97	25.92	0.00	19.01	17.30	0.00	3.23	2.17	0.00	0.32	11.20	49.65	9.83	2.66
03CAM300	**Inspiration**	49.55	0.92	6.83	26.17	25.70	0.00	18.21	17.35	0.00	2.84	1.65	0.00	0.34	10.78	49.18	10.42	2.64
03CAM122	**Jackfish Island**	44.08	0.00	2.35	12.01	9.46	1.17	14.19	0.00	55.04	3.23	2.23	0.00	0.31	17.46	69.86	9.28	2.92
03CAM227	**Jackfish Island**	45.42	0.00	2.03	11.54	9.60	0.00	15.03	7.26	49.39	2.98	1.90	0.00	0.27	16.92	70.54	8.68	2.90
03CAM228	**Jackfish Island**	44.97	0.00	2.10	12.53	10.24	0.00	14.57	6.86	48.33	3.06	2.00	0.00	0.31	16.91	69.89	8.82	2.90
ADH3-33	**Nipigon**	47.91	0.00	7.73	25.88	23.81	0.00	17.39	11.64	7.78	3.24	2.18	0.00	0.34	13.35	45.63	4.26	2.69
ADH5-17	**Nipigon**	22.79	3.99	9.53	36.42	10.75	0.00	13.35	17.86	0.00	4.05	3.19	0.00	0.84	17.49	19.20	4.44	2.67
ADH6-13	**Nipigon**	52.32	0.00	4.28	22.69	24.89	0.00	25.79	15.24	1.83	3.09	1.98	0.00	0.22	12.27	49.27	3.22	2.69
ADH6-98	**Nipigon**	57.68	0.36	2.11	23.50	32.03	0.00	16.93	20.68	0.00	2.67	1.42	0.00	0.30	11.34	49.69	3.00	2.67
AML-01-44	**Nipigon**	53.40	0.84	2.89	22.53	25.82	0.00	20.58	21.88	0.00	3.13	2.00	0.00	0.32	14.57	41.46	3.03	2.71
AML03-08	**Nipigon**	49.83	1.78	3.41	25.25	25.08	0.00	20.37	18.70	0.00	3.12	2.01	0.00	0.28	12.88	44.14	3.39	2.68
AML03-56	**Nipigon**	59.23	0.00	2.10	22.94	33.33	0.00	15.89	18.46	3.14	2.62	1.36	0.00	0.17	11.67	50.04	2.60	2.68
LN - 120	**Nipigon**	49.95	1.36	3.10	24.86	24.81	0.00	20.61	18.57	0.00	3.64	2.67	0.00	0.39	15.01	36.91	3.07	2.71
LN - 129	**Nipigon**	57.18	0.01	1.60	20.14	26.90	0.00	27.15	19.74	0.00	2.73	1.50	0.00	0.21	11.57	54.14	2.68	2.69
LN - 76	**Nipigon**	51.60	0.86	3.14	23.85	25.42	0.00	21.85	18.89	0.00	3.37	2.32	0.00	0.30	14.16	40.90	3.49	2.70
LN 70	**Nipigon**	51.93	0.00	3.01	24.68	26.66	0.00	18.44	17.58	3.98	3.21	2.13	0.00	0.32	14.04	44.36	3.12	2.71
LN 203	**Nipigon**	49.29	0.00	3.49	27.20	26.44	0.00	17.32	7.56	12.20	3.26	2.20	0.00	0.33	13.94	45.88	3.57	2.71
LN 221	**Nipigon**	50.38	2.60	3.99	28.18	28.61	0.00	14.90	15.61	0.00	3.35	2.31	0.00	0.45	12.82	35.39	3.42	2.66
LN 229	**Nipigon**	57.48	0.00	2.44	27.66	37.39	0.00	12.02	10.85	5.32	2.61	1.36	0.00	0.36	9.87	48.92	4.08	2.65
LN 231	**Nipigon**	54.88	0.00	2.79	22.97	27.94	0.00	18.77	12.18	10.69	2.84	1.65	0.00	0.17	13.24	51.07	3.47	2.71
LN 233	**Nipigon**	51.15	0.00	5.27	25.86	27.08	0.00	16.57	19.80	0.18	3.02	1.88	0.00	0.34	12.48	44.82	5.57	2.67
LN 239	**Nipigon**	60.28	0.00	1.76	23.03	34.95	0.00	16.63	7.66	12.19	2.41	1.10	0.00	0.28	10.40	57.14	5.52	2.68
LN 259	**Nipigon**	48.66	2.18	5.27	26.96	25.56	0.00	16.60	19.05	0.00	2.62	1.34	0.00	0.43	11.92	43.64	4.45	2.65
LN 301	**Nipigon**	53.90	1.61	3.36	29.15	34.08	0.00	13.29	13.91	0.00	2.71	1.48	0.00	0.40	10.18	40.92	4.89	2.63
LN 306	**Nipigon**	53.91	1.97	5.30	22.62	26.46	0.00	18.02	19.99	0.00	3.16	2.06	0.00	0.43	12.26	47.35	5.84	2.67
LN 311	**Nipigon**	61.23	0.00	1.90	19.15	30.24	0.00	20.85	15.04	8.89	2.54	1.26	0.00	0.13	11.63	57.83	3.40	2.71
LN 313	**Nipigon**	54.84	1.01	2.74	25.14	30.54	0.00	18.36	16.54	0.00	3.21	2.12	0.00	0.34	12.55	40.97	3.29	2.68
LN - 101	**McIntyre**	32.61	0.27	3.70	37.00	17.90	0.00	18.89	12.25	0.00	4.94	4.44	0.00	0.60	13.41	40.34	9.04	2.68
LN - 45	**McIntyre**	33.45	0.23	4.12	36.20	18.19	0.00	20.55	10.64	0.00	4.98	4.49	0.00	0.60	13.51	38.56	9.01	2.69
LN 161	**McIntyre**	40.90	0.00	3.92	29.20	20.20	0.00	17.59	16.18	3.92	4.57	3.93	0.00	0.48	15.23	43.20	9.30	2.73
LN 167	**McIntyre**	35.59	0.00	4.67	32.62	18.03	0.00	22.24	11.98	0.63	4.90	4.37	0.00	0.55	14.36	39.18	9.23	2.70
LN 170	**McIntyre**	37.41	0.22	3.91	33.75	20.17	0.00	18.41	13.90	0.00	4.83	4.29	0.00	0.51	13.73	40.38	9.47	2.69
03CAM030	**Pillar Lake Volcanics**	26.75	0.00	2.47	45.39	16.58	1.57	24.13	0.00	5.03	2.85	1.72	0.00	0.25	5.96	64.70	6.47	2.56
03CAM044	**Pillar Lake Volcanics**	50.71	0.00	17.75	20.84	21.43	0.00	13.70	21.17	0.24	2.86	1.68	0.00	0.32	8.57	61.95	6.29	2.60
03CAM123	**Pillar Lake Volcanics**	50.75	0.06	18.09	20.87	21.50	0.00	15.45	19.19	0.00	2.83	1.66	0.00	0.34	7.10	67.43	12.32	2.59
03CAM126	**Pillar Lake Volcanics**	28.89	0.00	5.88	36.57	14.86	2.76	22.78	0.00	13.02	1.82	1.66	0.66	0.00	4.25	81.49	5.08	2.57
03CAM142	**Pillar Lake Volcanics**	34.61	0.01	6.77	37.88	20.05	0.00	19.13	10.66	0.00	2.94	1.79	0.00	0.76	5.66	68.00	12.62	2.57
ADH3-28	**Shillabeer**	15.49	0.00	1.93	42.96	7.88	1.10	22.06	0.00	15.32	4.37	3.74	0.00	0.64	11.79	58.17	17.51	2.68
ADH5-2	**Shillabeer**	24.59	0.00	7.03	34.45	11.23	0.00	16.75	7.60	13.81	4.50	3.89	0.00	0.75	12.68	57.66	17.16	2.70

Table 2. continued

Sample	Suite	Rare Earth Elements [1]														
		LaN	CeN	PrN	NdN	SmN	EuN	GdN	TbN	DyN	HoN	ErN	TmN	YbN	LuN	EuN Anomaly
03CAM033	Inspiration	92.52	71.55	54.50	43.81	27.61	22.34	21.47	18.56	16.21	14.96	14.65	13.53	13.02	13.15	0.92
03CAM128	Inspiration	96.96	75.28	57.70	46.06	28.50	22.68	21.15	18.13	16.32	15.05	14.66	13.75	13.12	13.13	0.92
03CAM265	Inspiration	83.39	65.02	49.59	40.06	25.49	21.32	18.92	16.72	14.84	13.37	13.29	12.26	11.83	11.83	0.97
03CAM300	Inspiration	103.24	80.03	61.23	49.09	30.42	24.32	22.38	19.53	17.34	16.11	15.93	14.40	13.81	13.82	0.93
03CAM122	Jackfish Island	43.90	39.96	34.96	32.57	23.57	20.69	17.33	14.39	11.65	9.73	8.57	7.37	6.60	6.08	1.02
03CAM227	Jackfish Island	35.79	33.42	29.30	27.30	20.39	18.25	15.60	12.77	10.25	8.49	7.41	6.33	5.75	5.26	1.02
03CAM228	Jackfish Island	36.71	34.38	30.66	28.85	21.23	18.76	16.16	13.06	10.58	8.77	7.71	6.49	5.80	5.49	1.01
ADH3-33	Nipigon	53.65	46.30	39.46	35.61	29.08	24.20	25.54	23.63	21.63	20.16	20.01	18.44	17.57	17.56	0.89
ADH5-17	Nipigon	123.69	109.83	93.42	84.45	67.87	47.02	59.68	53.72	49.31	45.46	44.22	40.41	38.86	39.09	0.74
ADH6-13	Nipigon	32.54	30.25	26.10	23.79	21.02	18.87	19.68	17.35	17.23	15.81	16.29	14.29	14.10	13.18	0.93
ADH6-98	Nipigon	33.81	31.72	28.77	26.51	22.92	21.62	21.95	19.06	18.98	17.74	17.79	16.40	15.70	15.08	0.96
AML-01-44	Nipigon	42.74	38.04	33.39	32.27	27.58	24.98	25.54	24.12	22.73	21.61	21.82	20.27	19.65	19.76	0.94
AML03-08	Nipigon	41.14	37.54	32.81	28.94	25.02	22.97	23.66	20.50	20.17	18.24	18.99	16.74	16.94	15.62	0.94
AML03-56	Nipigon	20.67	19.07	17.26	16.50	14.82	15.97	13.79	12.86	12.80	11.66	12.11	10.80	11.10	10.54	1.12
LN - 120	Nipigon	47.09	42.53	38.16	36.87	30.72	28.12	28.89	27.25	25.52	24.17	24.44	22.27	21.35	21.46	0.94
LN - 129	Nipigon	24.73	22.42	20.67	20.15	17.78	17.12	16.96	16.28	15.51	14.89	15.00	13.61	12.88	13.31	0.99
LN - 76	Nipigon	44.62	39.19	34.15	31.89	26.44	23.31	24.00	22.76	21.05	20.28	20.36	18.77	17.85	18.18	0.93
LN 70	Nipigon	41.39	37.06	32.96	31.01	26.86	24.50	25.10	23.82	22.08	20.85	20.31	18.98	18.47	18.66	0.94
LN 203	Nipigon	41.55	37.37	33.15	30.33	25.58	22.45	23.03	21.36	19.87	18.58	18.54	17.13	16.24	16.16	0.93
LN 221	Nipigon	51.90	46.02	40.37	37.16	31.14	29.89	28.30	26.68	24.82	23.73	23.60	21.94	21.14	20.85	1.01
LN 229	Nipigon	38.08	33.47	29.50	27.37	22.46	21.93	20.16	17.86	16.66	15.54	15.43	13.95	13.02	12.62	1.03
LN 231	Nipigon	32.77	28.79	25.49	23.89	20.33	18.86	18.56	17.09	16.17	15.10	15.00	13.93	13.16	13.43	0.97
LN 233	Nipigon	61.44	50.10	40.34	35.16	25.97	22.55	22.18	20.04	18.92	17.54	17.50	16.21	15.37	15.48	0.94
LN 239	Nipigon	33.54	27.79	22.98	20.38	15.26	15.44	13.83	12.03	11.08	10.13	9.81	9.00	8.46	8.32	1.06
LN 259	Nipigon	60.81	51.87	43.57	40.66	32.14	28.01	28.57	25.90	23.31	21.79	21.57	19.76	19.03	18.77	0.92
LN 301	Nipigon	54.93	46.83	40.03	36.20	28.49	23.61	24.86	22.56	20.25	18.58	18.35	16.62	15.66	15.54	0.89
LN 306	Nipigon	70.66	57.51	47.14	41.30	29.51	21.24	26.33	23.34	21.12	19.45	19.18	17.63	16.88	17.10	0.76
LN 311	Nipigon	22.36	19.41	16.83	16.10	13.73	15.09	12.76	11.95	11.06	10.46	10.26	9.61	9.18	9.25	1.14
LN 313	Nipigon	40.65	36.10	32.37	30.60	26.12	24.02	24.07	22.39	20.63	19.80	19.37	17.87	17.20	17.23	0.96
LN - 101	McIntyre	97.39	88.64	77.48	70.29	51.07	41.94	37.97	31.22	25.55	21.50	19.48	16.68	15.03	14.17	0.95
LN - 45	McIntyre	100.58	91.65	80.59	73.69	53.67	45.44	40.01	32.82	26.82	22.65	20.38	17.28	15.57	14.10	0.98
LN 161	McIntyre	84.05	74.52	64.79	58.45	42.79	38.94	32.93	26.12	21.41	18.02	15.90	13.82	12.60	11.94	1.04
LN 167	McIntyre	95.74	87.20	75.14	69.47	49.90	44.24	37.89	30.50	24.89	20.77	18.64	15.93	14.46	13.70	1.02
LN 170	McIntyre	95.24	86.21	73.52	67.66	49.24	44.69	37.06	30.00	24.43	20.25	18.13	15.56	14.03	13.45	1.05
03CAM030	Pillar Lake Volcanics	68.78	60.95	50.93	44.13	29.93	21.72	23.28	20.51	18.07	16.78	16.53	15.33	14.82	15.00	0.82
03CAM044	Pillar Lake Volcanics	60.55	54.28	45.76	39.98	27.65	22.24	21.65	19.01	16.71	15.42	15.09	14.00	13.41	13.78	0.91
03CAM123	Pillar Lake Volcanics	128.40	98.76	69.79	53.40	30.72	23.53	22.84	20.19	18.07	16.71	16.30	15.29	14.53	14.76	0.89
03CAM126	Pillar Lake Volcanics	60.68	70.03	67.47	59.36	39.80	18.78	28.16	24.41	21.33	19.51	18.62	17.45	16.65	16.18	0.56
03CAM142	Pillar Lake Volcanics	140.59	111.37	86.24	68.03	40.13	24.19	27.92	23.10	19.98	18.11	17.41	16.04	15.53	15.31	0.72
ADH3-28	Shillabeer	141.24	135.32	118.98	104.27	65.43	48.76	40.77	29.13	22.12	17.18	14.75	12.33	11.24	10.07	0.94
ADH5-2	Shillabeer	142.64	138.25	123.56	108.76	69.29	52.38	42.16	30.35	23.19	18.31	15.46	12.76	11.59	10.47	0.97

[1] normalized to the chondrite values of Sun and McDonough (1989)

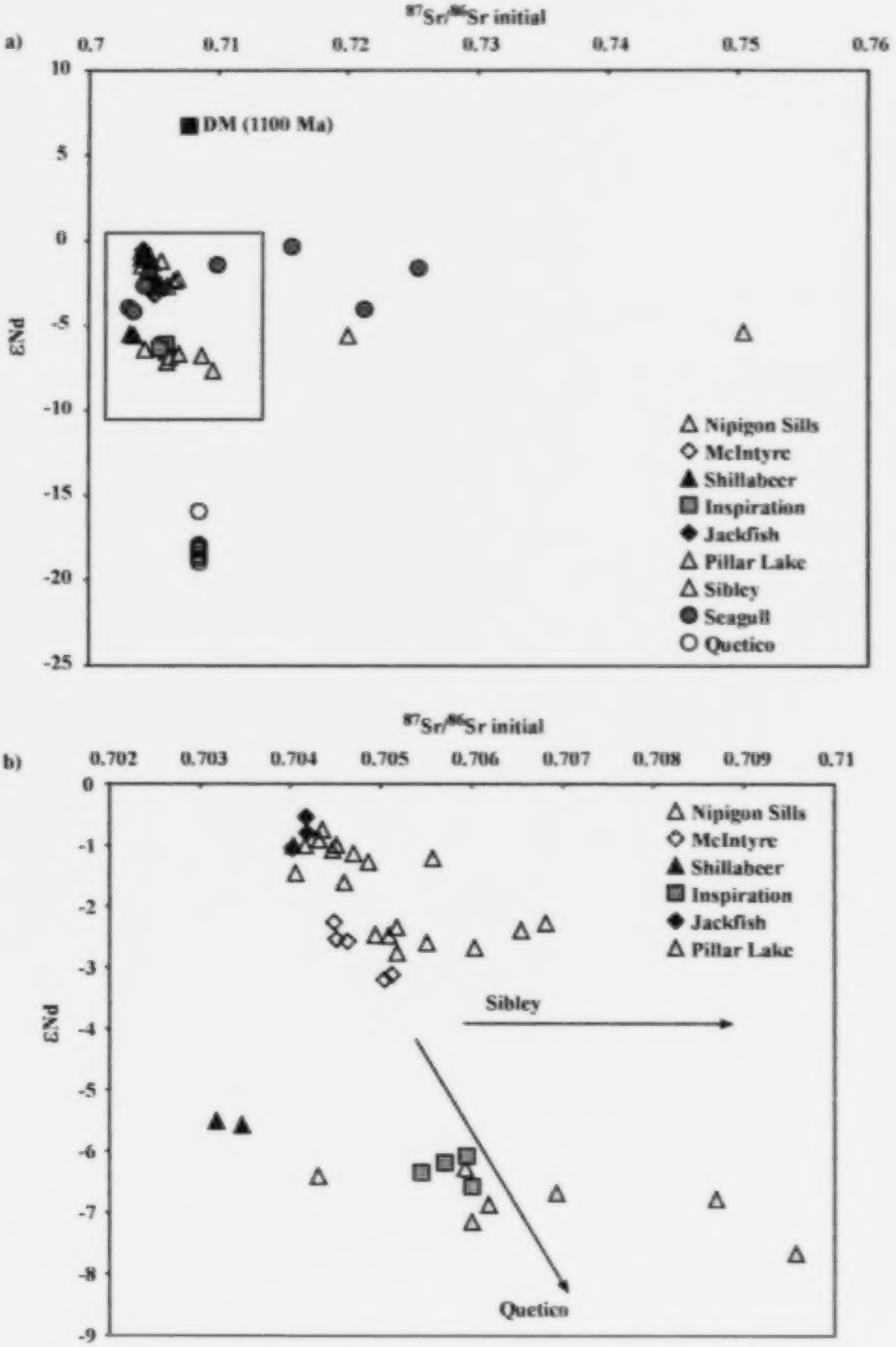

Figure 10. a) Plot of $^{87}Sr/^{86}Sr$ versus ε_{Nd} for the sills of the Nipigon Embayment. Volcanic rocks from Pillar Lake are also shown. Sibley data *from* R. Metsaranta (Lakehead University, personal communication, 2005); Seagull data *from* Heggie (2005); Quetico data *from* Henry, Stevenson and Gariepy (1998) and Pan, Fleet and Longstaffe (1999); depleted mantle (DM) values *from* Shirey et al. (1994). b) Detail of Figure 10a, arrows point toward Sibley and Quetico data on Figure 10a.

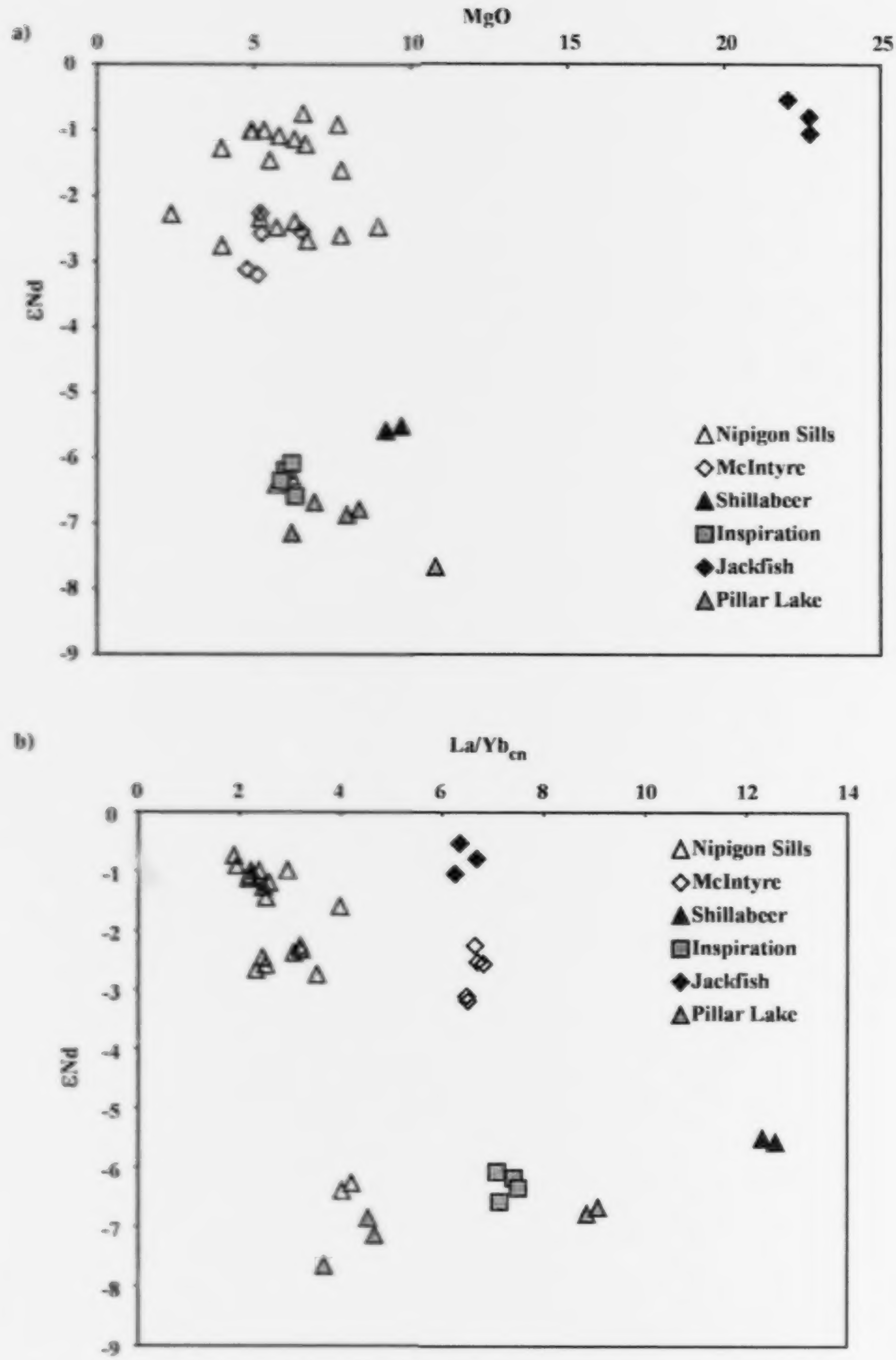

Figure 11. a) Plot of MgO versus ε_{Nd} for all diabase sills. b) Plot of chondrite-normalized La/Yb versus ε_{Nd} showing the effects of crustal contamination on LREE abundance. Inspiration and Jackfish Island whole rock data *from* MacDonald (2004).

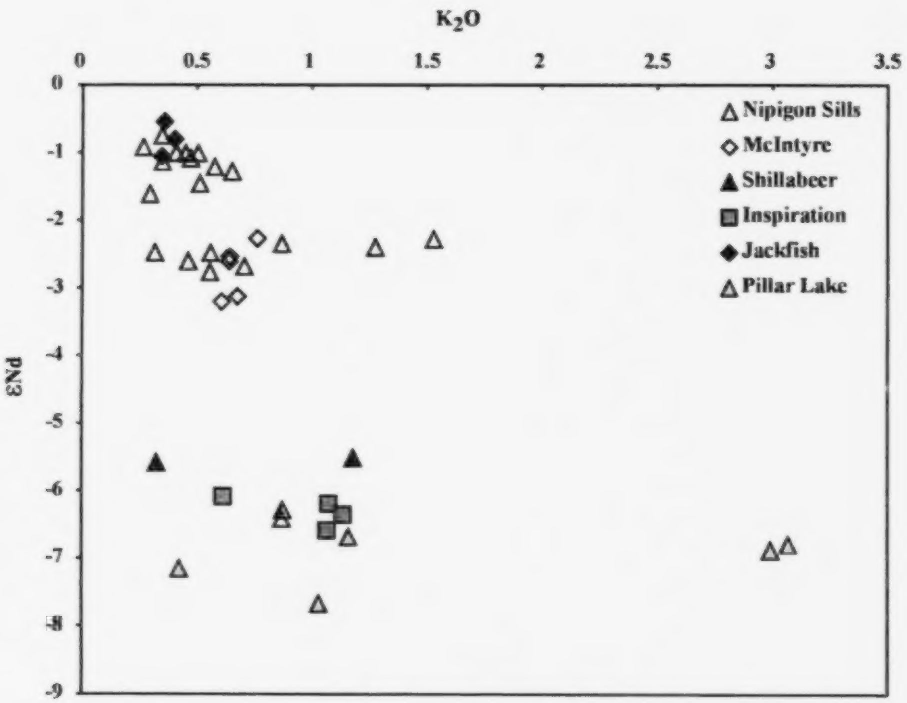

Figure 12. Plot of K_2O versus ε_{Nd} values for the diabase sills of the Nipigon Embayment. Samples with elevated K_2O also have elevated $^{87}Sr/^{86}Sr$ ratios, which is consistent with contamination by a Sibley-like component. Jackfish Island and Inspiration whole rock data *from* MacDonald (2004).

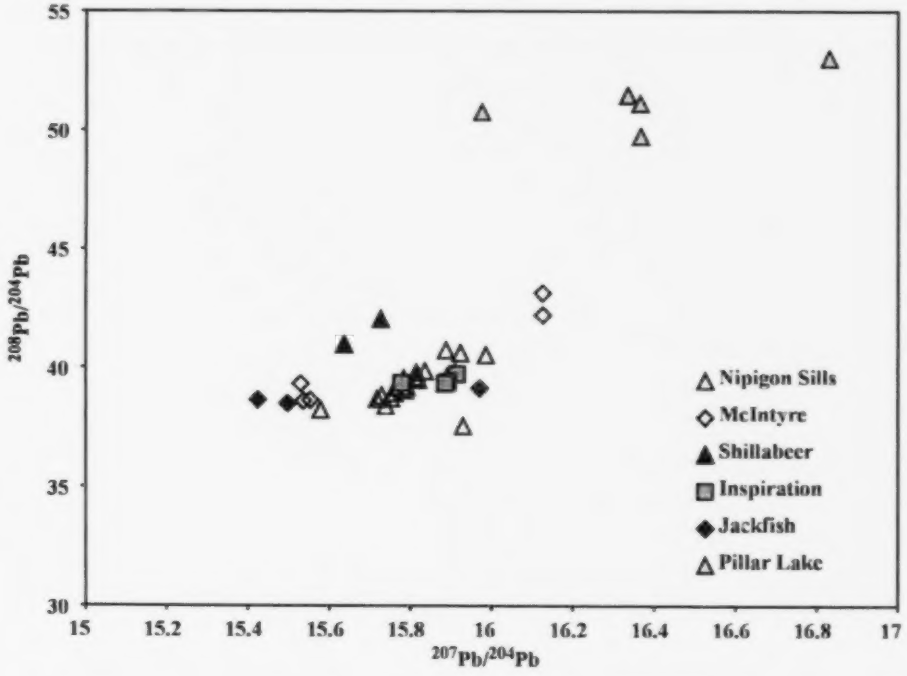

Figure 14. Plot of $^{207}Pb/^{204}Pb$ versus $^{208}Pb/^{204}Pb$ for the sills of the Nipigon Embayment.

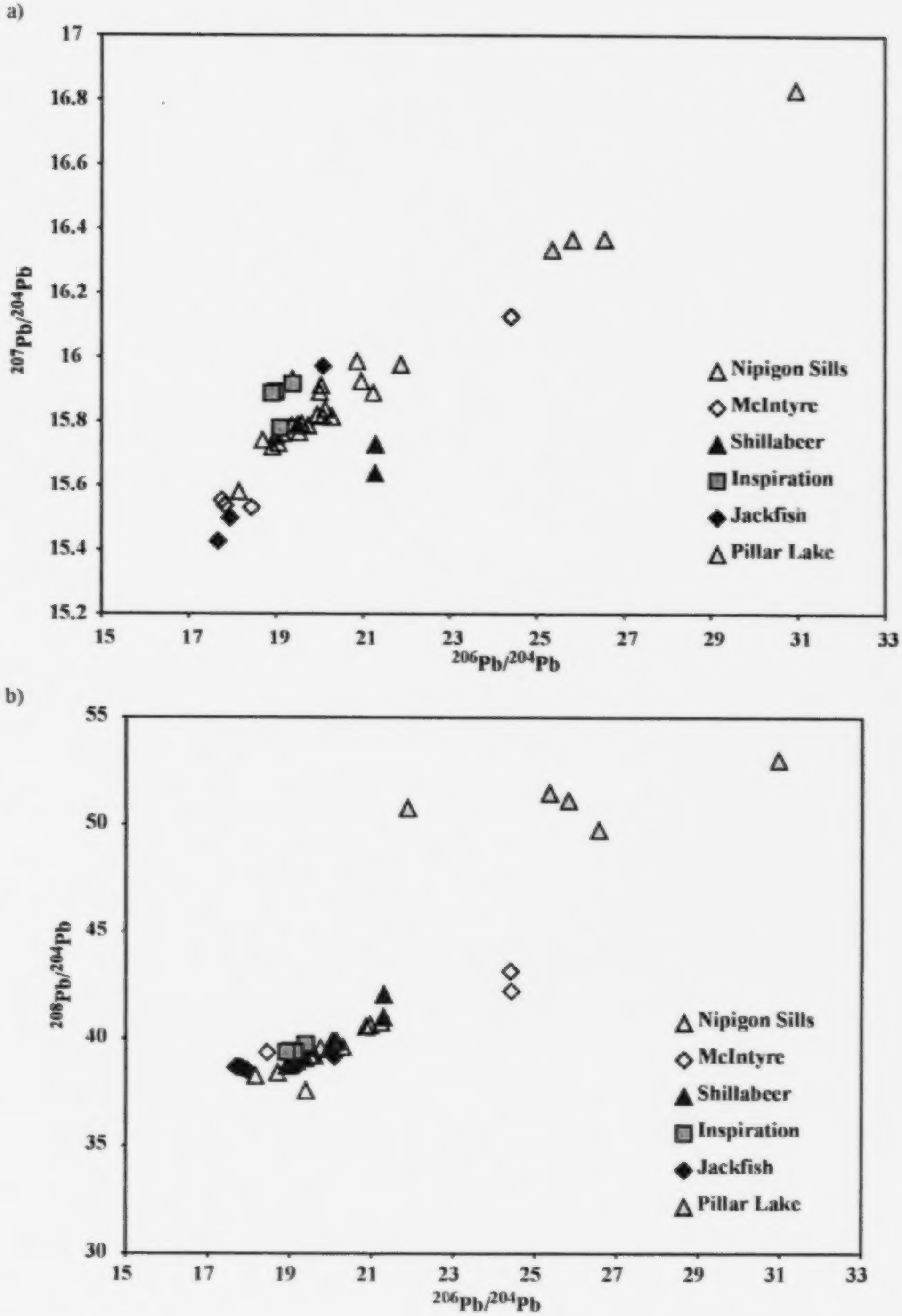

Figure 13. Plots of a) $^{206}Pb/^{204}Pb$ versus $^{207}Pb/^{204}Pb$; and b) $^{206}Pb/^{204}Pb$ versus $^{208}Pb/^{204}Pb$ for the sills of the Nipigon Embayment.

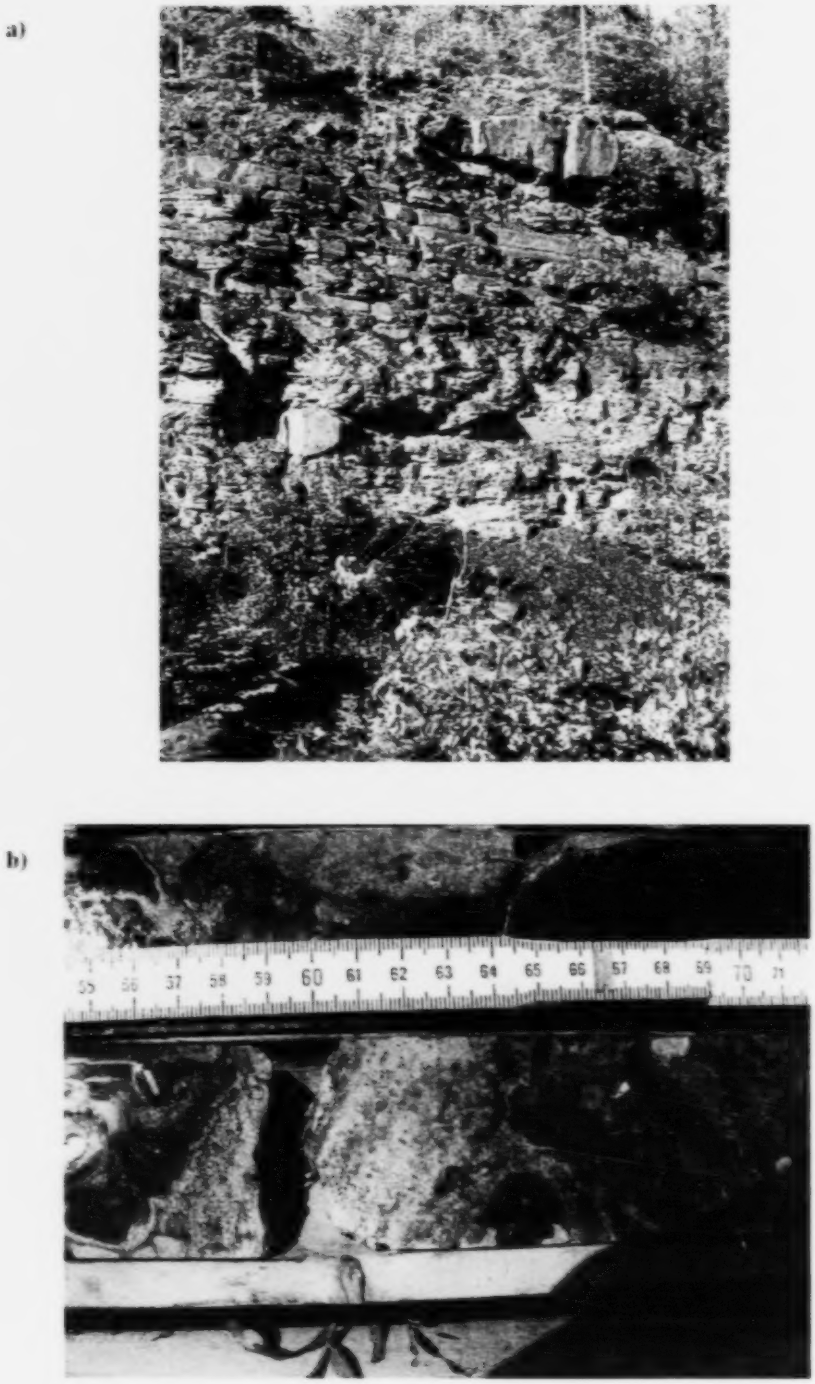

Photo 6. Diabase sill relationships with country rock: a) diabase sill intruding Rove Formation metasedimentary rocks near Great Lakes Nickel deposit, south of Thunder Bay; and b) diabase sill assimilating Sibley Group metasedimentary rocks in core from DDH 6.

Discussion

EMPLACEMENT MECHANISMS

One of the principal objectives of this study was to investigate the emplacement mechanism of the diabase sills. The sills range in thickness from a few metres to 150 m in cliff sections and over 250 m in drill core. Drill core data were used both to investigate internal variations within the sills and to correlate between closely spaced drill holes in order to examine emplacement mechanisms. The thickest sills appear to be homogeneous in outcrop with little evidence to indicate an emplacement mechanism. Preliminary data from diamond-drill core logs have revealed variations in textural relationships and mineral concentrations. The absence of clear internal chill contacts within the sills combined with layer-like changes in grain size, particularly within what appear to be single sills in diamond-drill core, may be evidence of several pulses of magma being injected within a short period of time. This is consistent with the work of Hart, Hollings et al. (2005) who have presented evidence for rare layering within sills, marked by magnetite-rich layers, variations in grain size and feldspar content, which may indicate they cooled as a single unit. Hart, MacDonald et al. (2005) reported major and trace element data from drill hole ML01-01 where they identified trends in TiO_2 and MgO values which were interpreted to reflect multiple magma injections. The elevated TiO_2 values correlate with an increase in magnetite abundance within the hole (Hart, MacDonald et al. 2005). This mineralogical and textural zoning is evident in all 3 ML-series diamond-drill holes where a very coarse to pegmatitic zone up to 30 m thick has been recognized. The pegmatitic unit retains a reasonably constant thickness and is present at the same elevation in all 3 holes. These holes were drilled over approximately 2.5 km indicating that some sills are laterally continuous over at least that interval.

In contrast, stratigraphic correlation between the Shillabeer (DDH-series, *see* Figure 5) diamond-drill holes is more difficult. Figure 9 depicts drill hole DDH 1 and DDH 6 (for locations, *see* Figure 5) separated by 300 m along an east to west axis and approximately 15 m vertically. The distribution of sedimentary units and the character of the diabase within these holes cannot be easily stratigraphically correlated despite the geographic proximity of the diamond-drill holes. Drill hole DDH 1 was collared in Sibley Group sedimentary rocks with multiple thin intercalated beds of diabase and highly metamorphosed sediments from 40 m extending to approximately 93 m (for location, *see* Figure 5). A significant thickness of Sibley Group sediments appears at 194 m down the hole and extends to nearly 275 m. Diabase injected into the Sibley Group near the top of the hole is very fine grained to aphanitic, and lighter coloured, which possibly indicates contamination by assimilated Sibley Group sediments, although this does not appear to be reflected in the trace element geochemistry. Similar diabase–Sibley Group contacts to those observed in DDH 1 are present in DDH 6. However, the Sibley Group sedimentary rocks were intersected at the top of the hole and between 130 and 170 m in DDH 6 with no other units of Sibley Group sedimentary rocks in the remainder of the diamond-drill hole (for location, *see* Figure 5). The remaining 4 Shillabeer diamond-drill holes (DDH-2 through -5) are shallower (<170 m in total length) and contain multiple units of highly metamorphosed Sibley Group sedimentary rocks and very fine-grained to aphanitic diabase.

The lack of stratigraphic correlation of rock types between the 2 diamond-drill holes (*see* Figure 9) suggests that the diabase units may be apophyses from a single, thicker sill. Similar apophyses can be observed in outcrop where thin diabase sills have intruded into sediments of the Rove Formation in the vicinity of Great Lakes Nickel deposit south of Thunder Bay, where 2 sills can be seen to terminate within the outcrop (Photo 6a). Thomson and Hutton (2004), in a study of doleritic sills in the North Rockall Trough, used three-dimensional seismic images to interpret the sill geometry. Among the features they recognized were stepped sill fingers radiating from a parent sill, which they interpret as flow-parallel features (*see also* Thomson and Hutton 2004, Figure 10). These stepped fingers are similar

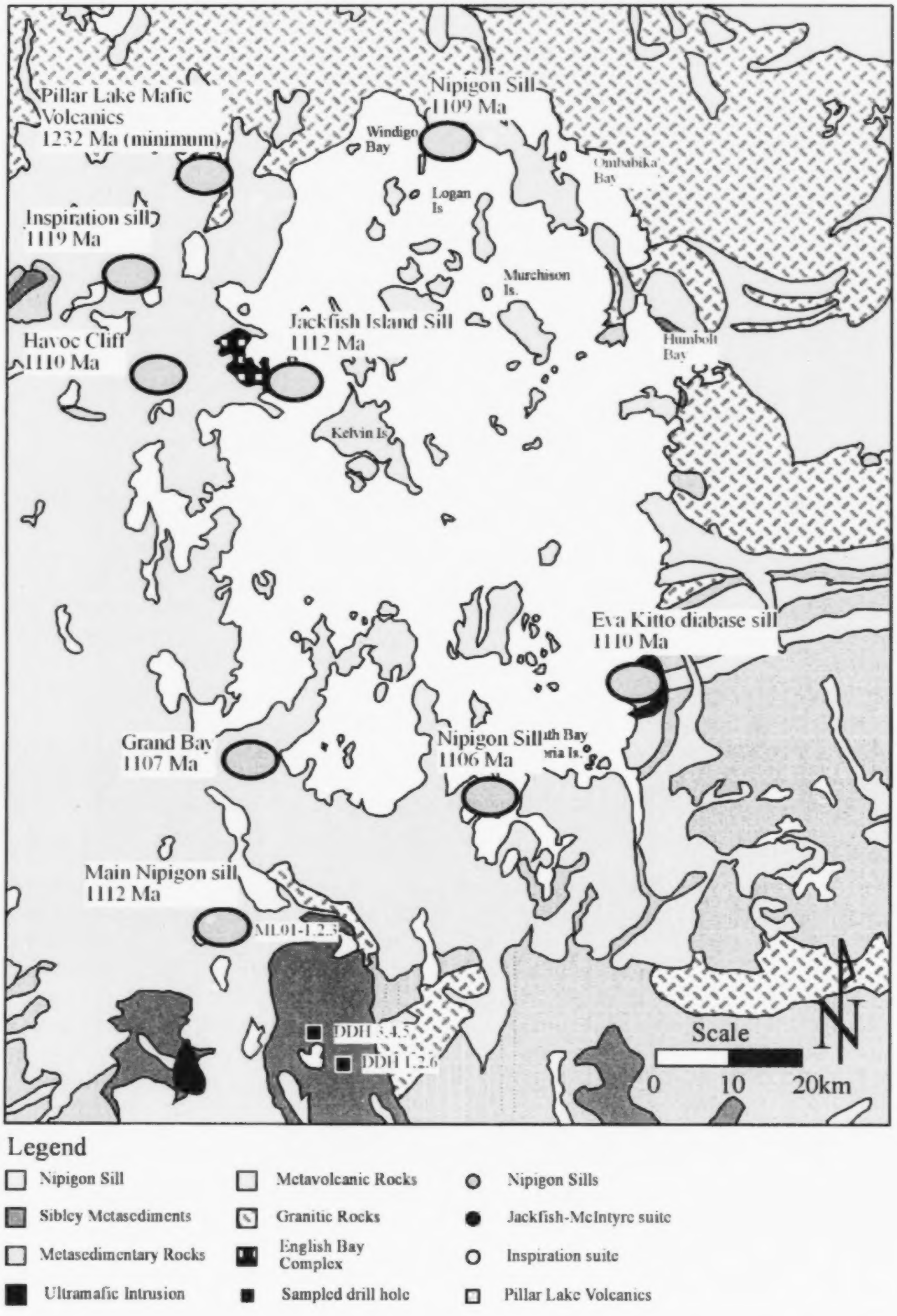
Pillar Lake Mafic Volcanics
1232 Ma (minimum)
Nipigon Sill
1109 Ma
Windigo Bay
Ombabika Bay
Logan Is
Inspiration sill
1119 Ma
Murchison Is.
Jackfish Island Sill
1112 Ma
Havoc Cliff
1110 Ma
Humbolt Bay
Kelvin Is
Eva Kitto diabase sill
1110 Ma
Grand Bay
1107 Ma
Nipigon Sill
1106 Ma
Main Nipigon sill
1112 Ma
ML01-1.2.3
DDH 3.4.5
DDH 1.2.6
Scale
0
10
20km
N
Legend
Nipigon Sill
Sibley Metasediments
Metasedimentary Rocks
Ultramafic Intrusion
Metavolcanic Rocks
Granitic Rocks
English Bay Complex
Sampled drill hole
Nipigon Sills
Jackfish-McIntyre suite
Inspiration suite
Pillar Lake Volcanics

Figure 15. Map showing the locations of U/Pb ages from the Nipigon Embayment. Ages *from* Heaman and Easton (2005). Map *modified after* Sutcliffe (1986).

in appearance to the features observed in this study. However, an alternative explanation is offered by 2 sills in the Kama Hill Formation of the Sibley Group. These sills crop out at different topographic levels on opposite sides of the hill suggesting the style of emplacement does not follow specific stratigraphic horizons and the sills appear to "climb up" stratigraphy. In the North Rockall Trough, Thomson and Hutton (2004) observed that the sills were bilaterally symmetrical and formed a trough-like geometry as they climbed away from the magma source (*see also* Thomson and Hutton 2004, Figure 7) and a similar model may be applicable in the Nipigon Embayment. An alternative explanation is that the layers of sedimentary rocks in these diamond-drill holes may be preserved remnants of a continuous unit that has been partially assimilated as the sill was emplaced, or possibly detached blocks of Sibley Group sedimentary rocks, which have either detached from the roof of the sill or been "floated" by the diabase as it intruded into the sedimentary sequence. Hart (2005b) has proposed that hornfelsed blocks of Sibley Group within a diabase dike on Highway 11/17 east of Thunder Bay may have been displaced or rotated by the intrusion of the sill. He suggested that the chaotic structure and lack of preservation of bedding structures within the blocks were evidence that the blocks had fallen through a thick sill rather than being *in situ* blocks. No bedding structures were recognized within the Sibley Group sediments in the Shillabeer drill holes, however, the fact that contact angles between the diabase and the sediment in the vertical drill holes were uniformly horizontal suggests that these are *in situ* sedimentary units. This supports the model that the diabase intrusions are apophyses of a larger sill that have intruded into and, in places, assimilated the sedimentary units. The presence of partially assimilated sediments within the diabase sills is also consistent with this mechanism (Photo 6b).

Samples of widely geographically distributed sills were submitted for U/Pb age determinations in order to investigate if there was any systematic variation of the ages of the sills that could offer insights into the emplacement history. The uranium-lead ages shown on Figure 15 are preliminary, but they show that there does not appear to be any north to south, or east to west progression in ages. A north-to-south age progression might have been expected if the sills were emplaced in a northward-propagating arm of the Midcontinent Rift. Similarly, work by Middleton et al. (2004) has shown that the magnetic fabrics of the diabase sills possess east to west flow fabrics in the vicinity of Lake Nipigon. However, the sills appear to have been emplaced throughout the embayment in a relatively short time period. The notable exceptions to this are the Inspiration sills, which appear to be somewhat older than the other suites.

GEOCHEMISTRY

At least 5 geochemically distinct sill suites have been recognized in the Nipigon basin: Nipigon, McIntyre, Shillabeer (this study), Inspiration (MacDonald 2004; *see* Table 1) and Jackfish Island (Sutcliffe 1986). The geographical proximity of the Jackfish Island and McIntyre suites (*see* Figure 5) in conjunction with their near-identical primitive mantle-normalized patterns (*see* Figure 8) suggests that these 2 suites may be related, with the Jackfish Island sills being the more primitive and less contaminated end member. This is supported by the higher ^{86}Sr/^{87}Sr ratios and more negative ε_{Nd} values in the McIntyre suite (*see* Figure 10). Contamination of the high MgO Jackfish Island sills by a felsic contaminant could account for the lower MgO contents of the McIntyre sills (*see* Figure 11a).

On a plot of MgO versus TiO_2, the various sills fall into 2 distinct groups, a high TiO_2 group, which includes the Jackfish Island, McIntyre and Shillabeer sills, and a low TiO_2 group, which includes the Inspiration and Nipigon suites (*see* Figure 6a). Samples from the Logan sills from the vicinity of Thunder Bay fall within the high titanium field, as do samples from the ultramafic Disraeli intrusion (*see* Figure 6a). This feature has been noted in other flood basalt provinces (e.g., Parana–Etendeka, Karoo and Ferrar: Peate and Hawkesworth 1996). In the Parana continental flood basalts, the high- and low-TiO_2 suites have been shown to occur in distinct areas and this has been argued to suggest that they are the result of a major compositional boundary within the lithospheric mantle (Hergt, Peate and Hawksworth 1991; Peate and

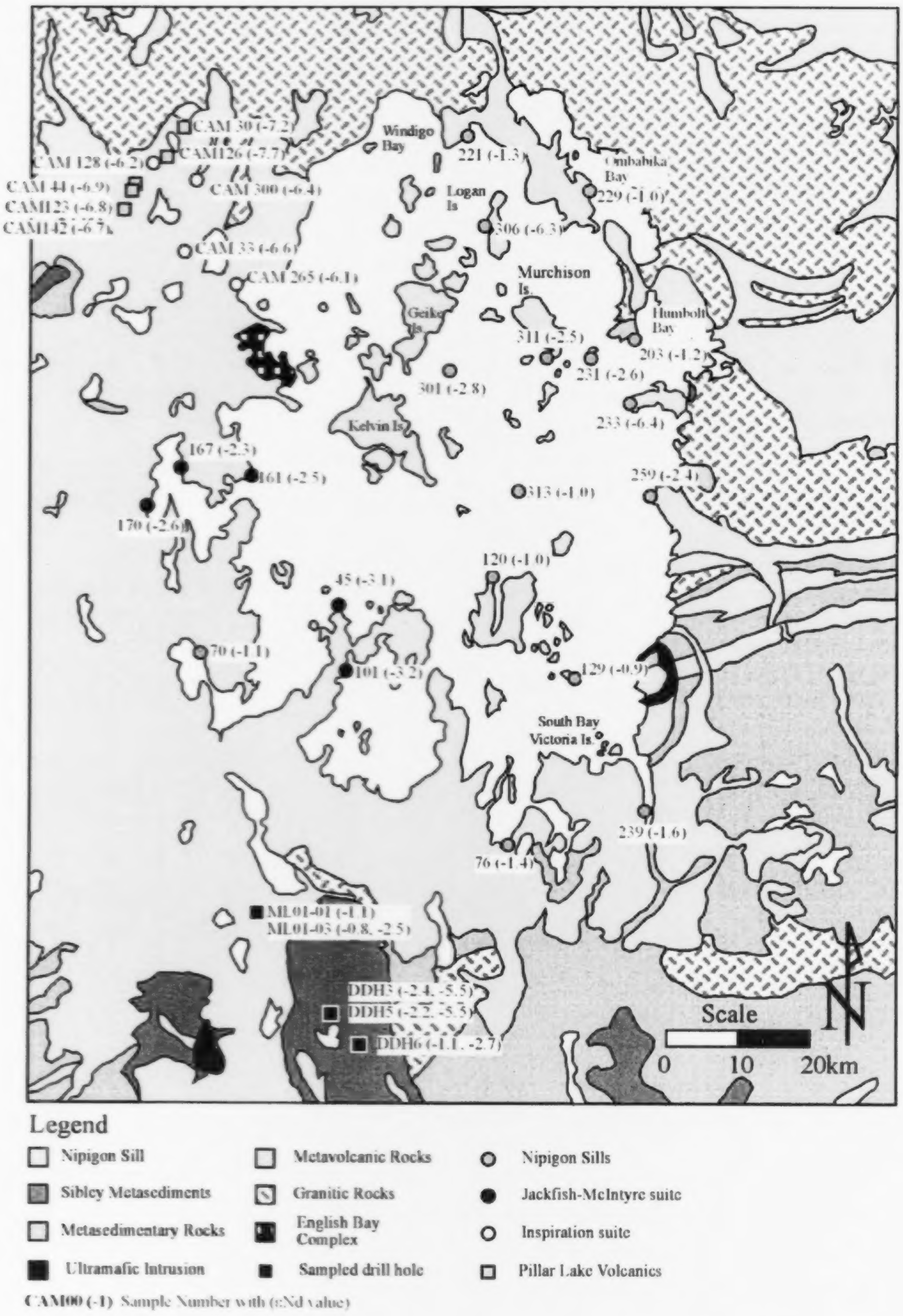
CAM 30 (-7.2)
CAM126 (-7.7)
CAM 128 (-6.2)
CAM 44 (-6.9)
CAM123 (-6.8)
CAM142 (-6.7)
CAM 300 (-6.4)
CAM 33 (-6.6)
CAM 265 (-6.1)
Windigo Bay
221 (-1.3)
Ombabika Bay
229 (-1.0)
Logan Is
306 (-6.3)
Murchison Is.
Geike Is.
Humbolt Bay
311 (-2.5)
203 (-1.2)
231 (-2.6)
301 (-2.8)
233 (-6.4)
Kelvin Is
167 (-2.3)
161 (-2.5)
259 (-2.4)
313 (-1.0)
170 (-2.6)
120 (-1.0)
45 (-3.1)
70 (-1.1)
101 (-3.2)
129 (-0.9)
South Bay Victoria Is.
239 (-1.6)
76 (-1.4)
ML01-01 (-1.1)
ML01-03 (-0.8, -2.5)
DDH3 (-2.4, -5.5)
DDH5 (-2.2, -5.3)
DDH6 (-1.1, -2.7)
Scale
0
10
20km
N
Legend
Nipigon Sill
Sibley Metasediments
Metasedimentary Rocks
Ultramafic Intrusion
Metavolcanic Rocks
Granitic Rocks
English Bay Complex
Sampled drill hole
Nipigon Sills
Jackfish-McIntyre suite
Inspiration suite
Pillar Lake Volcanics
CAM00 (-1) Sample Number with (εNd value)

Figure 16. Map showing the locations of samples analyzed for radiogenic isotopes and measured ε_{Nd} values for each sample *(modified after* Sutcliffe 1986).

Hawkesworth 1996) or, alternatively, that the low-titanium basalts were derived from an iron-depleted source formed as a result of previous melt extraction events likely within the continental mantle lithosphere (Turner and Hawkesworth 1995). The fact that the low- and high-titanium basalts from this study are closely spatially associated would appear to preclude the presence of a major compositional boundary and it is more likely that the 2 groups have been formed from distinct mantle source regions.

The high incompatible element abundances, in conjunction with LREE enrichment and strongly fractionated HREE of all diabase suites, are broadly comparable to modern plume-derived oceanic island basalt, albeit at lower absolute abundances (*see* Figure 7). This is particularly true of the Jackfish, McIntyre and Shillabeer suites. When compared to other rift-related basalts, the sills closely resemble basalts from the Parana–Etendeka flood basalt province (*see* Figure 7; Peate and Hawkesworth 1996; Gibson, Thompson and Dickin 2000). However, the majority of the sill suites display a pronounced negative Nb anomaly, which is not typical of oceanic island basalt, but is found in some continental flood basalts (e.g., Parana; Peate and Hawkesworth 1996; *see* Figure 7). The negative Nb anomalies in the sills, particularly the Nipigon and Inspiration suites, in conjunction with the high Th contents, are comparable to basalts formed in a supra-subduction environment. However, this is not consistent with the tectonic setting inferred for the Midcontinent Rift, where it is now generally accepted that an upwelling mantle plume was responsible for the large volumes of mafic magmas emplaced or erupted around 1.1 Ga (e.g., Nicholson and Shirey 1990). The higher LREE abundances in the Inspiration sills (~80–100× primitive mantle as opposed to 10–50× for the other suites), which display some of the most pronounced Nb anomalies, is consistent with the sills having been contaminated by a source with elevated Th and REE (*see* Figure 7). The majority of Archean granites exposed in the Superior Province are tonalite-trondhjemite-granodiorite (TTG) with geochemical characteristics similar to the proposed contaminant. Sediments derived from the erosion of these granites (e.g., the Quetico Subprovince metasedimentary rocks) are likely to display broadly similar geochemical signatures to the granites.

RADIOGENIC ISOTOPES

Rubidium–Strontium (Rb/Sr) and Neodymium–Samarium (Nd/Sm)

The radiogenic isotope characteristics of the sills offer a tool for evaluating the role of crustal contamination (*see* Figure 10). Depleted mantle at 1100 Ma would have had an ε_{Nd} value of +6, whereas an enriched plume source would have ε_{Nd} less than that of depleted mantle (Nicholson and Shirey 1990; Shirey et al. 1994). Nicholson and Shirey (1990) proposed that the main volume of rift basalt was produced from an enriched mantle plume with an ε_{Nd} value close to 0 and chondrite-normalized La/Sm of 2 to 3, which is consistent with isotopic and trace element data from many basalt sequences in the rift (Paces 1988; Nicholson et al. 1997; Wirth, Vervoort and Naiman 1997). Sill suites analyzed in this study have ε_{Nd} values of less than 0 with a range of –0.5 from the Jackfish suite to –6.5 from the Inspiration suite. This is consistent with contamination of the magma by an older crustal source. There are a number of potential contaminants in the basement rocks underlying the Nipigon Embayment (*see* Figure 5). These include the recently recognized Badwater Creek gabbro and Badwater Creek syenite (~1590 Ma: MacDonald, Tremblay and Easton 2005; Heaman and Easton 2005; *see* Table 1) and the English Bay complex (~1540 Ma), however, these are of limited extent (*see* Figure 5). More widespread contaminants include the metasediments of the Sibley Group and Quetico Subprovince as well as Archean granites. Vervoort and Green (1997) calculated that Archean TTG underlying the Midcontinent Rift would have had ε_{Nd} values of –18 to –13. Data for the Quetico Subprovince metasedimentary rocks have been determined by Pan, Fleet and Longstaffe (1999) and from the Sibley Group as part of the LNRGI (R. Metsaranta, Lakehead University, personal communication, 2004). For the majority of samples, there does not appear to be a strong correlation between the ε_{Nd} values and the basement rock (Figure 16). This is perhaps most clearly illustrated in drill holes DDH 3 and DDH 5 where Nipigon sills have very different ε_{Nd} values to the Shillabeer sills from the same hole. The exception to this are the Inspiration sills, which show strongly negative ε_{Nd} values in a relatively confined area close at the northern limit of the diabase sills.

Radiogenic data for samples from the Sibley Group and Quetico Subprovince may be used to investigate the role of different contaminants, however, it is recognized that the limited data set for the sediments may not be representative. The isotopic characteristics of the 2 metasedimentary contaminants are very different, with the Quetico characterized by strongly negative ε_{Nd} and low $^{87}Sr/^{86}Sr$ and the Sibley by ε_{Nd} of approximately –5 and high $^{87}Sr/^{86}Sr$ ratios. On a plot of $^{87}Sr/^{86}Sr$ versus ε_{Nd}, contamination by Sibley Group material should produce a horizontal trend toward increased $^{87}Sr/^{86}Sr$ isotopic values without a corresponding decrease in ε_{Nd}, whereas contamination by Quetico Subprovince material should result in a vertical trend toward decreased ε_{Nd} without a corresponding increase in Sr isotope ratios. In a study of the Seagull ultramafic intrusion, Heggie (2005) observed that ε_{Nd} data were consistent with contamination by Sibley Group metasediments and this is supported by the horizontal trend toward elevated $^{87}Sr/^{86}Sr$ (*see* Figure 10a). In general, the data for the diabase sills show a near-vertical trend consistent with contamination by an Archean source; however, a number of Nipigon sills show a horizontal trend towards a Sibley contaminant for at least some samples (*see* Figure 10a). One interpretation of these trends is that the source of the diabase sills assimilated an Archean contaminant within a lower crustal magma chamber, whereas the relatively thin Sibley horizons were assimilated during emplacement of the sills. Data from studies of komatiites are broadly supportive of this model; Huppert and Sparks (1985) have calculated that up to 50% contamination of komatiites might occur during the ascent of the magma, whereas post-eruptive contamination is unlikely to exceed 10%. It is plausible that a similar ratio could be applied to the ascent and emplacement of the sills with the Archean signature reflecting a deeper, more extensive, contamination consistent with its greater thickness and extent. In contrast, the less extensive and thinner (a few hundred metres in the vicinity of Lake Nipigon) Sibley Group only acted as a contaminant source during emplacement of the sills.

Studies of komatiites have shown that there is sometimes a correlation between MgO and crustal contamination as the higher MgO magmas are emplaced at a higher temperature allowing for an increase in the amount of country rocks that can be assimilated (e.g., Hollings and Kerrich 1998). The MgO–contamination relationship does not appear to hold true for the Nipigon sills as increasingly negative ε_{Nd} values are not accompanied by a corresponding increase in MgO (*see* Figure 11a). The Jackfish suite is the most mafic sill suite of the basin with MgO values approaching 23 weight % MgO, but shows the most primitive ε_{Nd} values (~ –0.5). In contrast, the most contaminated suite, the Inspiration, has MgO values of approximately 5 weight %, but ε_{Nd} values of –6 to –7. Even within individual sills, there does not appear to be any significant correlation (*see* Figure 11a).

On a plot of La/Yb_{cn} versus ε_{Nd}, data from the different sill suites show distinctive trends (*see* Figure 11b). Although there is a broad correlation between ε_{Nd} and increasing La/Yb_{cn} for the Nipigon suite, the same is not true of the other suites, which show no correlation. This implies that different sources have contaminated the various suites with the Nipigon suite being contaminated by a source with elevated LREE compared to the other suites. In the Kama Hill cliff section, Hart, Hollings et al. (2005) reported that thin sills contained elevated K_2O and MgO values and suggested that this was the result of assimilation of Sibley Group metasedimentary rocks of the Kama Hill Formation. In order to test this hypothesis, ε_{Nd} was plotted against K_2O for the regional-scale database from this study (*see* Figure 12). Samples from the Nipigon sills that showed a trend towards a Sibley contaminant on Figure 10 are also characterized by an elevated K_2O content, consistent with a Sibley source. However, there is also a correlation between ε_{Nd} and increasing K_2O for the Inspiration sills (*see* Figure 12), which do not show a Sibley $^{87}Sr/^{86}Sr$ contamination signature. Similarly, the Shillabeer sills, which are intruded into and, in places, have partially assimilated (Photo 6b), Sibley Group sediments, has the lowest $^{87}Sr/^{86}Sr$ ratios, which is not consistent with contamination by Sibley Group material. However, it is recognized that there may be many different Sibley contaminants with distinct geochemical signatures. It is noteworthy that 2 of the sill suites that show evidence for significant contamination (Kama Hill and Shillabeer) are also 2 of the thinner sills, however, the relatively thin Jackfish sills do not share this feature. The Shillabeer suite is also unusual in that it lacks the Th enrichment seen in the other suites, suggesting a unique contaminant. The Shillabeer suite, as well as displaying strongly negative ε_{Nd} values indicative of contamination, is also characterized by negative Zr and Hf anomalies not seen in any of the other sill suites (*see* Figure 7a). The negative Zr and Hf anomalies are also observed in the ultramafic Disraeli intrusion to the south (*see* Figure 7a) as well as in the Seagull intrusion (Heggie 2005). The LREE enrichment in the Shillabeer sill, relative to the Disraeli intrusion, may be a result of the contamination that produced the negative ε_{Nd} values. The variable isotopic and trace element signatures seen in the various sill suites indicates that they have undergone a complicated contamination history.

The fact that the Inspiration sills are the oldest known sill suite and are among the most contaminated (*see* Figures 10 and 15) may provide some insights into the early development of the rift. In a study of the Mamainse Point basalts, Shirey et al. (1994) and Nicholson et al. (1997) observed that basalts from the base of the sequence (1109–1107 Ma) underwent little interaction with the crust, whereas those towards the top of the sequence were contaminated by Archean basement. They proposed that, in the early phases of rifting, extension rates were high and magmas were able to rise through the crust quickly with little contamination; later, as extension decreases, magma is forced to pond at or near the base of the crust where it assimilates greater amounts of crustal material. If indeed the degree of contamination is related to the extension rate, then this implies that the older, most contaminated sills were emplaced when the rate of extension was initially low and then increased with time allowing the emplacement of the less contaminated sills. Following the emplacement of the sills, the extension rate may have increased further to allow the emplacement of the uncontaminated basalts at Mamainse Point.

Lead–Lead (Pb/Pb)

Lead isotopic data have been used to typify the source and contamination history of many suites of mafic volcanic and intrusive rocks. Examples include Vervoort et al. (1991), Vervoort, White and Thorpe (1994), Tosdal, Wooden and Bouse (1999), Cameron et al. (2004) and Lundstrom et al. (1995). The various mafic units in the Lake Nipigon area are not pervasively altered or hydrated, as they contain fresh olivine and feldspar. Some units may be the product of melt contamination, as manifested by a small amount of biotite (and potassium enrichment). The Pillar Lake volcanic rocks are the subject of an ongoing investigation; preliminary observations indicate that they have been subject to halmyrolytic alteration and, thus, have reacted with seawater (M.A. Magee, Ontario Geological Survey and Lakehead University, personal communication, 2005). The measured lead isotope composition of these units (*see* Table 2) are the products of "common lead", that which was present during crystallization of melt, and radiogenic lead, that which was added to the rocks from uranium and thorium that coexists with the lead-bearing phase or, in the case of the present study, in the host rock. If the melt was well mixed and the sample is representative, then the data will form a cluster or short linear trend. If the U/Pb and Th/Pb ratios vary considerably through the rock, then the data will usually form a linear array, or isochron that may provide an age that determines the time at which U, Th and Pb were deposited in the rock. In the study of Vervoort et al. (1991), lead isotopic data for volcanic rocks in the Noranda region of Quebec formed an excellent linear array, but had been reset during regional metamorphism. For a more extensive treatment of lead isotope analytical methods and data analysis, see Faure (1986) or Franklin et al. (1983).

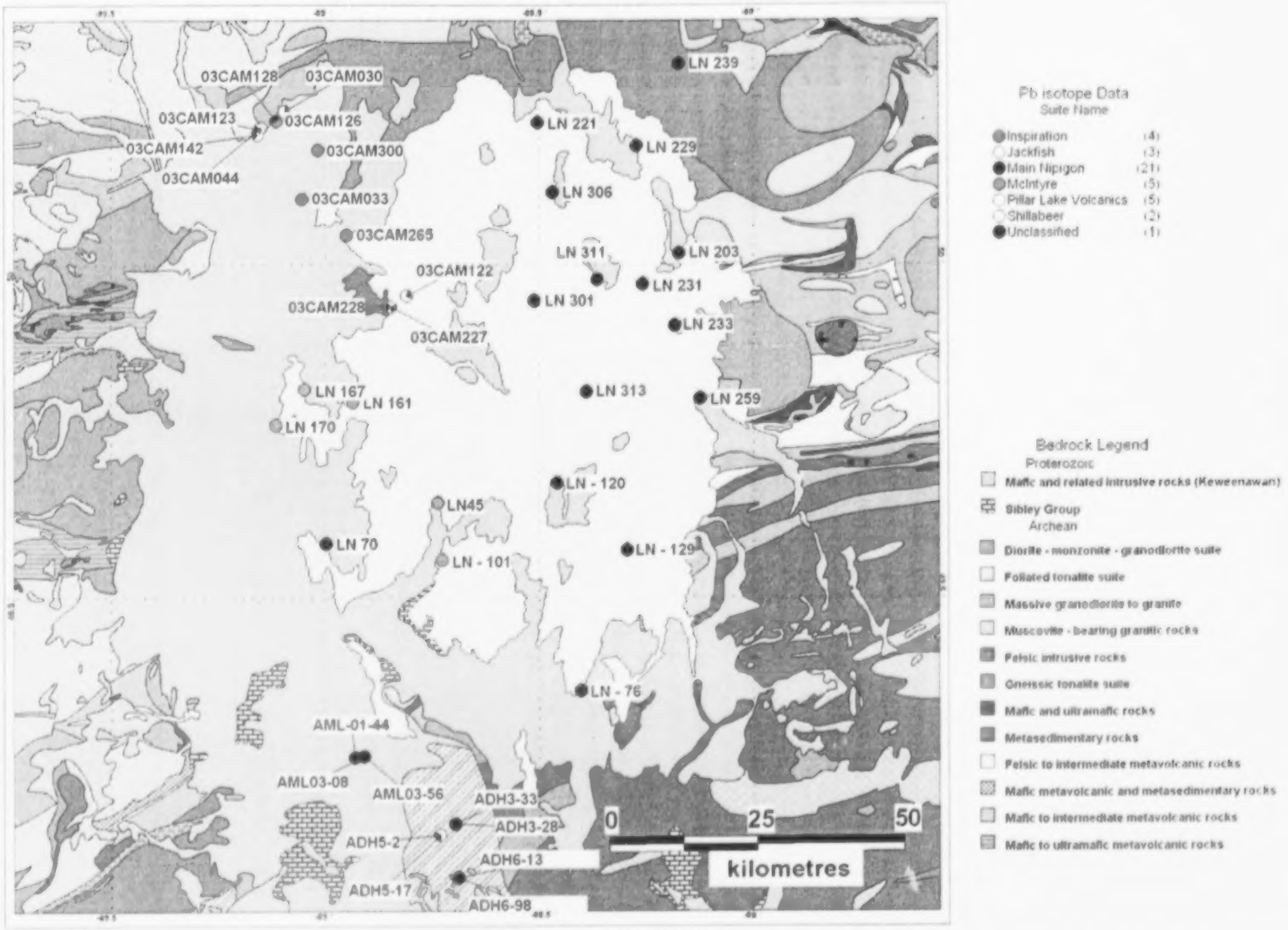
03CAM128
03CAM030
03CAM123
03CAM126
03CAM142
03CAM300
03CAM044
03CAM033
03CAM265
03CAM122
03CAM228
03CAM227
LN 239
LN 221
LN 229
LN 306
LN 311
LN 203
LN 231
LN 301
LN 233
LN 313
LN 259
LN 167
LN 161
LN 170
LN - 120
LN45
LN 70
LN - 129
LN - 101
LN - 76
AML-01-44
AML03-08
AML03-56
ADH3-33
ADH3-28
ADH5-2
ADH6-13
ADH5-17
ADH6-98
0
25
50
kilometres
Pb isotope Data
Suite Name
Inspiration (4)
Jackfish (3)
Main Nipigon (21)
McIntyre (5)
Pillar Lake Volcanics (5)
Shillabeer (2)
Unclassified (1)
Bedrock Legend
Proterozoic
Mafic and related intrusive rocks (Keweenawan)
Sibley Group
Archean
Diorite - monzonite - granodiorite suite
Foliated tonalite suite
Massive granodiorite to granite
Muscovite - bearing granitic rocks
Felsic intrusive rocks
Gneissic tonalite suite
Mafic and ultramafic rocks
Metasedimentary rocks
Felsic to intermediate metavolcanic rocks
Mafic metavolcanic and metasedimentary rocks
Mafic to intermediate metavolcanic rocks
Mafic to ultramafic metavolcanic rocks

Figure 17. Location of samples for isotopic studies of Proterozoic mafic igneous suites in the Lake Nipigon area, Ontario. Geology map is from the digital version of OGS (2003).

The present investigation involved only whole-rock lead isotope analyses. Lead usually resides in feldspar, and future work could involve leaching lead from feldspar (which usually contains little U or Th), which may yield better data for common-lead compositions. The objectives of this preliminary study are to see if

1. the various petrogenetic units have distinct lead isotopic compositions or trends?
2. melt contamination can be detected and, if so, what constraints might be placed on the source of this?
3. there is any age information contained in this data set?

Six different units were analyzed, along with one sample that was not classified. The sample locations are provided in Table 2 and are shown in Figure 17. The data were treated using a series of programs written by J.M. Franklin that calculate model ages, $^{238}U/^{204}Pb$ (μ), $^{232}Th/^{204}Pb$ (ψ) and $^{232}Th/^{238}U$ ratios for each sample, enable the calculation of a Yorkfit two-error regression line (*see* York 1969 for the method), and facilitate two-stage age calculations. In addition, a program provided by Ludwig (2000) was used for some of the calculations. The Stacey and Kramers (1975) growth curve is used for reference in various diagrams.

The major and trace element data (*see* Table 2) are plotted in a series of diagrams (Figure 18) to determine if the field-assigned units are petrogenetically distinct. From the various plots in Figure 18 it is clear that many, but not all of the units are geochemically distinct. The geochemical data were collected for the LNRGI study; for comparison (not shown), similar plots were made of the entire data set available to Franklin, including MacDonald and Tremblay (2004a), Hart and Magyarosi (2004b), and data collected by East-West Resource Corporation, and by Teck–Cominco Ltd., the latter of which was provided to LNRGI (Franklin 2003). The plot of Mg Number versus La_N/Yb_N ratio (*see* Figure 18D) most clearly illustrates the compositional uniqueness of each suite. All except the Pillar Lake volcanic samples are well grouped on most plots. Some other salient points arising from these plots are

1. The Jackfish Island sill is clearly ultramafic, but has a slightly lower La/Yb ratio than most of the peridotite in the Seagull (Wolf Mountain) and Hele areas.
2. The Shillabeer sill is characterized by elevated MgO contents and may belong to the same suite as the peridotite and picritic rocks defined by Franklin (2003).
3. The Nipigon sills has a bimodal La/Yb; this group may contain more than one petrogenetic suite.
4. The Pillar Lake volcanics are possibly alkaline, and probably have been seawater altered (halmyrolysis), given its narrow range of contents of immobile elements, but considerable variation in Mg.
5. The Inspiration sills are similar to the Nipigon sills in major element contents, but have distinctly higher contents of REEs. They seem to form a distinct petrogenetic group.

Further analysis of the geochemical data is not warranted; the above observations are made in order to provide a framework in which to examine the lead isotopic data.

The conventional lead isotope plots are presented in Figure 19. On inspection of the $^{206}Pb/^{204}Pb$ versus $^{207}Pb/^{204}Pb$ diagram (*see* Figure 19a), the data form 4 clusters or arrays. The least radiogenic is composed of some of the Jackfish Island (1112.4±2.8 Ma) and McIntyre samples (one of each of these suites is anomalously radiogenic); the diabase Jackfish Island samples form a distinct linear array with a steep slope. The Nipigon sills (1109.9±2.2 Ma) and Inspiration (1159.6±33) samples form a moderately

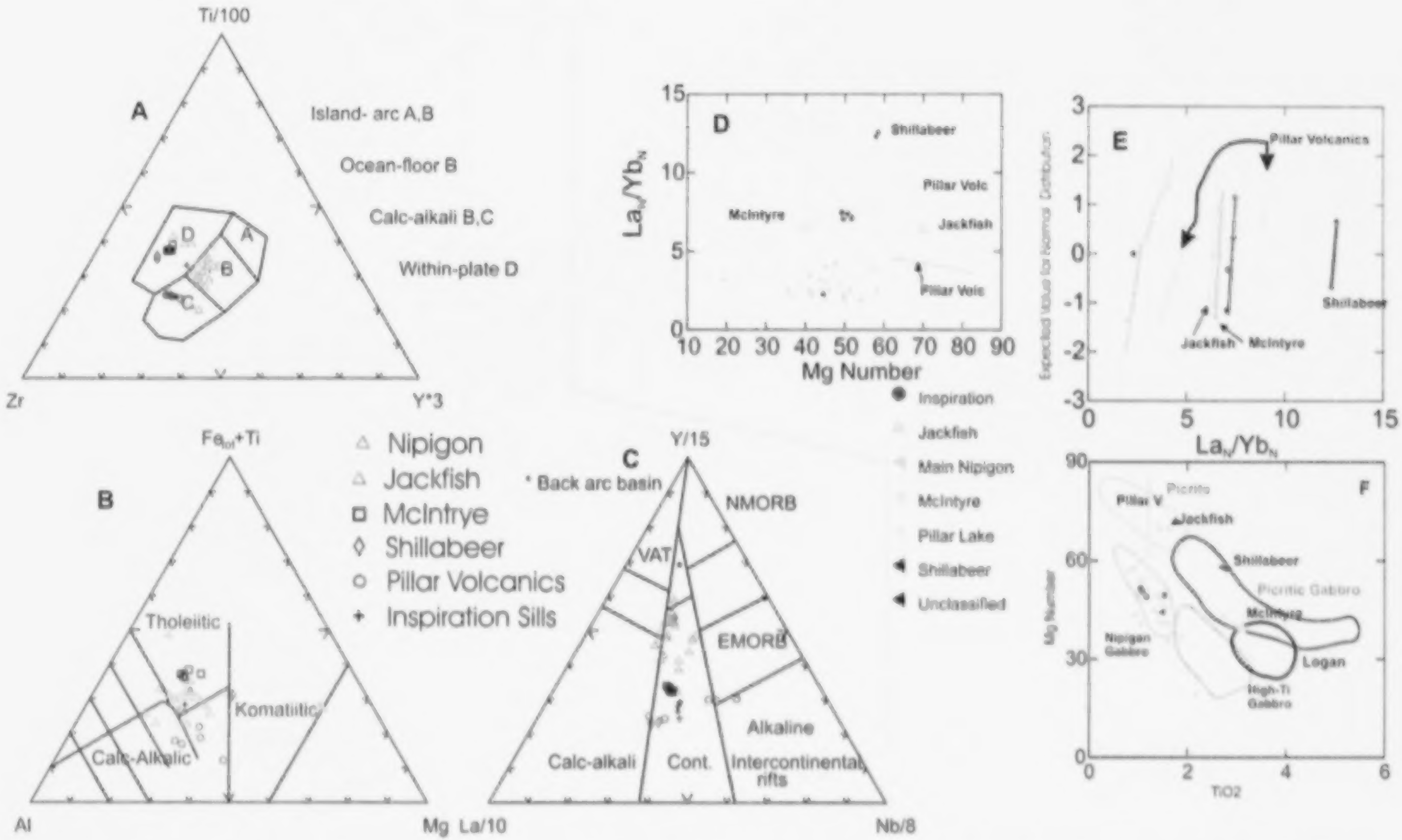

Figure 18. Petrochemistry plots: Plots A and C are for immobile elements (*see* Pearce 1996 and references therein) and B is a Jensen plot (Jensen 1976). Plots D and F combine Mg number, chondrite-normalized La/Yb ratio and TiO_2 to illustrate the separation of lithogroups, and Plot E is a probability plot, illustrating the coherence of each of the suites. REEs are normalized *after* Sun and McDonough (1989).

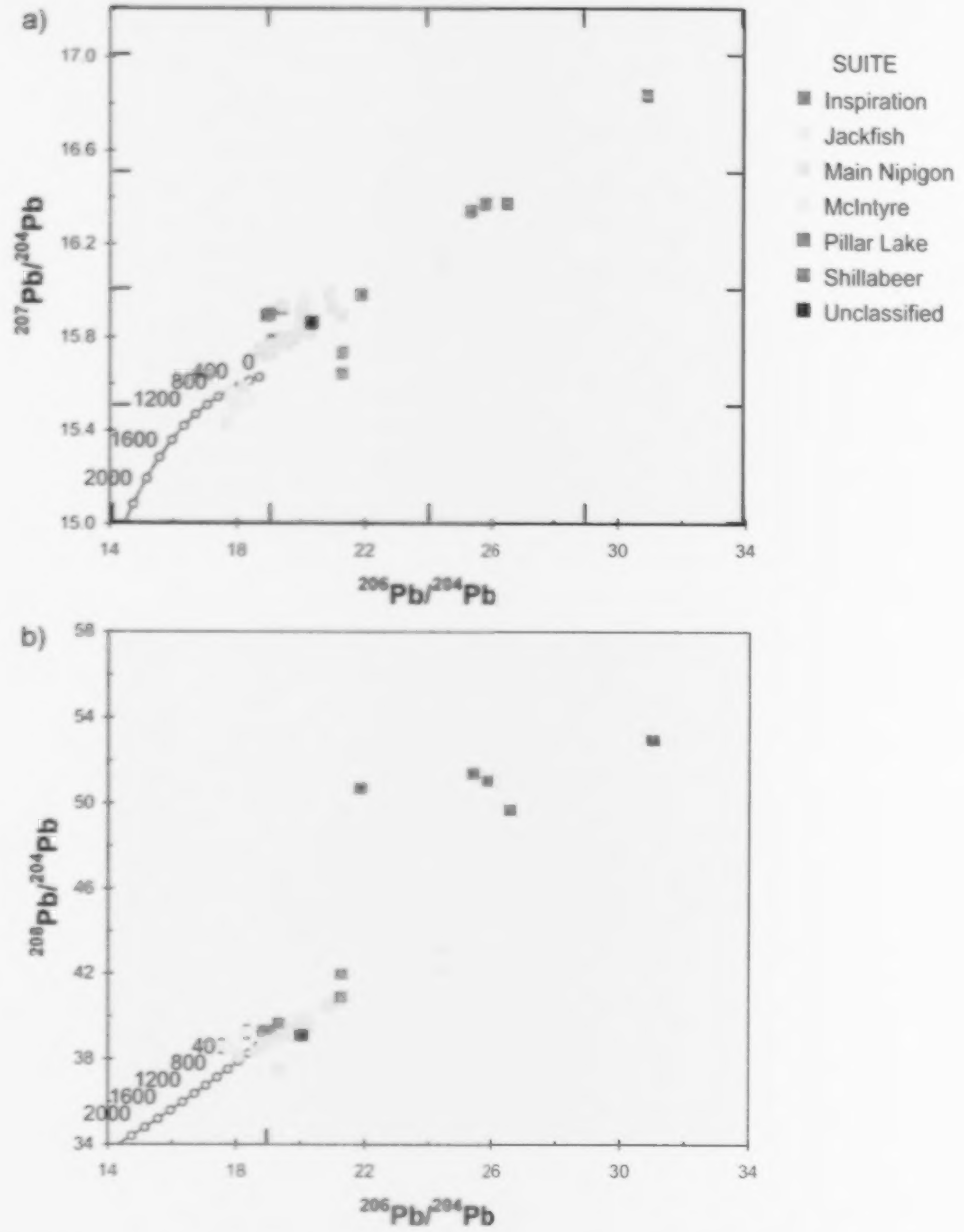

Figure 19. a) Uranogenic lead (^{206}Pb/^{204}Pb versus ^{207}Pb/^{204}Pb) isotope plot. Growth curve is *from* Stacey and Kramers (1975); the line is for reference only. b) Thorogenic lead (^{206}Pb/^{204}Pb versus ^{208}Pb/^{204}Pb) isotope plot.

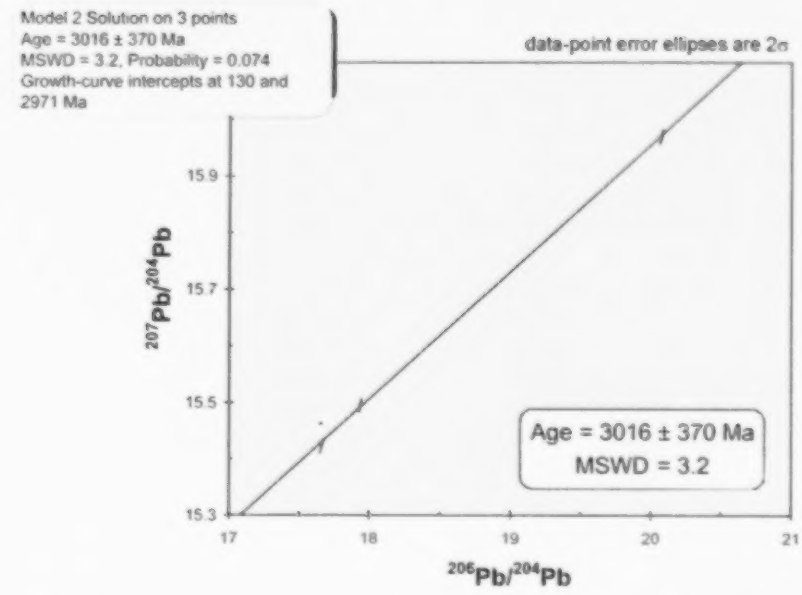

Figure 20. ^{206}Pb/^{204}Pb versus ^{207}Pb/^{204}Pb diagram of the Jackfish Island sill lead isotopic data.

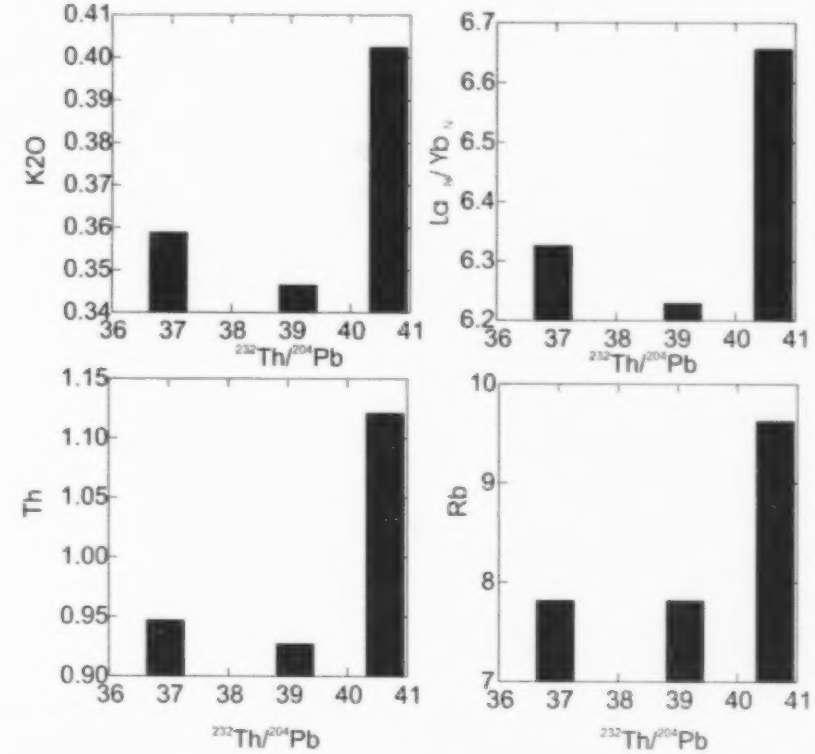

Figure 21. Histograms showing the anomalous content in sample 03CAM228 (Jackfish Island sill) of elements that are commonly associated with crustal contamination of a melt.

radiogenic cluster. The 2 Shillabeer samples form a distinct cluster (no age determination, but they are petrologically similar to the Disraeli intrusion, which has an age of 1112 Ma). The samples from Pillar Lake volcanics (>1232 Ma) are distinctly radiogenic and form a moderately good linear array. Overall, the data define a linear trend. On the thorogenic plot (*see* Figure 19b), all of the data form a distinct linear trend, except the Pillar Lake data, which is highly radiogenic and clearly not related to the other samples.

Discussion of Lead Isotope Data

The data for each suite were examined separately; only some contain enough data, or formed distinct arrays, to merit more detailed interpretation.

JACKFISH ISLAND SILLS

This distinct linear array of lead isotopic data forms a line with a slope of 0.227±0.004, which yields an isochron age of 3016±370 Ma (Figure 20). This steep slope and geologically impossible age indicates that this is a secondary isochron or a binary mixing line. Using the established age of 1112 Ma for a two-stage calculation yields a source age of about 2546 Ma. Given the uncertainties in the determination of the slope and age of this unit, and limited number of samples, this source age indicates that the Jackfish Island sill may have been extracted from mantle material that was last tapped during the Archean. To examine this further, the element contents for various possible contaminants were plotted against ^{232}Th/^{204}Pb (ψ) (Figure 21). In other studies (Franklin 2003; Hart and Magyarosi 2004), it was noted that the ultramafic rocks are contaminated, as indicated by the presence of a small amount of biotite (typically ~1%). This is also consistent with radiogenic isotope data from the Seagull intrusion (Heggie 2005). The highest ^{232}Th/^{204}Pb (ψ) sample (03CAM228) has higher LREE contents (i.e., a higher La_N/Yb_N ratio) and enhanced Th, K and Rb (*see* Figure 21). The Rb/Sr and Sm/Nd data for this suite are consistent with it being the least contaminated suite, however, the ε_{Nd} of –0.5 indicates that even the most radiogenic sample (i.e., sample 03CAM228, *see* Table 2) may have been contaminated by crustal material. If so, the linear array is a binary mixing line, and has no age significance.

MCINTYRE SILLS

The lead isotopic data form an errorchron with a slope of 0.09 (Figure 22). They are anchored by a scatter of 3 points, and the line is thus controlled by 2 near-coincident radiogenic points. With such poor data distribution, the age determination is suspect. Nevertheless, the age is within error for the overall Logan igneous suite. This indicates that the data distribution may be due to *in situ* radiogenic growth and may also be related to melt contamination. Data for initial ^{86}Sr/^{87}Sr and elements that may represent melt contamination are plotted against ^{238}U/^{204}Pb (μ), a measure of radiogenicity, in Figure 23. These plots indicate an excellent correlation between ^{238}U/^{204}Pb (μ) and Th, U and initial ^{86}Sr/^{87}Sr, a negative correlation with the La/Yb_{cn} ratio, and no correlation with either K or Rb. The errorchron in this case is related to primary variability in U and Th. The correlation with initial ^{86}Sr/^{87}Sr indicates some relationship of this inhomogeneity to melt contamination, but there is no clear evidence that the contamination source was enriched in K or Rb. Thus, the best candidate for a contamination source would be carbonate from the Rossport Formation of the Sibley Group, which is enriched in radiogenic Sr (Franklin, Poulsen and McIlwaine 1972), as all other contamination sources should contain K and Rb. No REE data are currently available for the carbonate-rich portions of the Rossport Formation.

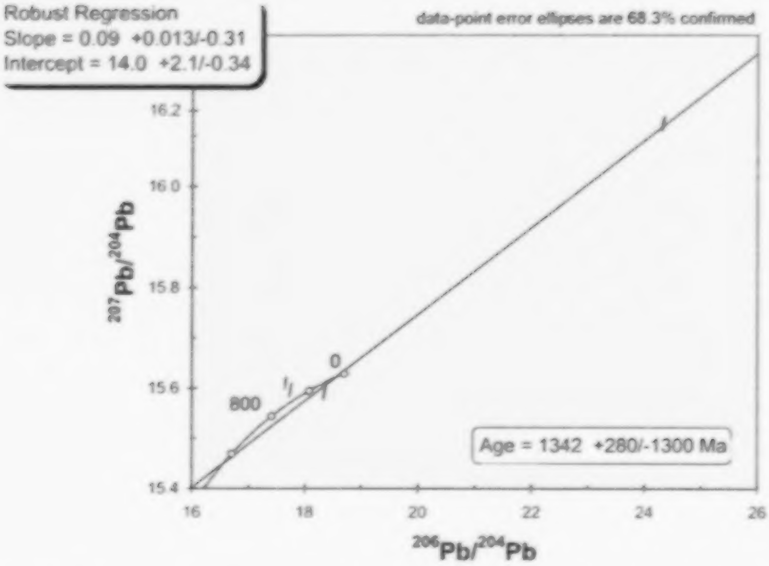

Figure 22. Uranogenic lead isotopic ($^{206}Pb/^{204}Pb$ versus $^{207}Pb/^{204}Pb$) diagram with isochron age and slope data for the McIntyre sills sample suite.

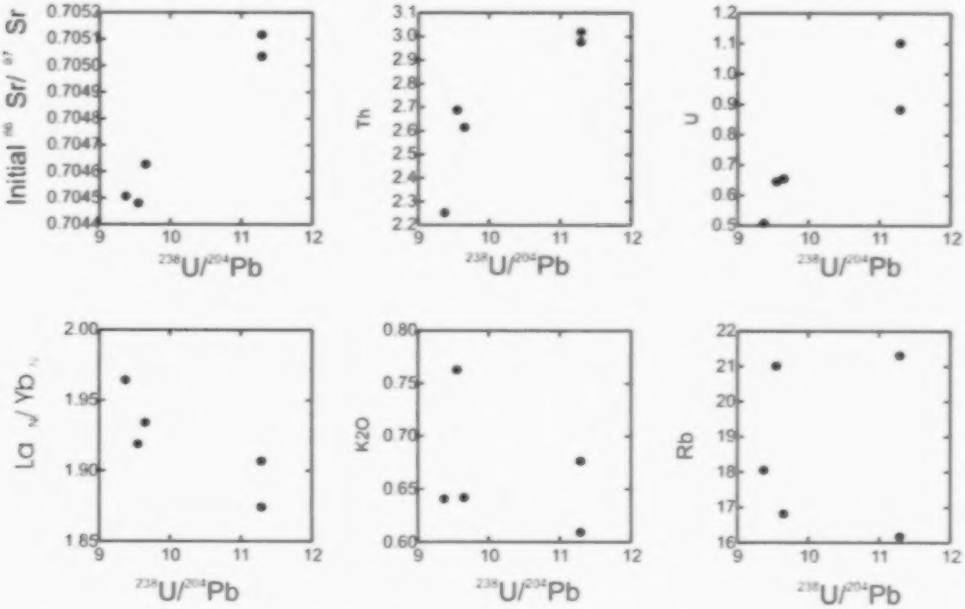

Figure 23. Plots for the McIntyre sills sample suite showing relationship between radiogenicity of the lead isotope determinations and various elements of isotopic ratios that are commonly indicators of melt contamination.

NIPIGON SILLS

The lead isotopic data form an elongate cluster (Figure 24), which parallels that for the McIntyre sills, but is of more limited extent and is also more radiogenic. One sample (ADH6-13) has very low ^{208}Pb/^{204}Pb composition and another (LN301) has a non-radiogenic ^{206}Pb/^{204}Pb composition. The thorogenic lead plot (*see* Figure 24) illustrates a distinctly linear data distribution.

These data were also compared with the same suite of elements or isotopic data that indicate melt contamination (Figure 25). These illustrate a moderately good correlation between all of the contamination indicators except Rb. This may indicate that the melt was contaminated by a feldspathic source, and not one containing abundant K mica. The Sibley Group rocks meet this criterion, but Archean granite cannot be excluded. A similar plot (not shown) for thorogenic lead (^{232}Th/^{204}Pb) shows almost no correlation between radiogenicity and the various indicators of melt contamination. The initial ^{86}Sr/^{87}Sr and K_2O contents of the Nipigon samples are strongly correlated (correlation co-efficient (r) =0.8), but not with Rb (r=0.1) also consistent with a potassium feldspar-rich contamination source.

Close inspection of these data indicate that one subset forms a distinctive linear array that is sufficiently coherent to permit a two-stage interpretation. These data are presented in Figure 26. This good linear array has an isochron age of 1255±490 Ma, and is within error of the well established ages for the Nipigon sills (Heaman and Easton 2005).

The significant variability amongst the overall sample set for the Nipigon sills is not easily explained. There are other, similar linear arrays of data that may be extracted from it, and yet others that are randomly more radiogenic than the array used above. This indicates that there may have been several magma pulses involved in forming this extensive suite, and that melt contamination may not have been consistent at either the melt batch or local scale. The best explanation will require a more robust examination of all of the geochemical data available.

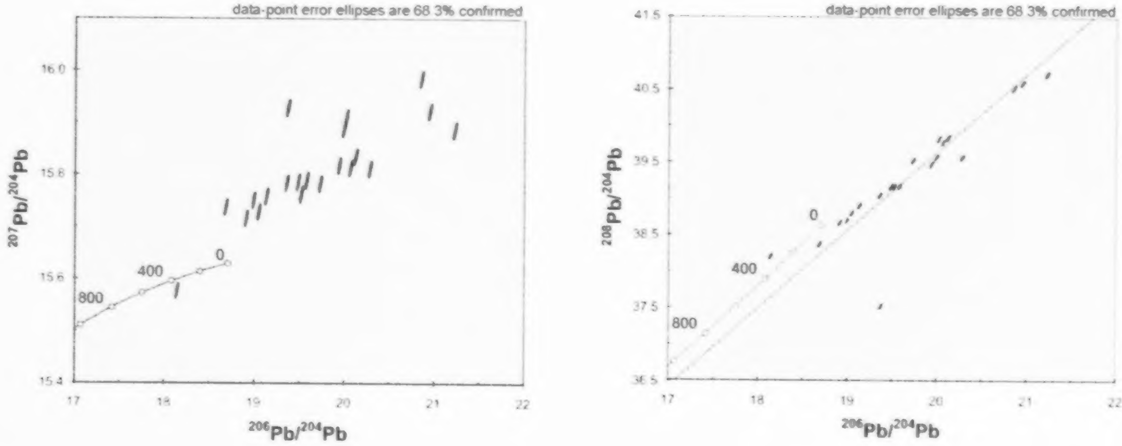

Figure 24. Lead isotopic (^{206}Pb/^{204}Pb versus ^{207}Pb/^{204}Pb) diagram of Nipigon sills samples.

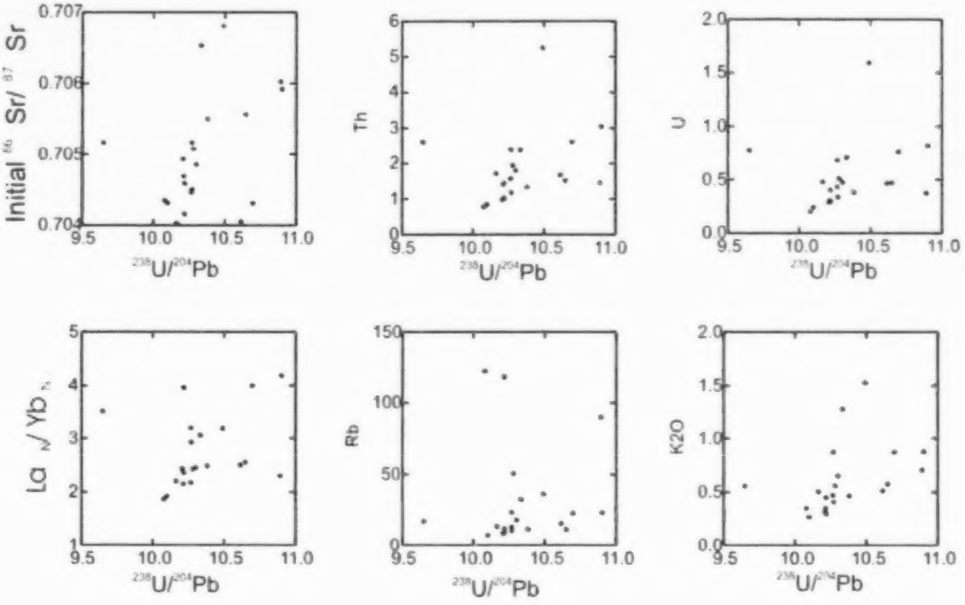

Figure 25. Plots for the Nipigon sills sample suite showing the relationship between radiogenicity of the lead isotope determinations and various elements of isotopic ratios that are commonly indicators of melt contamination.

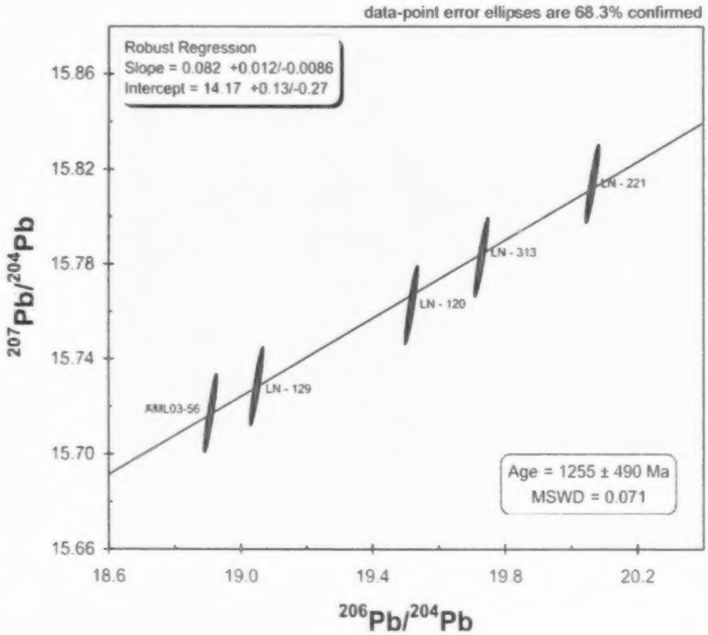

Figure 26. Lead isotopic ($^{206}Pb/^{204}Pb$ versus $^{207}Pb/^{204}Pb$) diagram for a subset of the Nipigon suite that forms a distinct linear array.

Table 3. Derived isotopic variables for the Lake Nipigon radiogenic isotope study. Note that the $^{238}U/^{204}Pb$ and $^{232}Th/^{204}Pb$ are calculated using the Stacey and Kramers (1975) model system. The choice of system is not critical, as the values will remain relatively the same regardless of the system used.

Unit	Number of Samples	Initial $^{87}Sr/^{86}Sr$	Initial $^{238}U/^{204}Pb$	Initial $^{232}Th/^{204}Pb$
Inspiration	4	0.706	10.691	43.126
Jackfish Island	3	0.704	9.789	38.897
Nipigon	21	0.705	10.343	37.163
McIntyre	5	0.705	10.229	37.979
Pillar Lake	5	0.707	12.190	54.740
Shillabeer	2	0.703	9.711	34.819
Unclassified	1	0.705	10.438	37.682

PILLAR LAKE VOLCANICS

The Proterozoic pillow basalt samples are unique within the overall data set; as noted above, the samples are all very radiogenic, are clearly compositionally separate from all other samples, form a reasonable Pb-isotopic linear array on the uranogenic plot (Figure 27, left) and are completely scattered on the thorogenic plot (Figure 27, right). They are typified by an anomalously high initial $^{86}Sr/^{87}Sr$ (Table 3) as well as distinctive geochemical attributes (*see* Figure 18).

The age of the Pillar Lake volcanics has not been accurately determined, and the Pb-isochron age presented here must be considered as a minimum value. In comparison with isochron ages for McIntyre and Nipigon sills, it appears to be older, consistent with the preliminary data provided elsewhere herein. The age is consistent with that for the mafic portion of the Badwater Creek gabbro (1598.7±1.1 Ma). The exceptionally high initial $^{86}Sr/^{87}Sr$ indicates that the flows interacted with seawater. The initial $^{86}Sr/^{87}Sr$ for the Sibley Group is 0.7056; all of the initial $^{86}Sr/^{87}Sr$ values for the Pillar Lake volcanics are higher than this value, consistent with a possible alteration source. Alternatively, given the apparent alkalic chemical composition of these rocks, this may represent a unique petrogenetic suite.

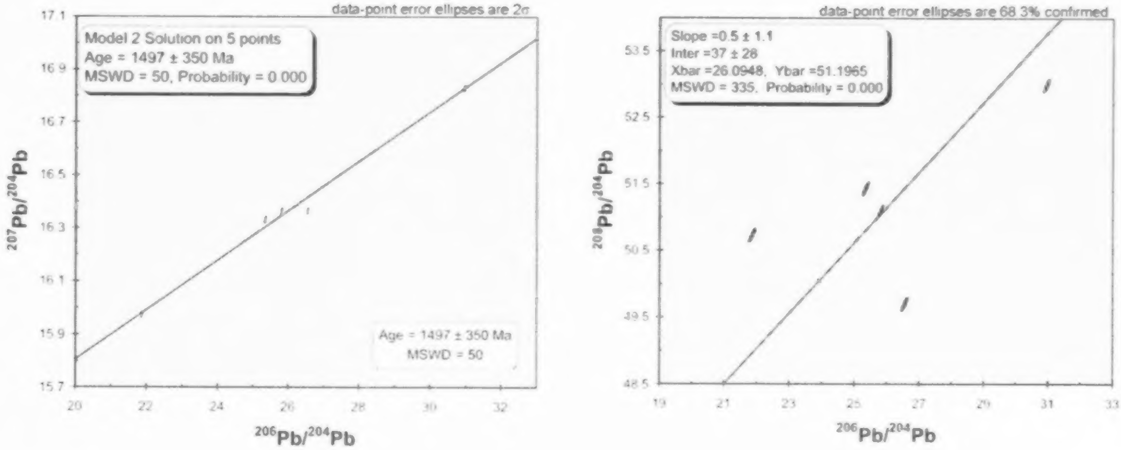

Figure 27. Lead isotopic ($^{206}Pb/^{204}Pb$ versus $^{207}Pb/^{204}Pb$) diagram of the Pillar Lake volcanics.

OTHER UNITS

Data for the Inspiration and Shillabeer samples (Figure 28) form clusters and can only be interpreted in the context of the other suites. The Inspiration samples are remarkably homogeneous, and formed from a melt that was remarkably well mixed with respect to U and Th. Data for the Inspiration sills are similar to those for the Nipigon sills, indicating that these may have a common parentage. The similar trace element geochemistry is consistent with this, but the ε_{Nd} data indicate that the Inspiration sills have undergone significantly more contamination by an older source. The compositions of the Inspiration sills have higher $^{207}Pb/^{204}Pb$ values than the Nipigon sills, perhaps indicating that the former are slightly older than the latter. This is consistent with their measured ages of 1159± 33 and 1109 to 1114 Ma ages, respectively.

The Shillabeer compositions are distinct from all others in this study (*see* Figures 18 and 19), and have the lowest $^{238}U/^{204}Pb$ and $^{232}Th/^{204}Pb$ values (*see* Table 3) of all. The Shillabeer sills are geochemically similar to the main ultramafic suite in the region (high La/Yb, high Mg number, Ti rich), including the Disraeli and Seagull intrusions. The Shillabeer samples also have the lowest initial $^{86}Sr/^{87}Sr$ of the entire analyzed suite, indicating a paucity of upper crustal contamination. The distinct isotopic characteristics of the Shillabeer sills should be re-considered after more data are collected for the ultramafic rocks in the region.

The only remaining sample, labelled "unclassified" in the sample data provided for this analysis (*see* Table 3), has compositional characteristics identical to the Nipigon sills, and probably is part of that suite.

SUMMARY OF LEAD ISOTOPE DATA

1. Lead isotope data from Proterozoic intrusive and volcanic sills in the Lake Nipigon area form several distinct clusters, and a few linear arrays that reflect both the ages and petrogenesis of these units.

2. The Jackfish Island sills, which have an ultramafic composition, appears to be unique in showing little evidence of post-emplacement radiogenic addition. It has formed from a mantle melt that was last tapped during the late Archean.

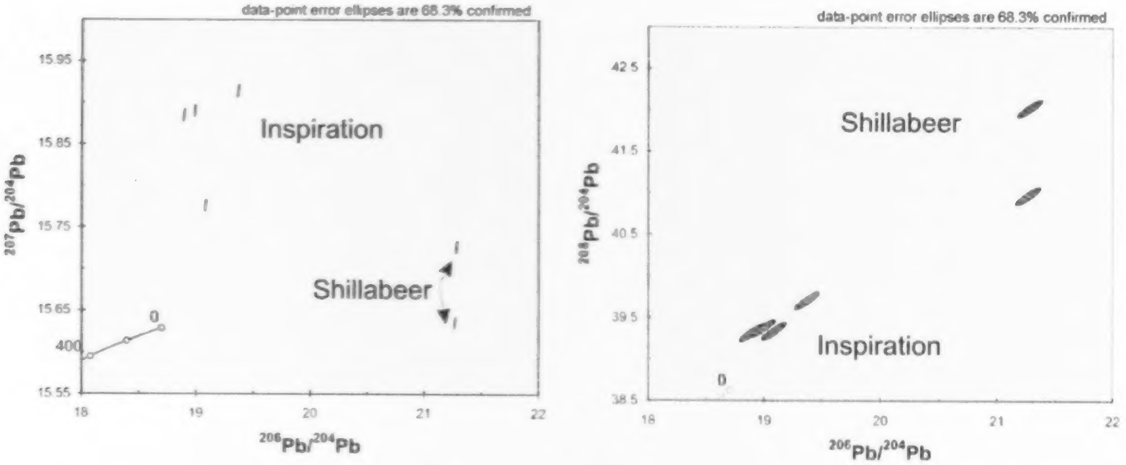

Figure 28. Lead isotopic ($^{206}Pb/^{204}Pb$ versus $^{207}Pb/^{204}Pb$) diagram of samples from the Inspiration and Shillabeer suites.

3. The Nipigon and McIntyre sills form linear arrays with slopes approximately 0.08 to 0.09, consistent with continuous addition of uranogenic lead from time of crystallization until present. The variability in the Nipigon sills may indicate a small, but variable, component of crustal contamination of melt batches. The Nipigon and McIntyre sills are isotopically separate, indicating that the McIntyre sills are older than the Nipigon sills.

4. The Inspiration sills are isotopically very distinct from all of the others. The relatively homogeneous composition indicates that these sills formed from a well-mixed melt, are significantly (~50 my) older than the Nipigon and McIntyre sills, and have not been strongly contaminated.

5. The Shillabeer sills have a unique lead isotope composition relative to all others in this study. The exceptionally low radiogenic content of these samples indicates that they came from a unique melt. These sills have not been strongly contaminated by upper crustal material.

6. The Pillar Lake volcanics are completely different in their lead isotopic attributes as compared to the other units in this study. They are marked by exceptionally radiogenic lead, but the uranogenic lead ratios form a distinct linear array, which enables the calculation of a minimum age of approximately 1500 Ma. This is consistent with ages determined for the felsic and mafic components of the Badwater Creek intrusion, and suggests that this volcanic unit did not form as apart of the Midcontinent Rift magmatic suite, but rather at a significantly earlier time. The strongly radiogenic nature of these samples may be related to their melt composition (alkaline?) or to exceptional seawater alteration. The high initial $^{86}Sr/^{87}Sr$ in these samples is consistent with the latter.

Conclusions

The geochemical and isotopic data generated as part of this study and the work of MacDonald (2004) have demonstrated that the diabase sills around Lake Nipigon are not the homogenous sequence they were thought to be. Four geochemically distinct suites can be recognized: the Nipigon sills, which are areally the most extensive; the Inspiration sills in the northwest; and the spatially restricted Shillabeer and Jackfish–McIntyre sills. All these sills show trace element and isotopic evidence that they have been contaminated by older basement material during ascent and emplacement. This contamination appears to be highly varied and, in some cases, very localized (e.g., the Shillabeer sills). The Inspiration and Shillabeer sills show the most negative ε_{Nd} values, but the Pb and Rb/Sr data suggest very different contaminants. The variable contamination of the sills may in part be a product of the extension rate in the rift, which would imply that the extension rate in the rift increased between the emplacement of the Inspiration and the Nipigon sills.

Acknowledgments

We are grateful to Tom Hart, Carol Anne MacDonald, Michael Easton, Mark Smyk and Larry Heaman for insightful discussions during the course of this project. Geoff Heggie and Riku Metsaranta assisted with the field work component of this study and their efforts are greatly appreciated. Anne Hammond provided invaluable assistance with sample preparation. Wally Rayner is thanked for his efforts co-ordinating the Lake Nipigon Region Geoscience Initiative.

References

Addison, W.D., Brumpton, G.R., Vallini, D.A., McNaughton, N.J., Davis, D.W., Kissin, S.A., Fralick, P.W. and Hammond, A.L. 2005. Discovery of distal ejecta from the 1850 Ma Sudbury impact event; Geology, v.33, p.193-196.

Anglin, C.D. and Franklin, J.M. 1985. Gold mineralization in the Beardmore–Geraldton area of northwestern Ontario: structural considerations and role of iron formation; Geological Survey of Canada, Paper 85-1A, p.193-201.

Anglin, C.D., Franklin, J.M., Loveridge, W.D., Hunt, P.A. and Osterburg, S.A. 1988. Use of zircon U-Pb ages of felsic intrusive and extrusive rocks in eastern Wabigoon Subprovince, Ontario, to place constraints on base metal and gold mineralization; *in* Radiogenic Age and Isotopic Studies, Report 2, Geological Survey of Canada, Paper 88-2, p.109-115.

Bell, R. 1870. Report of Mr. Robert Bell on lakes Superior and Nipigon; Geological Survey of Canada, Report of Progress 1866–69, Part IX, p.313-364.

Blackburn, C.E., Johns, G.W., Ayer, J. and Davis, D.W. 1991. Wabigoon Subprovince, *in* Geology of Ontario, Ontario Geological Survey, Special Volume 4, Part 1, p.303-382.

Cameron, K.L., Lopez, R., Ortega-Gutiérrez, F., Solari, L.A., Keppie, J.D. and Schulze, C. 2004. U-Pb geochronology and Pb isotopic compositions of leached feldspars: constraints on the origin and evolution of Grenville rocks from eastern and southern Mexico; *in* Proterozoic tectonic evolution of the Grenville Orogen in North America, Geological Society of America, Memoir 197, p.755-769.

Cannon, W.F., Green, A.G., Hutchinson, D.R., Lee, M., Milkereit, B., Behrendt, J.C., Halls, H.C., Green, J.C., Dickas, A.B., Morey, G.B., Sutcliffe, R.H. and Spencer, C. 1989. The North American Midcontinent Rift beneath Lake Superior from GLIMPSE seismic reflection profiling; Tectonics, v.8, p.305-332.

Card, K.D. and Ciesielski, A. 1986. DNAG #1. Subdivisions of the Superior Province of the Canadian Shield; Geoscience Canada, v.13, p.5-13.

Cheadle, B.A. 1986. Alluvial-playa sedimentation in the lower Keweenawan Sibley Group, Thunder Bay District, Ontario; Canadian Journal of Earth Sciences, v.23, p.527-542.

Coates, M.E. 1972. Geology of the Black Sturgeon River area, District of Thunder Bay; Ontario Department of Mines and Northern Affairs, Geoscience Report 98, 41p.

Creaser, R.A., Erdmer, P., Stevens, R.A. and Grant, S.L. 1997. Tectonic affinity of Nisutlin and Anvil assemblage strata from the Teslin tectonic zone, northern Canadian Cordillera: constraints from neodymium isotope and geochemical evidence; Tectonophysics, v.16, p.107-121.

Cumming, G.L. and Krstic, D. 1991. Geochronology at the Namew Lake Cu-Ni deposit, Flin-Flon area, Manitoba, Canada: a Pb–Pb study of whole rocks and ore minerals, Canadian Journal of Earth Sciences, v.28, p.1328-1339.

Davis, D.W. 1999. Report for the Ontario Geological Survey on the U–Pb geochronology of rocks from the Onaman Lake belt; Earth Science Department, Royal Ontario Museum, Toronto, Ontario, 20p.

Davis, D.W. and Green, J.C. 1997. Geochronology of the North American Midcontinent Rift in western Lake Superior and implications for its geodynamic evolution; Canadian Journal of Earth Sciences, v.34, p.476-488.

Davis, D.W. and Jackson, M.C. 1988. Geochronology of the Lumbey Lake greenstone belt: a 3 Ga complex within the Wabigoon Subprovince, northwest Ontario; Geological Society of America, Bulletin, v.100, p.818-824.

Davis, D.W. and Sutcliffe, R.H. 1985. U-Pb ages from the Nipigon Plate and northern Lake Superior; Geological Society of America Bulletin, v.96, p.1572-1579.

Faure, G. 1986. Principles of isotope geology; John Wiley and Sons, New York, 589p.

Franklin, J.M. 2003. Review of the petrochemistry of the mafic and ultramafic rocks in the Teck–Cominco drill core (2002) for the Nipigon region and Summary comments on the petrochemistry of the Nipigon Embayment and Keweenawan Rift Sequence; unpublished report, Teck–Cominco Ltd., 34p.

Franklin, J.M., McIlwaine, W.H., Poulsen, K.H. and Wanless, R.K. 1980. Stratigraphy and depositional setting of the Sibley Group, Thunder Bay District, Ontario, Canada; Canadian Journal of Earth Sciences, v.17, p.633-651.

Franklin, J.M., Poulsen, K.H. and McIlwaine, W.H. 1972. Stratigraphy of the Sibley Group, a Helikian red bed sequence; Geological Society of America, Abstracts with Programs, v.4, p.509.

Franklin, J.M., Sangster, D.F., Roscoe, S.M. and Loveridge, W.D. 1983. Lead isotope studies in Superior and Southern provinces; Geological Survey of Canada, Bulletin 351, 60p.

Gibson, S.A., Thompson, R.N. and Dickin, A.P. 2000. Ferropicrites: geochemical evidence for Fe-rich streaks in upwelling mantle plumes; Earth and Planetary Science Letters, v.174, p.355-374.

Green, J.C. 1971. The North Shore Volcanic Group; Institute on Lake Superior Geology, 17th Annual Meeting, Duluth, Minnesota, May 1971, Program, v.17, p.73-96.

——— 1989. Physical volcanology of mid-Proterozoic plateau lavas: the Keweenawan North Shore Volcanic Group, Minnesota; Geological Society of America Bulletin, v.101, p.486-500.

Green, J.C. and Fitz, T.J. 1993. Extensive felsic lavas and rheoignimbrites in the Keweenawan Midcontinent Rift plateau volcanics, Minnesota: petrographic and field recognition; Journal of Volcanology and Geothermal Research, v.54, p.177-196.

Halls, H.C. 1974. Magnetic studies in northern Lake Superior; Canadian Journal of Earth Sciences, v.9, p.1349-1367.

Hart, T.R. 2005a. Precambrian geology of the southern Black Sturgeon River and Seagull Lake area, Nipigon Embayment, northwestern Ontario; Ontario Geological Survey, Open File Report 6165, 63p.

——— 2005b. Field Trip 5. Geology of the Black Sturgeon area; Institute on Lake Superior Geology, 51st Annual Meeting, Nipigon, Ontario, Part 2 – Guidebooks, v.51, pt.2, p.85-104.

Hart, T.R., Hollings, P., Heggie, G. and MacDonald, C.A. 2005. Proterozoic platinum group element mineralization of the Nipigon Embayment, northwest Ontario; poster abstract *in* 10th International Platinum Symposium, 8-11 August, 2005, Oulu, Finland, Geological Survey of Finland, 10th International Platinum Symposium, Extended Abstracts, p.362-364.

Hart, T.R. and MacDonald, C.A. 2005. Geology and mineralization of the Proterozoic and Archean rocks of the Nipigon Embayment: Lake Nipigon Region Geoscience Initiative; Ontario Exploration and Geoscience Symposium, December 13-15, 2005, Toronto, Ontario.

Hart, T.R., MacDonald, C.A., Hollings, P. and Richardson, A. 2005. Proterozoic intrusive rocks of the Nipigon Embayment and Midcontinent Rift; poster abstract *in* 10th International Platinum Symposium, 8-11 August, 2005, Oulu, Finland, Geological Survey of Finland, 10th International Platinum Symposium, Extended Abstracts, p.365-368.

Hart, T.R. and Magyarosi, Z. 2004a. Precambrian geology of the northern Black Sturgeon River and Disraeli Lake area, Nipigon Embayment, northwestern Ontario; Ontario Geological Survey, Open File Report 6138, 56p.

——— 2004b. Northern Black Sturgeon River–Disraeli Lake area, Nipigon Embayment, northwestern Ontario: lithogeochemical, assay and compilation data; Ontario Geological Survey, Miscellaneous Release—Data 133.

Hart, T.R. and Préfontaine, S. 2004a. Precambrian geology of the northern Black Sturgeon River area, Nipigon Embayment, northwestern Ontario; Ontario Geological Survey, Preliminary Map P.3538, scale 1:50 000.

——— 2004b. Precambrian geology of the Disraeli Lake area, Nipigon Embayment, northwestern Ontario; Ontario Geological Survey, Preliminary Map P.3539, scale 1:50 000.

Hart, T.R., ter Meer, M. and Jolette, C. 2002. Precambrian geology of Kitto, Eva, Summers, Dorothea and Sandra townships, Beardmore area, northwestern Ontario; Ontario Geological Survey, Open File Report 6095, 206p.

Hart, T.R., Whaley, A.G. and Pace, A. 2005. Precambrian geology of the southern Black Sturgeon River–Seagull Lake–Disraeli Lake area, Nipigon Embayment, northwestern Ontario; Ontario Geological Survey, Preliminary Map P.3562, scale 1:50 000.

Heaman, L.M. and Easton, R.M. 2005. Proterozoic history of the Lake Nipigon area, Ontario: constraints from U-Pb zircon and baddeleyite dating; abstract *in* Institute on Lake Superior Geology, 51st Annual Meeting, Nipigon, Ontario, Part 1 – Proceedings and Abstracts, v.51, pt.1, p.24-25.

Heggie, G.J. 2005. Whole rock geochemistry, mineral chemistry, petrology and Pt, Pd mineralization of the Seagull intrusion, northwestern Ontario; unpublished MSc thesis, Lakehead University, Thunder Bay, Ontario, 156p.

Henry, P., Stevenson, R.K. and Gariepy, C. 1998. Late Archean mantle composition and crustal growth in the western Superior Province of Canada: neodymium and lead isotopic evidence from the Wawa, Quetico and Wabigoon subprovinces; Geochimica et Cosmochimica Acta, v.62, p.143-157.

Hergt, J.M., Peate, D.W. and Hawkesworth, C.J. 1991. The petrogenesis of Mesozoic Gondwana low-Ti flood basalts; Earth and Planetary Science Letters, v.105, p.134-148.

Hinchey, J.G., Hattori, K.H. and Lavigne, M.J. 2005. Geology, petrology and controls on PGE mineralization of the southern Roby and Twilight zones, Lac des Iles Mine, Canada; Economic Geology, v.100, p.43-61.

Hollings, P., Fralick, P. and Kissin, S. 2004. Geochemistry and geodynamic implications of the Mesoproterozoic English Bay granite-rhyolite complex, northwestern Ontario; Canadian Journal of Earth Sciences, v.41, p.1329-1338.

Hollings, P. and Kerrich, R. 1998. Trace element systematics of ultramafic and mafic volcanic rocks from the 3 Ga North Caribou greenstone belt, northwestern Superior Province; Precambrian Research, v.93, p.257-279.

Holmden, C., Creaser, R.A., Muehlenbachs, K., Bergstrom, S.M. and Leslie, S.A. 1996. Isotopic and elemental systematics of Sr and Nd in 454 Ma biogenic apatites: implication for paleoseawater studies; Earth and Planetary Science Letters, v.142, p.425-437.

Huppert, H.E. and Sparks, S.J. 1985. Cooling and contamination of mafic and ultramafic magmas during ascent through continental crust; Earth and Planetary Science Letters, v.74, p.371-386.

Jenner, G.A. 1996. Trace element geochemistry of igneous rocks: geochemical nomenclature and analytical geochemistry; *in* Trace element geochemistry of volcanic rocks: applications for massive sulphide exploration; Geological Association of Canada, Short Course Notes, v.12, p.51-77.

Jenner, G.A., Longerich, H.P., Jackson, S.E. and Fryer, B.J. 1990. ICP-MS – A powerful tool for high precision trace-element analysis in earth sciences: evidence from analysis of selected USGS reference samples; Chemical Geology, v.83, p.133-148.

Jensen, L.S. 1976. A new cation plot for classifying subalkalic rocks; Ontario Geological Survey, Miscellaneous Paper 66, 22p.

Klasner, J.S., Cannon, W.F. and Van Schmus, W.R. 1982. The pre-Keweenawan tectonic history of the southern Canadian Shield and its influence on formation of the Midcontinent Rift; *in* Geology and tectonics of the Lake Superior Basin, Geological Society of America, Memoir 156, p.27-45.

Klewin, K.W. and Shirey, S.B. 1992. The igneous petrology and magmatic evolution of the Midcontinent rift system; Tectonophysics, v.213, p.33-40.

Lawson, A.C. 1885. Report on the geology of the Lake of the Woods region, with special reference to the Keewatin (Huronian?) belt of the Archean rocks; Geological Survey of Canada, Annual Report (new series), v.1, Report CC, 151p.

——— 1888. Report on the geology of the Rainy Lake region; Geological Survey of Canada, Annual Report, v.13, pt.1, Report F, 182p.

——— 1913. The Archean geology of the Rainy Lake region restudied; Geological Survey of Canada, Memoir 40, 115p.

Lightfoot, P.C., Sage, R.P., Doherty, W., Naldrett, A.J. and Sutcliffe, R.H. 1999. Mineral potential of Proterozoic Keweenawan intrusions: implications of major and trace element geochemical data from bimodal mafic and felsic volcanic sequences of Mamainse Point and the Black Bay Peninsula, Ontario; Ontario Geological Survey, Open File Report 5998, 91p.

Lightfoot, P., Sutcliffe, R. and Doherty, W. 1991. Crustal contamination identified in Keweenawan Osler Group tholeiites, Ontario: a trace element perspective; Journal of Geology, v.99, p.739-760.

Logan, W.E. 1863. Report on the geology of Canada; Canadian Geological Survey, Geological Report Program 1863, 983p.

Longerich, H.P., Jenner, G.A., Fryer, B.J. and Jackson, S.E. 1990. Inductively coupled plasma-mass spectrometric analysis of geological samples: a critical evaluation based on case studies; Chemical Geology, v.83, p.105-118.

Ludwig, K.R. 2000. User's manual for Isoplot/Ex, version 2.2: a geochronological toolkit for Microsoft® Excel; University of California–Berkeley, Berkeley, California, Berkeley Geochronology Center, Special Publication No. 1a, 56p.

Lugmair, G.W. and Galer, S.J.G. 1992. Age and isotope relationships among the angrites Lewis Cliff 86010 and Angra dos Reis; Geochimica et Cosmochimica Acta, v.56, p.1673-1694.

Lundstrom, C., Gill, J., Williams, Q. and Perfit, M.P. 1995. Mantle melting and basalt extraction by equilibrium porous flow; Science, v.270, p.1958-1962.

MacDonald, C.A. 2004. Precambrian geology of the south Armstrong–Gull Bay area, Nipigon Embayment, northwestern Ontario; Ontario Geological Survey, Open File Report 6136, 42p.

MacDonald, C.A., ter Meer, M., Lepage, L., Préfontaine, S. and Tremblay, E. 2004a. Precambrian geology of the Waweig–Wabinosh lakes area, western Nipigon Embayment, northwestern Ontario; Ontario Geological Survey, Preliminary Map P.3536, scale 1:50 000.

——— 2004b. Precambrian geology of the English Bay–Havoc Lake area, western Nipigon Embayment, northwestern Ontario; Ontario Geological Survey, Preliminary Map P.3537, scale 1:50 000.

MacDonald, C.A. and Tremblay, E. 2004a. Geological and lithogeochemical data from the northwest Nipigon Embayment, Lake Nipigon Region Geoscience Initiative (LNRGI); Ontario Geological Survey, Miscellaneous Release—Data 132.

——— 2004b. Lake Nipigon Region Geoscience Initiative: Results of bedrock mapping in the northern part of the western Nipigon Embayment, northwestern Ontario, Canada; oral presentation abstract *in* Institute on Lake Superior Geology, Proceedings, v.50, pt.1, Programs and Abstracts, p.102-103.

——— 2004c. Precambrian geology of the south Armstrong–Gull Bay area, Nipigon Embayment, northwestern Ontario, Canada; poster abstract *in* Institute on Lake Superior Geology, Proceedings, v.50, pt.1, Programs and Abstracts, p.104-105.

MacDonald, C.A., Tremblay, E. and Easton, R.M. 2005. Precambrian geology of the west-central map area, Nipigon Embayment, northwestern Ontario: Lake Nipigon Region Geoscience Initiative; Ontario Geological Survey, Open File Report 6164, 49p.

MacDonald, C.A., Tremblay, E. and ter Meer, M. 2005a. Precambrian geology of the Kabitotikwia Lake area, west-central Nipigon Embayment, northwestern Ontario, Ontario Geological Survey, Preliminary Map P.3559, scale 1:50 000.

——— 2005b. Precambrian geology of the Cheeseman–Black Sturgeon lakes area, west-central Nipigon Embayment, northwestern Ontario; Ontario Geological Survey, Preliminary Map P.3560, scale 1:50 000.

MacDonald, C.A., Tremblay, E., ter Meer, M., Hart, T.R. and Easton, R.M. 2005. Precambrian geology of the Max–Muskrat lakes area, west-central Nipigon Embayment, northwestern Ontario; Ontario Geological Survey, Preliminary Map P.3561, scale 1:50 000.

Mason, J.K. and White, G.D. 1986. Gold occurrences, prospects and deposits of the Beardmore–Geraldton area; Ontario Geological Survey, Open File Report 5630, 680p.

McCuaig, T.C., Kerrich, R. and Xie, Q. 1994. Phosphorous and high field strength anomalies in Archean high-magnesian magmas as possible indicators of source mineralogy and depth; Earth and Planetary Science Letters, v.124, p.221-239.

Middleton, R.S., Borradaile, G.J., Baker, D. and Lucas, K. 2004. Proterozoic diabase sills of northern Ontario: magnetic properties and history; Journal of Geophysical Research, v.109, B02103, doi:10.1029/2003JB002581.

Miller, J.D., Green, J.C., Severson, M.J., Chandler, V.W., Hauck, S.A., Peterson, D.M. and Wahl, T.E. 2002. Geology and mineral potential of the Duluth Complex and related rocks of northeastern Minnesota; Minnesota Geological Survey, Report of Investigations 58, 207p.

Morton, R.L. and Franklin, J.M. 1987. Two-fold classification of Archean volcanic-associated massive sulfide deposits; Economic Geology, v.82, p.1057-1063.

Nicholson, S.W. and Shirey, S.B. 1990. Midcontinent Rift volcanism in the Lake Superior Region: Sr, Nd and Pb isotopic evidence for a mantle plume origin; Journal of Geophysical Research, v.95, no.B7, p.10 851-10 868.

Nicholson, S.W., Shirey, S., Schulz, K. and Green, J. 1997. Rift-wide correlation of 1.1 Ga Midcontinent rift system basalts: implications for multiple mantle sources during rift development; Canadian Journal of Earth Sciences, v.34, p.504-520.

Ontario Geological Survey 2003. 1:250 000-scale bedrock geology of Ontario; Ontario Geological Survey, Miscellaneous Release—Data 126.

——— 2004a. Airborne magnetic and gamma-ray spectrometric surveys, residual magnetic field and Keating coefficients, Lake Nipigon Embayment area (Lake Nipigon Geoscience Initiative); Ontario Geological Survey, Geophysical Maps 81 812 to 81 823, scale 1:50 000.

——— 2004b. Airborne magnetic and gamma-ray spectrometric surveys, residual magnetic field and Keating coefficients, Lake Nipigon Embayment area (Lake Nipigon Geoscience Initiative); Ontario Geological Survey, Geophysical Maps 81 848 to 81 849, scale 1:100 000.

——— 2004c. Airborne magnetic and gamma-ray spectrometric surveys, shaded image of the second vertical derivative of the magnetic field and Keating coefficients, Lake Nipigon Embayment area (Lake Nipigon Geoscience Initiative); Ontario Geological Survey, Geophysical Maps 81 824 to 81 835, scale 1:50 000.

——— 2004d. Airborne magnetic and gamma-ray spectrometric surveys, shaded image of the second vertical derivative of the magnetic field and Keating coefficients, Lake Nipigon Embayment area (Lake Nipigon Geoscience Initiative); Ontario Geological Survey, Geophysical Maps 81 850 to 81 851, scale 1:100 000.

——— 2004e. Airborne magnetic and gamma-ray spectrometric surveys, ternary radioelement image, Lake Nipigon Embayment area (Lake Nipigon Geoscience Initiative); Ontario Geological Survey, Geophysical Maps 81 836 to 81 847, scale 1:50 000.

——— 2004f. Airborne magnetic and gamma-ray spectrometric surveys, ternary radioelement image, Lake Nipigon Embayment area (Lake Nipigon Geoscience Initiative); Ontario Geological Survey, Geophysical Maps 81 852 to 81 853, scale 1:100 000.

——— 2004g. Ground gravity survey, terrain-corrected Bouguer anomaly, southern part, Lake Nipigon Embayment area (Lake Nipigon Region Geoscience Initiative); Ontario Geological Survey, Geophysical Map 81 930, scale 1:100 000.

——— 2004h. Ground gravity survey, terrain-corrected Bouguer anomaly, northern part, Lake Nipigon Embayment area (Lake Nipigon Region Geoscience Initiative); Ontario Geological Survey, Geophysical Map 81 931, scale 1:100 000.

——— 2004i. Ground gravity survey, first vertical derivative of the terrain-corrected Bouguer anomaly, southern part, Lake Nipigon Embayment area (Lake Nipigon Region Geoscience Initiative); Ontario Geological Survey, Geophysical Map 81 932, scale 1:100 000.

——— 2004j. Ground gravity survey, first vertical derivative of the terrain-corrected Bouguer anomaly, northern part, Lake Nipigon Embayment area (Lake Nipigon Region Geoscience Initiative); Ontario Geological Survey, Geophysical Map 81 933, scale 1:100 000.

——— 2004k. Ground gravity survey, residual of the terrain-corrected Bouguer anomaly, southern part, Lake Nipigon Embayment area (Lake Nipigon Region Geoscience Initiative); Ontario Geological Survey, Geophysical Map 81 934, scale 1:100 000.

——— 2004l. Ground gravity survey, residual of the terrain-corrected Bouguer anomaly, northern part, Lake Nipigon Embayment area (Lake Nipigon Region Geoscience Initiative); Ontario Geological Survey, Geophysical Map 81 935, scale 1:100 000.

——— 2005. Ontario airborne geophysical surveys, magnetic and gamma-ray spectrometric data, grid and vector data and profile data, Lake Nipigon Embayment area (Lake Nipigon Region Geoscience Initiative: PU 03-103); Ontario Geological Survey, Geophysical Data Set 1047.

Osmani, I.A. and Rees, K. 1998. Report on the Phase I Exploration Program, Wolf Mountain property, north of Lake Superior, District of Thunder Bay, Leckie Lake Area G-67; Thunder Bay Resident Geologist's office, assessment file, 52H0SW2001, 2.19142.

Paces, J.B. 1988. Magmatic processes, evolution and mantle source characteristics contributing to the petrogenesis of Midcontinent Rift basalts: Portage Lake volcanics, Keweenaw Peninsula, Michigan; unpublished PhD thesis, Michigan Technological University, Houghton, Michigan, 432p.

Paces, J.B. and Miller, J.D. 1993. Precise U-Pb ages of Duluth Complex and related mafic intrusions, northeastern Minnesota; geochronological insights to physical, petrogenetic, paleomagnetic, and tectonomagnetic processes associated with the 1.1 Ga Midcontinent Rift System; Journal of Geophysical Research, Part B - Solid Earth and Planets, v.B98, p.13,997-14,013.

Pan, Y., Fleet, M.E. and Longstaffe, F.J. 1999. Melt related metasomatism in mafic granulites of the Quetico Subprovince of Ontario: constraints from O-Sr-Nd isotopic and fluid inclusion data; Canadian Journal of Earth Sciences, v.36, p.1449-1462.

Pearce, J.A. 1996. A user's guide to basalt discrimination diagrams; *in* Trace element geochemistry of volcanic rocks: applications for massive sulphide exploration, Geological Association of Canada, Short Course Notes, v.12, p.79-113.

Peate, D.W. and Hawkesworth, C.J. 1996. Lithospheric to asthenospheric transition in low-Ti flood basalts from southern Parana, Brazil; Chemical Geology, v.127, p.1-24.

Percival, J.A. and Williams, H.R. 1989. The Quetico accretionary complex, Superior Province, Canada; Geology, v.17, p.23-25.

Pettijohn, F.J. 1935. Stratigraphy and structure of Vermillion Township, District of Kenora, Ontario; Geological Society of America Bulletin, v.46, p.1891-1908.

Richardson, A.J. 2003. Pass Lake Formation sediment provenance; unpublished BSc(Hons) thesis, Lakehead University, Thunder Bay, Ontario, 40p.

Richardson, A.J. and Hollings, P. 2004. Lake Nipigon Region Geoscience Initiative. Geochemistry and mineralogy of the Nipigon diabase sills; *in* Summary of Field Work and Other Activities 2004, Ontario Geological Survey, Open File Report 6145, p.51-1 to 51-5.

Rogala, B. 2003. The Sibley Group: a lithostratigraphic, geochemical and paleomagnetic study; unpublished MSc thesis, Lakehead University, Thunder Bay, Ontario, 254p.

Schandl, E.S. 2004. Petrographic data from the northwest Nipigon Embayment: Lake Nipigon Region Geoscience Initiative (LNRGI); Ontario Geological Survey, Miscellaneous Release—Data 141.

——— 2005. Petrographic data from the west-central Nipigon Embayment: Lake Nipigon Region Geoscience Initiative; Ontario Geological Survey, Miscellaneous Release—Data 156.

Schwerdtner, W.M. 1984. Foliation patterns in large gneiss bodies of the Archean Wabigoon Subprovince, southern Canadian Shield; Journal of Geodynamics, v.1, p.313–337.

Scott, J.F. 1987. Uranium occurrences of the Thunder Bay–Nipigon–Marathon area; Ontario Geological Survey, Open File Report 5634, 158p.

Shirey, S., Klewin, K., Berg, J. and Carlson, R. 1994. Temporal changes in the sources of flood basalts: isotopic and trace element evidence from the 1100 Ma old Keweenawan Mamainse Point Formation, Ontario, Canada; Geochimica et Cosmochimica Acta, v.58, p.4475-4490.

Stacey, J.S. and Kramers, J.D. 1975. Approximation of terrestrial lead isotope evolution by a two-stage model; Earth and Planetary Science Letters, v.26, p.207-221.

Stott, G.M. and Davis, D.W. 1999. Contributions to the tectonostratigraphic analysis of the Onaman–Tashota greenstone belt, eastern Wabigoon Subprovince; *in* Western Superior Transect Annual Meeting, Lithoprobe Report #70, Lithoprobe Secretariat, University of British Columbia, Vancouver, British Columbia, p.122–124.

Sun, S.-s. and McDonough, W.F. 1989. Chemical and isotopic systematics of oceanic basalts: implications for mantle composition and processes; *in* Magmatism in the ocean basins, Geological Society, Special Publication No.42, p.313-345.

Sutcliffe, R.H. 1982. Precambrian geology of the Wabigoon–Quetico subprovince boundary, Orient Bay sheet, Thunder Bay District; Ontario Geological Survey, Preliminary Map P.2531, scale 1:50 000.

——— 1986. Proterozoic rift-related igneous rocks at Lake Nipigon, Ontario; unpublished PhD thesis, University of Western Ontario, London, Ontario, 325p.

——— 1991. Proterozoic geology of the Lake Superior area; *in* Geology of Ontario, Ontario Geological Survey, Special Volume 4, Part 1, p.627-658.

Sutcliffe, R.H. and Smith, A.R. 1988. Geology of the St. Ignace Island volcanic-plutonic complex; *in* Summary of Field Work and Other Activities 1988, Ontario Geological Survey, Miscellaneous Paper 141, p.368-371.

Thomson, K. and Hutton, D. 2004. Geometry and growth of sill complexes: insights using 3D seismic from the North Rockall Trough; Bulletin of Volcanology, v.66, p.364-375.

Thurston, P.C. 1991. Archean geology of Ontario: Introduction; *in* Geology of Ontario, Ontario Geological Survey, Special Volume 4, Part 1, p.73-78.

Tomlinson, K.Y., Davis, D.W., Percival, J.A., Hughes, D.J. and Thurston, P.C. 2001. Mafic to felsic magmatism and crystal recycling in the Obonga lake greenstone belt, western Superior Province: evidence from geochemistry, Nd isotopes and U-Pb geochronology; Precambrian Research, v.114, p.295-325.

Tomlinson, K.Y., Davis, D.W., Stone, D. and Hart, T.R. 2003. U-Pb age and Nd isotopic evidence for Archean terrane development and crustal recycling in the south-central Wabigoon Subprovince, Canada; Contributons to Mineralogy and Petrology, v.144, p.684-702.

Tomlinson, K.Y., Stott, G., Percival, J.A. and Stone, D. 2004. Basement terrane correlations and crustal recycling in the western Superior Province: Nd isotopic characterof granitoid and felsic volcanic rocks in the Wabigoon Subprovince, N. Ontario, Canada; Precambrian Research, v.132, p.245-274.

Tosdal, R.M., Wooden, J.L. and Bouse, R.M. 1999. Pb isotopes, ore deposits and metallogenic terrains; *in* Application of radiogenic isotopes to ore deposit research and exploration, Society of Economic Geologists, Reviews in Economic Geology, v.12, p.1-28.

Turner, S.P. and Hawkesworth, C.J. 1995. The nature of the sub-continental mantle: constraints from the major element composition of continental flood basalts; Chemical Geology, v.120, p.295-314.

Vervoort, J.D. and Green, J.C. 1997. Origin of evolved magmas in the Midcontinent rift system, northeast Minnesota: Nd-isotope evidence for melting of Archean crust; Canadian Journal of Earth Sciences, v.34, p.521-535.

Vervoort, J.D., White, W.M. and Thorpe, R.I. 1994. Nd and Pb isotope ratios of the Abitibi greenstone belt: new evidence for very early differentiation of the Earth; Earth and Planetary Science Letters, v.128, p.215-229.

Vervoort, J.D., White, W.M., Thorpe, R.I. and Franklin, J.M. 1991. Archean mantle Pb and Nd isotopic evolution: evidence from footwall rocks to the Noranda and Matagami volcanogenic massive sulphide deposits, Abitibi greenstone belt, Quebec; Geological Association of Canada–Mineralogical Association of Canada–Society of Economic Geologists, Joint Annual Meeting, Program with Abstracts, v.16, p.A128.

Weiblen, P.W. and Morey, G.B. 1980. A summary of the stratigraphy, petrology and structure of the Duluth Complex; American Journal of Science, v.280A, p.88-133.

Williams, H.R. 1988. Geological studies in the Wawa, Quetico and Wabigoon subprovinces, with emphasis on structure and tectonic development; *in* Summary of Field Work and Other Activities 1988, Ontario Geological Survey, Miscellaneous Paper 141, p.169-172.

——— 1990. Subprovince accretion tectonics in the south-central Superior Province; Canadian Journal of Earth Sciences, v.27, p.570-581.

——— 1991. Quetico Subprovince; *in* Geology of Ontario, Ontario Geological Survey, Special Volume 4, Part 1, p.383-404.

Wilson, A.W.G. 1910. Geology of the Nipigon Basin, Ontario, Canada; Department of Mines, Geological Survey Branch, Memoir 1, 152p.

Wirth, K.R., Vervoort, J.D. and Naiman, Z.J. 1997. The Chengwatana Volcanics, Wisconsin and Minnesota: petrogenesis of the southernmost volcanic rocks exposed in the Midcontinent Rift; Canadian Journal of Earth Sciences, v.34, p.536-548.

York, D. 1969. Least-squares fitting of a straight line with correlated errors; Earth and Planetary Science Letters, v.5, p.329-324.

Appendix 1

Major, Trace and Rare Earth Element Geochemical Data for the Nipigon Sills

Universal Transverse Mercator (UTM) co-ordinates are North American Datum 1927 (NAD 27), Zone 16.

Appendix 1. Major, trace and rare earth element geochemical data for the Nipigon suite.

Sample	**LN-01**	**LN-03**	**LN-05**	**LN-07**	**LN-09**	**LN-11**	**LN-13**	**LN-15**	**LN-17**
Easting	366728	366507	370382	378116	389731	381569	386490	389706	385040
Northing	5338006	5545514	5554415	5563047	5562861	5554010	5550248	5546135	5545091
Datum	NAD 27	NAD 27	NAD 27	NAD 27	NAD 27	NAD 27	NAD 27	NAD 27	NAD 27
SiO_2	49.69	48.42	51.43	48.33	49.25	5.29	51.16	5.82	5.26
TiO_2	1.45	1.15	1.27	1.35	1.81	1.23	1.14	1.40	1.33
Al_2O_3	15.83	15.54	15.47	16.13	14.12	16.72	17.78	15.26	15.97
Fe_2O_3	14.39	14.32	11.68	14.52	16.64	11.67	11.75	13.28	12.67
MnO	0.20	0.20	0.19	0.28	0.24	0.19	0.16	0.20	0.19
MgO	6.12	7.57	6.22	6.00	4.79	6.32	4.83	5.65	6.20
CaO	9.74	1.27	9.96	1.37	9.91	1.67	9.78	1.13	1.45
K_2O	0.65	0.44	1.88	0.47	0.52	0.53	0.95	0.72	0.56
Na_2O	2.56	2.33	2.81	2.55	2.59	2.57	3.15	2.68	2.57
P_2O_5	0.13	0.99	0.12	0.13	0.17	0.19	0.18	0.15	0.19
Mg#	0.48	0.54	0.54	0.48	0.39	0.55	0.43	0.48	0.52
Ti	8793	6954	624	819	114	677	6896	7891	6249
P	574	436	526	569	742	482	793	658	481
Cr									
Ni	19.25	164.00	82.38	11.34	59.00	116.43	69.63	89.43	126.29
Rb	2.69	11.62	29.68	11.24	14.22	14.51	25.22	19.21	15.84
Sr	17.35	155.80	269.46	152.99	145.40	22.55	214.27	189.44	198.15
Cs	1.16	0.39	0.65	0.47	0.44	0.43	0.57	0.56	0.41
Sc	29.44	26.40	27.27	29.30	32.20	27.57	21.80	3.75	28.16
V	315.92	261.20	22.63	36.13		243.89	21.41	29.19	245.56
Ta	0.45	0.34	1.47	0.36	0.48	0.42	0.57	0.54	0.42
Nb	6.27	4.60	15.47	5.12	6.90	5.63	7.88	7.13	5.51
Zr	112.29	85.00	127.80	93.31	123.90	8.90	112.92	11.28	82.19
Hf	3.35	2.30	3.21	2.69	3.50	2.29	3.27	2.91	2.25
Th	2.29	1.58	3.87	1.24	1.73	2.00	3.37	2.79	1.95
U	0.68	0.46	0.96	0.37	0.46	0.56	0.85	0.79	0.56
Y	28.38	21.46	21.49	26.22	34.73	19.82	26.72	25.94	2.62
La	13.22	8.74	22.28	8.70	11.50	1.47	16.12	14.87	1.82
Ce	29.21	19.25	44.57	19.80	26.49	22.17	33.74	3.13	22.72
Pr	3.85	2.55	5.37	2.72	3.66	2.82	4.26	3.79	2.88
Nd	16.95	11.72	21.58	12.72	17.12	12.39	17.99	16.68	12.55
Sm	4.20	3.13	4.22	3.59	4.73	3.32	4.19	4.19	3.57
Eu	1.35	1.95	1.32	1.24	1.61	1.54	1.40	1.34	1.13
Gd	5.43	3.89	4.27	4.53	6.18	3.55	4.76	4.82	3.59
Tb	0.81	0.64	0.67	0.77	1.10	0.58	0.80	0.78	0.59
Dy	5.19	4.14	4.49	4.86	6.46	3.71	4.97	5.42	3.74
Ho	1.89	0.85	0.85	1.48	1.38	0.78	1.62	1.51	0.79
Er	3.78	2.42	2.41	2.95	3.96	2.22	3.45	3.98	2.29
Tm	0.44	0.35	0.35	0.43	0.58	0.33	0.44	0.45	0.34
Yb	2.81	2.26	2.42	2.89	3.72	2.18	2.76	2.89	2.15
Lu	0.43	0.33	0.33	0.42	0.54	0.32	0.50	0.44	0.33

Appendix 1. continued

Sample	LN-19	LN-21	LN-23	LN 25	LN 27	LN 32	LN 36	LN 70	LN 71
Easting	383156	379404	378158	368685	363245	358050	365704	355536	406072
Northing	5540435	5536573	5532006	5527317	5528445	5482410	5485959	5493869	5467746
Datum	NAD 27	NAD 27	NAD 27	NAD 27	NAD 27	NAD 27	NAD 27	NAD 27	NAD 27
SiO_2	49.53	48.54	48.80	48.75	49.57	48.84	48.28	48.86	49.28
TiO_2	1.65	1.12	1.23	1.13	2.84	1.37	1.44	1.49	1.14
Al_2O_3	15.50	13.35	14.97	15.83	12.90	13.73	14.56	14.39	14.22
Fe_2O_3	13.19	14.37	14.56	13.37	1.73	15.93	15.55	15.67	14.14
MnO	0.19	0.22	0.28	0.18	0.14	0.22	0.22	0.22	0.22
MgO	7.57	8.98	6.48	6.59	8.90	6.63	6.52	6.28	6.98
CaO	1.25	11.84	1.86	11.14	11.95	1.37	1.39	9.91	11.89
K_2O	0.58	0.31	0.46	0.36	0.62	0.36	0.41	0.49	0.38
Na_2O	2.50	2.28	2.40	2.67	3.00	2.52	2.59	2.67	2.47
P_2O_5	0.12	0.69	0.89	0.11	0.24	0.12	0.14	0.15	0.19
Mg#	0.56	0.58	0.49	0.52	0.62	0.48	0.48	0.47	0.53
Ti	6452	6834	7465	6535	1724	7737	8573	8993	6800
P	527	35	394	48	167	524	62	655	438
Cr									
Ni	167.98	165.00	128.53						
Rb	16.86	7.32	1.15	1.62	18.23	1.17	11.34	15.12	1.57
Sr	195.34	121.90	154.94	169.90	4.15	148.58	156.90	16.40	169.13
Cs	0.52	0.28	0.35	0.32	0.19	0.41	0.43	0.67	0.58
Sc	27.96	34.80	31.54	36.83	29.64	43.76	37.93	4.78	39.28
V	241.33	312.00	31.15	35.56	399.81	373.85	367.73	37.76	312.40
Ta	0.46	0.32	0.39	0.29	0.89	0.32	0.36	0.39	0.31
Nb	6.14	3.10	4.22	4.50	14.17	4.82	5.70	6.00	4.52
Zr	89.72	59.70	79.33	8.30	199.87	92.35	13.90	16.40	79.19
Hf	2.41	1.70	2.50	2.20	5.20	2.51	2.80	2.90	2.18
Th	2.23	1.30	1.59	1.15	2.45	1.23	1.35	1.48	1.13
U	0.66	0.30	0.47	0.30	2.19	0.33	0.38	0.49	0.35
Y	21.64	18.85	22.31	23.94	39.67	26.58	27.54	3.60	22.13
La	12.98	5.82	8.64	7.99	25.40	8.45	9.60	9.81	7.57
Ce	25.22	13.36	19.49	18.45	7.24	19.25	21.74	22.68	16.82
Pr	3.18	1.88	2.64	2.50	9.93	2.62	2.97	3.13	2.30
Nd	13.43	8.78	12.98	11.46	42.27	12.32	13.84	14.48	1.79
Sm	3.28	2.48	3.23	3.28	1.13	3.54	3.82	4.11	3.11
Eu	1.13	0.87	1.21	1.21	2.98	1.25	1.33	1.42	1.96
Gd	3.89	3.17	4.12	4.29	9.74	4.44	4.80	5.16	3.72
Tb	0.65	0.54	0.72	0.68	1.42	0.76	0.79	0.89	0.63
Dy	4.11	3.42	4.43	4.38	8.30	4.89	5.30	5.69	3.93
Ho	0.87	0.73	0.95	0.92	1.53	1.35	1.54	1.18	0.85
Er	2.57	2.13	2.72	2.66	4.31	2.99	3.90	3.36	2.45
Tm	0.37	0.38	0.40	0.38	0.56	0.43	0.44	0.48	0.35
Yb	2.27	1.99	2.53	2.41	3.48	2.74	2.76	3.14	2.23
Lu	0.34	0.30	0.40	0.36	0.53	0.41	0.42	0.47	0.34

Appendix 1. continued

Sample	**LN - 76**	**LN 79**	**LN - 86**	**LN - 89**	**LN 92**	**LN - 95**	**LN 96**	**LN - 98**	**LN - 113**
Easting	398211	392267	390262	386998	388049	380298	377215	374660	386895
Northing	5468311	5476885	5489534	5489222	5479532	5474488	5476810	5482470	5494765
Datum	NAD 27	NAD 27	NAD 27	NAD 27	NAD 27	NAD 27	NAD 27	NAD 27	NAD 27
SiO_2	49.54	51.28	47.25	49.65	47.36	49.87	47.96	48.56	48.29
TiO_2	1.65	2.40	0.85	1.23	0.99	1.24	1.25	0.98	1.26
Al_2O_3	13.75	12.14	17.44	15.18	15.47	15.00	12.92	15.32	14.87
Fe_2O_3	15.74	18.77	14.15	11.58	14.49	13.95	15.61	13.16	14.58
MnO	0.24	0.24	0.20	0.18	0.19	0.22	0.21	0.19	0.28
MgO	5.49	3.35	7.12	6.86	8.42	6.35	8.72	8.37	7.69
CaO	1.43	8.34	1.16	12.88	1.26	11.14	1.64	11.28	11.36
K_2O	0.51	0.72	0.26	0.29	0.28	0.46	0.32	0.34	0.30
Na_2O	2.56	2.97	2.54	2.27	2.43	2.49	2.28	2.39	2.35
P_2O_5	0.14	0.27	0.78	0.89	0.92	0.19	0.11	0.89	0.99
Mg#	0.43	0.28	0.53	0.57	0.56	0.51	0.55	0.58	0.52
Ti	9786	12137	5216	6200	5875	7515	7374	5535	7319
P	612	119	349	394	393	481	436	394	437
Cr	67.99		41.00	373.52		164.46		239.85	246.17
Ni	53.78		136.00	88.36		95.26		17.64	118.82
Rb	15.38	18.33	8.47	7.67	8.27	12.15	1.12	8.78	7.25
Sr	154.27	162.97	165.70	138.86	155.00	163.65	136.20	155.95	143.70
Cs	0.62	0.56	0.20	0.19	0.31	0.40	0.29	0.30	0.30
Sc	34.75	43.73	19.10	36.95	32.28	31.19	41.43	25.99	3.82
V	32.47	389.73	194.40	291.18	274.70	35.25	34.50	223.59	292.32
Ta	0.43	0.69	0.20	0.25	0.25	0.34	0.29	0.28	0.25
Nb	6.60	1.92	2.80	3.41	3.60	4.71	4.20	3.61	3.52
Zr	11.62	189.83	53.50	68.75	69.90	91.55	79.60	68.84	68.65
Hf	3.44	5.11	1.50	1.98	1.90	2.57	2.20	1.97	1.91
Th	1.67	2.99	0.71	0.88	0.90	1.63	1.90	1.25	0.93
U	0.46	0.85	0.19	0.24	0.25	0.48	0.28	0.36	0.26
Y	29.58	53.62	15.74	2.92	19.18	23.66	22.88	17.92	21.65
La	1.58	2.70	4.89	5.87	6.27	9.75	7.28	6.98	6.25
Ce	23.99	47.32	11.90	13.64	14.21	2.22	16.74	15.69	14.48
Pr	3.24	6.31	1.55	1.93	1.92	2.74	2.25	2.98	2.32
Nd	14.89	29.25	7.19	9.25	9.16	12.22	1.73	9.53	9.67
Sm	4.46	7.75	2.50	2.69	2.58	3.40	3.10	2.57	2.74
Eu	1.35	2.42	0.85	0.98	0.97	1.26	1.73	0.92	1.87
Gd	4.93	9.43	2.57	3.40	3.26	4.97	3.84	3.14	3.54
Tb	0.85	1.59	0.44	0.59	0.55	0.69	0.65	0.53	0.61
Dy	5.35	9.94	2.87	3.86	3.52	4.40	4.18	3.33	3.85
Ho	1.15	2.57	0.62	0.82	0.74	0.92	0.88	0.70	0.82
Er	3.37	5.91	1.80	2.39	2.14	2.72	2.54	2.23	2.38
Tm	0.48	0.86	0.26	0.34	0.38	0.38	0.37	0.29	0.34
Yb	3.34	5.43	1.67	2.18	2.10	2.47	2.33	1.83	2.22
Lu	0.46	0.82	0.25	0.33	0.30	0.36	0.35	0.28	0.33

Appendix 1. continued

Sample	**LN 115**	**LN - 120**	**LN - 122**	**LN - 129**	**LN - 130**	**LN - 140**	**LN 142**	**LN 155**	**LN 201**
Easting	387280	394781	399725	406356	404460	397600	401913	362116	417284
Northing	5497535	5503064	5504576	5491671	5491595	5477810	5477107	5513967	5542580
Datum	NAD 27	NAD 27	NAD 27	NAD 27	NAD 27	NAD 27	NAD 27	NAD 27	NAD 27
SiO_2	47.75	49.34	48.28	49.97	44.73	47.71	5.27	45.68	48.56
TiO_2	0.85	1.84	1.19	1.54	0.88	1.14	1.78	4.13	1.42
Al_2O_3	14.26	13.63	11.43	13.55	14.20	15.79	13.69	11.79	15.19
Fe_2O_3	15.57	16.68	16.41	12.86	15.98	13.51	16.58	22.52	15.15
MnO	0.22	0.24	0.24	0.22	0.21	0.19	0.25	0.28	0.22
MgO	9.46	4.93	9.57	7.66	11.43	8.16	4.57	3.64	6.67
CaO	1.85	1.89	1.34	12.13	1.18	11.12	9.43	8.39	9.70
K_2O	0.21	0.53	0.53	0.27	0.27	0.35	0.56	0.74	0.56
Na_2O	2.23	2.66	1.87	2.20	2.14	2.18	2.85	2.63	2.53
P_2O_5	0.54	0.18	0.13	0.98	0.86	0.89	0.20	0.20	0.14
Mg#	0.57	0.39	0.56	0.57	0.61	0.57	0.38	0.26	0.49
Ti	536	1116	7263	6415	5216	6175	1380	25120	8544
P	218	786	568	436	349	393	873	873	613
Cr		51.00	275.33	322.00	93.00	221.00			132.49
Ni		5.00	217.26	82.00	299.00	177.00			136.54
Rb	4.93	13.26	18.81	7.50	6.60	9.45	17.85	23.54	14.53
Sr	136.20	145.20	142.37	129.00	141.40	16.00	166.43	158.90	143.53
Cs	0.18	0.32	0.54	0.18	0.20	0.24	0.55	0.84	1.87
Sc	35.67	36.00	33.14	4.40	18.00	24.20	46.82	46.27	45.17
V	27.61	32.00	255.62	319.70	176.70	232.40	44.36	747.16	326.24
Ta	0.20	0.43	0.45	0.24	0.22	0.27	0.47	0.75	0.28
Nb	2.70	6.70	6.48	3.40	3.20	3.80	7.56	12.20	5.19
Zr	49.60	127.00	92.88	67.20	59.90	71.80	116.69	168.00	87.42
Hf	1.40	3.50	2.53	1.90	1.60	1.90	3.23	4.50	2.49
Th	0.57	1.71	2.15	0.85	0.78	1.27	1.58	2.68	1.18
U	0.16	0.48	0.61	0.24	0.22	0.37	0.49	0.89	0.32
Y	17.66	34.58	22.95	21.48	16.53	18.92	34.35	39.24	26.53
La	4.40	11.16	11.21	5.86	5.37	7.18	12.66	16.14	7.60
Ce	9.81	26.30	24.28	13.72	12.27	16.22	28.73	35.91	17.99
Pr	1.39	3.63	3.79	1.96	1.70	2.19	3.85	4.71	2.52
Nd	6.98	17.22	13.44	9.41	7.83	9.87	17.93	21.66	11.66
Sm	2.14	4.70	3.38	2.72	2.18	2.68	4.86	5.71	3.45
Eu	0.84	1.63	1.22	0.99	0.83	0.99	1.65	1.96	1.24
Gd	2.79	5.94	3.98	3.49	2.80	3.27	6.57	6.97	4.30
Tb	0.48	1.19	0.66	0.69	0.48	0.55	1.98	1.17	0.74
Dy	3.18	6.48	4.29	3.94	3.32	3.48	6.38	7.28	4.83
Ho	0.68	1.37	0.90	0.84	0.65	0.72	1.33	1.56	1.77
Er	2.60	4.44	2.62	2.48	1.88	2.13	3.80	4.36	2.96
Tm	0.29	0.57	0.37	0.35	0.27	0.32	0.55	0.62	0.43
Yb	1.92	3.63	2.42	2.19	1.77	1.93	3.51	3.99	2.82
Lu	0.29	0.55	0.37	0.34	0.27	0.29	0.52	0.59	0.42

Appendix 1. continued

Sample	**LN 203**	**LN 205**	**LN 207**	**LN 211**	**LN 213**	**LN 215**	**LN 217**	**LN 221**	**LN 223**
Easting	415974	412607	409472	413279	404745	401605	400698	392832	401382
Northing	5541109	5537139	5553098	5550206	5555477	5555628	5558155	5563478	5566365
Datum	NAD 27	NAD 27	NAD 27	NAD 27	NAD 27	NAD 27	NAD 27	NAD 27	NAD 27
SiO_2	47.99	5.53	49.45	49.53	5.57	48.85	47.69	5.78	49.43
TiO_2	1.54	3.71	1.85	1.42	1.72	1.49	1.69	1.63	1.76
Al_2O_3	14.93	12.90	16.41	13.95	16.94	15.84	11.75	15.85	15.94
Fe_2O_3	15.49	18.59	14.15	14.75	14.29	14.35	18.34	14.25	15.74
MnO	0.18	0.25	0.19	0.29	0.19	0.19	0.25	0.20	0.28
MgO	6.63	2.58	4.12	6.65	2.76	5.13	7.14	3.94	3.86
CaO	9.66	7.52	9.87	1.35	9.19	1.19	1.54	9.49	9.85
K_2O	0.58	1.15	0.66	0.54	0.76	0.56	0.33	0.65	0.67
Na_2O	2.95	3.71	3.22	2.94	3.29	3.29	2.28	3.37	2.94
P_2O_5	0.15	0.50	0.32	0.14	0.39	0.18	0.87	0.28	0.32
Mg#	0.48	0.23	0.40	0.50	0.30	0.45	0.46	0.38	0.36
Ti	9214	18585	12	8549	1342	8823	172	973	1655
P	662	2182	14	614	1663	786	349	917	142
Cr	16.17	29.00	72.20	138.59	36.18	95.12	142.00	67.60	86.36
Ni	141.56	2.00	51.14	18.46	34.12	84.13	96.00	44.39	51.21
Rb	11.23	26.43	16.51	16.23	16.57	13.70	7.12	17.82	18.67
Sr	29.15	15.60	197.34	186.50	183.45	178.42	122.90	176.56	169.43
Cs	0.54	0.76	0.51	0.49	0.58	0.56	0.26	0.59	0.57
Sc	39.43	46.00	36.98	46.20	33.99	36.44	5.00	38.34	38.16
V	333.67	148.00	313.85	336.44	242.73	251.35	388.00	232.27	324.35
Ta	0.32	0.72	0.48	0.33	0.39	0.34	0.27	0.42	0.42
Nb	5.66	12.80	8.52	5.52	7.12	6.73	4.40	7.47	7.53
Zr	122.55	272.00	199.14	14.45	152.26	12.15	73.30	141.53	157.52
Hf	3.13	6.90	4.81	2.81	3.81	3.36	2.10	3.73	4.17
Th	1.52	3.53	2.75	1.45	2.56	1.54	0.77	1.82	2.38
U	0.47	1.28	0.76	0.44	0.58	0.49	0.21	0.47	0.62
Y	27.51	58.88	42.72	3.38	36.98	26.99	26.68	35.52	39.65
La	9.85	23.50	17.40	11.29	13.29	1.56	5.48	12.39	15.75
Ce	22.87	52.64	39.88	23.76	3.83	23.79	13.34	28.17	35.36
Pr	3.15	7.35	5.47	3.15	4.21	3.18	1.96	3.84	4.72
Nd	14.17	31.75	24.84	14.28	19.27	14.49	9.43	17.36	22.25
Sm	3.91	8.43	6.58	3.97	5.26	3.91	2.94	4.76	5.94
Eu	1.32	2.63	1.59	1.30	1.78	1.52	1.12	1.73	1.82
Gd	4.73	1.19	7.73	5.54	6.19	4.81	3.93	5.82	7.89
Tb	0.80	1.68	1.25	0.86	1.42	0.78	0.71	1.00	1.15
Dy	5.48	1.66	7.79	5.42	6.64	4.95	4.78	6.34	7.22
Ho	1.52	2.21	1.61	1.14	1.37	1.17	1.17	1.34	1.51
Er	3.69	6.38	4.55	3.31	4.32	2.95	3.12	3.96	4.27
Tm	0.44	0.91	0.64	0.48	0.57	0.42	0.45	0.56	0.60
Yb	2.76	5.76	3.90	3.93	3.69	2.66	2.98	3.59	3.82
Lu	0.42	0.84	0.57	0.46	0.55	0.40	0.45	0.53	0.56

Appendix 1. continued

Sample	LN 225	LN 227	LN 229	LN 231	LN 233	LN 235	LN 239	LN 243	LN 247
Easting	398748	398059	409197	409778	415032	417883	416391	413372	408729
Northing	5568632	5571189	5559243	5536087	5529128	5530032	5572872	5579692	5579729
Datum	NAD 27	NAD 27	NAD 27	NAD 27	NAD 27	NAD 27	NAD 27	NAD 27	NAD 27
SiO_2	5.55	51.19	49.33	48.26	5.27	51.54	48.25	49.86	49.27
TiO_2	1.15	1.35	0.97	1.16	1.31	0.88	0.78	2.32	1.41
Al_2O_3	18.28	18.44	18.99	14.64	15.23	19.43	17.22	13.93	14.79
Fe_2O_3	11.57	1.99	1.97	14.72	13.87	9.72	11.56	17.21	14.57
MnO	0.15	0.14	0.15	0.19	0.20	0.14	0.16	0.23	0.19
MgO	4.58	4.18	5.33	7.75	5.68	4.28	7.77	3.62	6.92
CaO	9.81	9.75	1.67	1.24	9.60	1.26	11.31	8.73	9.66
K_2O	0.82	0.84	0.48	0.46	0.87	0.79	0.30	0.83	0.75
Na_2O	3.40	3.19	3.44	2.53	2.87	2.90	2.54	3.89	3.14
P_2O_5	0.30	0.25	0.17	0.84	0.16	0.13	0.13	0.23	0.13
Mg#	0.44	0.46	0.52	0.54	0.47	0.49	0.60	0.32	0.48
Ti	692	6259	5825	6918	7980	4756	4645	1428	8527
P	919	195	743	35	699	570	58	14	572
Cr	67.15	67.26	125.21	14.48	12.87	8.33	23.42	56.00	137.18
Ni	74.18	97.38	11.18	152.52	15.83	8.33	152.94	45.00	13.90
Rb	24.55	25.57	1.33	11.23	22.50	15.97	9.56	23.15	24.75
Sr	239.55	242.34	189.53	179.91	212.68	247.52	18.21	165.70	168.66
Cs	0.77	1.13	0.34	0.44	0.77	0.48	1.29	0.66	1.26
Sc	27.63	27.15	29.49	43.15	41.32	26.18	32.20	42.00	42.37
V	18.41	153.59	185.31	27.92	264.29	144.60	184.14	374.00	312.70
Ta	0.46	0.53	0.24	0.26	0.46	0.34	0.19	0.59	0.37
Nb	7.32	8.33	4.47	4.42	7.66	5.82	3.42	1.20	6.25
Zr	114.36	146.47	88.65	75.86	113.59	79.13	59.97	173.90	126.49
Hf	2.97	3.61	2.24	2.68	2.92	2.83	1.70	4.50	3.23
Th	3.12	3.81	1.18	1.33	2.61	1.69	1.26	2.90	2.40
U	0.83	1.84	0.34	0.38	0.76	0.46	0.29	0.85	0.73
Y	23.72	29.23	23.70	22.88	26.72	18.95	15.31	38.87	28.31
La	16.64	2.30	9.25	7.77	14.56	9.47	7.95	15.80	11.81
Ce	34.39	42.85	2.48	17.62	3.66	18.58	17.49	35.41	26.66
Pr	4.13	5.24	2.83	2.42	3.83	2.35	2.18	4.70	3.52
Nd	17.62	21.91	12.78	11.16	16.51	1.18	9.52	21.21	15.68
Sm	3.97	5.20	3.44	3.12	3.97	2.57	2.33	5.61	4.26
Eu	1.44	1.49	1.27	1.94	1.38	1.27	0.90	1.97	1.39
Gd	4.35	5.67	4.14	3.81	4.56	3.74	2.84	6.93	4.91
Tb	0.68	0.86	0.67	0.64	0.75	0.51	0.45	1.12	0.90
Dy	4.29	5.40	4.23	4.17	4.87	3.22	2.81	7.30	5.16
Ho	0.88	1.93	0.88	0.85	0.99	0.68	0.57	1.57	1.58
Er	2.54	3.68	2.55	2.48	2.90	2.36	1.62	4.28	3.48
Tm	0.35	0.43	0.36	0.36	0.41	0.29	0.23	0.62	0.44
Yb	2.25	2.65	2.21	2.24	2.61	1.93	1.44	3.98	2.79
Lu	0.33	0.39	0.33	0.34	0.39	0.29	0.21	0.58	0.41

Appendix 1. continued

Sample	**LN 249**	**LN 253**	**LN 255**	**LN 257**	**LN 259**	**LN 263**	**LN 265**	**LN 300**	**LN 301**
Easting	406283	416102	416195	418101	419054	419988	421125	391527	391576
Northing	5478901	5483603	5480128	5473666	5516774	5512127	5508087	5531193	5533653
Datum	NAD 27	NAD 27	NAD 27	NAD 27	NAD 27	NAD 27	NAD 27	NAD 27	NAD 27
SiO_2	5.22	49.18	48.38	48.92	52.18	49.27	5.66	49.22	51.22
TiO_2	1.40	0.93	0.73	0.80	0.94	1.36	1.11	1.13	1.45
Al_2O_3	14.65	18.89	18.59	17.47	14.89	17.43	18.39	15.87	18.99
Fe_2O_3	14.15	11.18	11.90	11.28	13.26	13.19	11.17	13.33	11.39
MnO	0.21	0.16	0.15	0.16	0.20	0.19	0.16	0.19	0.17
MgO	5.43	6.44	7.38	7.58	5.18	4.90	4.12	6.69	3.95
CaO	1.69	1.76	1.54	11.49	9.36	1.56	1.52	1.51	1.27
K_2O	0.53	0.49	0.44	0.30	0.87	0.61	0.59	0.50	0.56
Na_2O	2.65	2.63	2.59	2.43	2.93	2.88	3.13	2.65	3.19
P_2O_5	0.16	0.17	0.15	0.70	0.20	0.19	0.19	0.12	0.19
Mg#	0.46	0.56	0.59	0.60	0.46	0.45	0.45	0.52	0.43
Ti	8363	565	4450	486	5679	83	6684	6789	6323
P	657	746	657	37	880	80	790	525	833
Cr	171.62	185.00	151.45	223.42	59.46				
Ni	63.23	147.79	179.53	147.28	56.44	112.34	61.43	138.93	4.81
Rb	11.96	16.30	13.94	7.37	23.38	16.82	16.42	12.13	16.84
Sr	162.79	195.45	193.88	177.23	176.36	191.27	196.28	174.38	26.12
Cs	0.31	0.43	0.46	0.89	0.63	0.67	0.50	0.44	0.77
Sc	44.16	28.16	25.74	33.62	42.33	26.71	28.57	33.47	27.91
V	285.29	17.92	15.45	218.41	168.32	284.63	273.55	292.23	215.52
Ta	0.33	0.28	0.25	0.24	0.42	0.42	0.38	0.37	0.42
Nb	5.82	4.62	3.81	3.46	6.56	6.44	5.93	4.50	6.27
Zr	98.46	96.11	79.84	6.11	13.55	134.68	121.75	96.51	135.13
Hf	2.80	2.51	2.16	1.63	3.33	3.52	3.21	2.66	3.52
Th	1.46	1.91	1.83	0.82	2.39	2.55	2.29	1.76	2.61
U	0.36	0.55	0.50	0.22	0.68	0.78	0.69	0.52	0.77
Y	27.18	22.59	18.95	16.30	32.94	27.42	23.12	2.87	27.41
La	9.43	12.43	1.79	5.22	14.41	13.59	11.49	9.44	13.19
Ce	19.98	26.41	23.61	11.83	31.75	29.95	25.29	2.69	28.66
Pr	2.79	3.43	3.92	1.62	4.14	3.96	3.28	2.73	3.83
Nd	12.88	15.21	13.38	7.74	18.99	17.64	14.66	12.25	16.95
Sm	3.55	3.89	3.29	2.13	4.92	4.37	3.69	3.13	4.36
Eu	1.33	1.16	1.25	0.89	1.62	1.42	1.19	1.27	1.37
Gd	4.48	4.34	3.78	2.64	5.87	5.25	4.45	3.83	5.18
Tb	0.76	0.69	0.59	0.45	0.97	0.83	0.71	0.64	0.84
Dy	4.93	4.16	3.58	2.96	5.93	5.15	4.33	3.95	5.14
Ho	1.48	0.84	0.72	0.62	1.23	1.41	0.94	0.82	1.52
Er	3.64	2.33	2.22	1.88	3.58	2.92	2.57	2.34	3.38
Tm	0.43	0.33	0.27	0.26	0.54	0.41	0.36	0.33	0.42
Yb	2.85	1.99	1.67	1.69	3.24	2.60	2.23	2.15	2.66
Lu	0.42	0.29	0.24	0.25	0.48	0.39	0.33	0.31	0.39

Appendix 1. continued

Sample	**LN 302**	**LN 303**	**LN 304**	**LN 305**	**LN 306**	**LN 307**	**LN 308**	**LN 309**	**LN 310**
Easting	395018	399229	400738	396130	395021	395549	404643	404902	404357
Northing	5536620	5539889	5543249	5548384	5551701	5556682	5534830	5532101	5530454
Datum	NAD 27	NAD 27	NAD 27	NAD 27	NAD 27	NAD 27	NAD 27	NAD 27	NAD 27
SiO_2	5.29	51.29	51.31	5.94	5.75	49.19	5.48	48.43	5.30
TiO_2	1.40	2.29	1.29	1.17	1.44	0.82	0.93	0.84	0.96
Al_2O_3	15.39	15.50	17.54	16.64	14.41	14.88	17.88	15.24	18.90
Fe_2O_3	12.53	14.62	11.99	12.50	13.63	12.85	11.13	12.73	1.11
MnO	0.17	0.19	0.18	0.19	0.19	0.19	0.16	0.19	0.15
MgO	5.72	3.11	4.13	4.97	6.18	8.65	5.38	8.92	4.54
CaO	1.47	8.25	9.89	9.96	9.87	1.52	1.46	11.37	11.51
K_2O	0.56	1.22	0.77	0.69	0.87	0.45	0.61	0.34	0.43
Na_2O	3.34	3.53	3.15	2.99	2.45	2.36	2.99	2.19	2.98
P_2O_5	0.15	0.38	0.24	0.99	0.20	0.18	0.14	0.89	0.12
Mg#	0.51	0.31	0.43	0.46	0.50	0.60	0.52	0.67	0.50
Ti	8362	11899	787	796	8723	4976	548	599	578
P	613	1618	149	438	876	48	437	393	526
Cr									
Ni	16.28	49.69	58.32	254.94	92.51	23.60	17.48	192.87	62.75
Rb	14.48	33.65	21.47	18.29	23.48	11.72	14.32	8.92	11.24
Sr	21.34	211.90	235.42	227.12	184.82	182.30	219.33	155.27	198.67
Cs	0.43	0.90	0.83	0.44	0.74	0.36	0.43	0.27	0.33
Sc	35.12	3.56	28.75	31.47	34.76	33.22	26.62	32.66	29.32
V			256.20	283.75		243.80	213.66	249.41	256.83
Ta	0.51	0.89	0.53	0.42	0.55	0.30	0.36	0.21	0.25
Nb	7.43	13.63	7.91	6.42	8.33	4.40	5.71	3.22	4.18
Zr	11.39	22.12	117.89	9.69	117.80	68.80	8.38	62.94	84.17
Hf	2.91	5.71	3.54	2.48	3.11	1.90	2.15	1.71	2.30
Th	2.55	6.24	2.92	2.26	3.42	1.71	1.78	1.19	1.54
U	0.78	1.79	0.84	0.54	0.83	0.49	0.49	0.35	0.45
Y	24.66	41.79	25.65	22.83	28.74	16.37	17.63	15.85	19.38
La	12.41	29.96	16.79	12.64	16.75	9.60	8.97	6.69	8.25
Ce	26.83	61.79	33.97	26.42	35.20	18.88	18.52	14.57	18.25
Pr	3.44	7.75	4.25	3.29	4.48	2.43	2.35	1.95	2.39
Nd	14.92	32.64	18.28	14.24	19.28	1.29	1.83	8.79	1.95
Sm	3.68	7.27	4.19	3.44	4.52	2.53	2.47	2.27	2.93
Eu	1.23	2.40	1.42	1.26	1.23	0.95	1.13	0.88	1.69
Gd	4.31	8.23	4.95	4.23	5.41	2.96	2.99	2.77	3.53
Tb	0.72	1.32	0.78	0.67	0.87	0.49	0.56	0.48	0.58
Dy	4.59	7.83	4.74	4.15	5.37	3.11	3.28	2.95	3.54
Ho	0.95	1.62	0.99	0.89	1.17	0.65	0.67	0.64	0.74
Er	2.76	4.58	2.78	2.54	3.17	1.83	1.95	1.74	2.16
Tm	0.40	0.64	0.39	0.36	0.45	0.26	0.28	0.24	0.33
Yb	2.55	3.95	2.49	2.33	2.87	1.65	1.84	1.56	1.98
Lu	0.39	0.59	0.37	0.36	0.43	0.25	0.28	0.24	0.29

Appendix 1. continued

Sample	**LN 311**	**LN 312**	**LN 313**	**ADH3-31**	**ADH3-33**	**ADH3-37**	**ADH3-40**	**ADH5-4**	**ADH5-17**
Easting	402264	403652	400038	376299	376299	376299	376299	373679	373679
Northing	5536935	5524057	5518293	5446449	5446449	5446449	5446449	5444646	5444646
Datum	NAD 27	NAD 27	NAD 27	NAD 27	NAD 27	NAD 27	NAD 27	NAD 27	NAD 27
SiO_2	48.57	5.19	49.67	49.69	49.24	5.69	49.67	49.84	52.61
TiO_2	0.89	1.89	1.48	1.54	1.52	1.71	1.83	1.52	2.17
Al_2O_3	14.72	15.45	15.82	15.92	14.53	13.54	14.33	15.66	11.78
Fe_2O_3	12.94	14.32	13.95	12.75	14.84	15.98	16.48	13.49	19.44
MnO	0.20	0.20	0.20	0.18	0.29	0.23	0.23	0.18	0.25
MgO	8.94	4.64	4.89	7.36	6.29	5.32	4.29	6.20	2.33
CaO	11.26	9.15	1.67	8.63	9.15	9.37	7.79	9.28	5.74
K_2O	0.32	0.78	0.45	1.15	1.28	1.29	1.59	0.73	1.53
Na_2O	2.12	3.15	2.72	3.46	2.89	2.74	3.61	2.96	3.84
P_2O_5	0.59	0.32	0.16	0.14	0.16	0.16	0.26	0.14	0.38
Mg#	0.64	0.42	0.44	0.56	0.48	0.42	0.36	0.53	0.29
Ti	5396	1877	8886	9297	9255	1433	1124	9237	139
P	262	1400	699	623	75	72	882	623	1675
Cr				164.26	151.36	83.49	4.41	149.99	
Ni	181.37	57.90	56.73	11.45	11.92	58.34	41.42	15.96	11.11
Rb	8.24	22.88	11.63	43.59	32.28	29.74	36.47	19.68	35.89
Sr	149.40	184.84	156.23	215.67	199.90	199.77	21.25	174.17	148.29
Cs	0.34	0.74	0.35	0.59	0.60	0.43	0.33	0.88	0.95
Sc	35.70	31.40	37.19	28.46	28.76	31.89	29.46	3.71	25.97
V	27.37			296.39	313.92	321.92	323.35	322.23	56.37
Ta	0.18	0.49	0.33	0.48	0.48	0.52	0.53	0.47	0.99
Nb	2.90	8.32	5.68	6.73	6.86	7.44	7.68	6.43	15.46
Zr	55.00	174.82	112.47	121.13	127.14	142.39	143.67	113.16	291.54
Hf	1.50	4.61	3.45	3.16	3.33	3.72	3.74	2.96	7.68
Th	0.98	3.87	1.44	2.25	2.38	2.60	2.53	2.18	5.24
U	0.29	0.95	0.43	1.11	0.76	0.76	0.77	0.66	1.59
Y	15.70	34.89	28.64	27.68	3.96	33.69	35.54	27.83	66.59
La	5.30	19.25	9.63	13.69	12.71	13.58	14.92	11.85	29.31
Ce	11.88	41.66	22.94	3.48	28.33	3.50	33.30	26.34	67.22
Pr	1.60	5.47	3.76	3.96	3.75	4.95	4.40	3.56	8.88
Nd	7.52	24.16	14.29	17.99	16.63	17.99	19.92	15.80	39.44
Sm	2.10	5.83	4.00	4.32	4.45	4.89	5.31	4.17	1.38
Eu	0.88	1.86	1.39	1.41	1.44	1.57	1.77	1.40	2.73
Gd	2.62	6.90	4.95	4.95	5.25	5.79	6.25	4.86	12.26
Tb	0.45	1.78	0.84	0.82	0.88	0.98	1.59	0.82	2.92
Dy	2.88	6.58	5.24	5.14	5.49	6.13	6.57	5.15	12.52
Ho	0.59	1.34	1.13	1.58	1.14	1.28	1.36	1.61	2.57
Er	1.70	3.73	3.26	3.67	3.31	3.70	3.93	3.68	7.32
Tm	0.25	0.52	0.46	0.44	0.47	0.53	0.56	0.45	1.34
Yb	1.56	3.38	2.92	2.85	2.99	3.36	3.52	2.96	6.66
Lu	0.24	0.50	0.44	0.43	0.45	0.58	0.54	0.45	0.99

Appendix 1. continued

Sample	**ADH5-29**	**)H6-13**	**ADH6-47**	**ADH6-66**	**)H6-98**	**ADH6-115**	**AML-01-01**	**AML-01-03**	**AML-01-05**
Easting	373679	376663	376663	376663	376663	376663	359505	359505	359505
Northing	5444646	5437496	5437496	5437496	5437496	5437496	5458026	5458026	5458026
Datum	NAD 27	NAD 27	NAD 27	NAD 27	NAD 27	NAD 27	NAD 27	NAD 27	NAD 27
SiO_2	49.83	49.76	47.66	48.96	6.00	49.98	48.78	48.35	48.17
TiO_2	1.34	1.38	1.41	1.31	1.00	2.27	1.30	1.13	1.55
Al_2O_3	13.76	13.71	14.61	15.31	16.11	12.88	15.51	15.37	15.52
Fe_2O_3	14.73	13.65	15.54	14.27	12.60	17.73	14.24	13.57	13.49
MnO	0.23	0.19	0.22	0.27	0.18	0.25	0.20	0.20	0.20
MgO	6.66	6.68	6.61	5.84	6.28	3.42	7.49	7.27	7.63
CaO	1.25	11.36	9.79	1.98	1.70	8.39	1.43	11.36	11.63
K_2O	0.53	0.77	1.14	0.49	0.35	0.98	0.42	0.43	0.39
Na_2O	2.82	2.46	3.52	2.59	2.57	3.74	2.35	2.54	2.38
P_2O_5	0.20	0.20	0.14	0.12	0.14	0.38	0.18	0.99	0.99
Mg#	0.50	0.52	0.48	0.47	0.52	0.30	0.54	0.54	0.55
Ti	8144	8268	8593	7922	5996	13773	7385	6855	6415
P	487	439	621	524	611	1671	49	438	436
Cr	51.73	322.74	132.14	151.16	25.82	32.25	136.21	27.61	221.00
Ni	59.81	61.88	118.93	7.76	58.98	42.32	166.26	132.39	149.00
Rb	15.22	89.92	29.37	14.52	118.66	29.90	11.97	11.55	1.14
Sr	155.52	182.36	168.43	152.26	164.32	124.65	16.85	156.26	157.30
Cs	0.62	0.49	0.73	0.64	0.53	1.71	0.34	0.43	0.32
Sc	33.46	45.89	29.48	31.73	38.88	28.11	25.14	28.28	25.90
V	321.47	423.42	317.85	317.24	236.97	235.29	265.42	267.39	239.20
Ta	0.39	0.99	0.37	0.34	1.72	0.87	0.44	0.37	0.32
Nb	5.27	7.26	4.99	4.65	6.92	14.51	5.69	5.12	4.50
Zr	97.20	88.17	91.79	91.40	92.85	243.45	84.43	81.84	75.30
Hf	2.53	2.20	2.44	2.53	2.66	6.45	2.44	2.37	2.10
Th	1.72	1.45	1.30	1.18	1.41	2.93	1.61	1.56	1.42
U	0.49	0.37	0.38	0.33	0.33	0.88	0.46	0.46	0.48
Y	24.79	23.53	26.44	25.68	22.42	61.55	21.87	21.13	19.67
La	9.75	7.71	8.87	8.15	8.13	2.53	8.85	8.53	7.76
Ce	21.46	18.51	2.37	18.56	19.42	48.46	19.84	18.98	17.49
Pr	2.88	2.48	2.83	2.57	2.73	6.77	2.66	2.56	2.39
Nd	12.96	11.19	12.90	12.74	12.38	31.57	12.18	11.73	1.84
Sm	3.53	3.22	3.64	3.42	3.56	8.93	3.25	3.18	2.95
Eu	1.26	1.95	1.24	1.23	1.25	2.69	1.17	1.14	1.59
Gd	4.27	4.44	4.44	4.29	4.51	1.80	3.98	3.82	3.48
Tb	0.73	0.65	0.76	0.73	0.71	1.86	0.67	0.65	0.59
Dy	4.56	4.38	4.82	4.63	4.82	11.25	4.19	4.56	3.76
Ho	0.96	0.89	1.14	0.98	1.49	2.36	0.86	0.85	0.79
Er	2.78	2.70	2.92	2.83	2.94	6.84	2.56	2.48	2.39
Tm	0.40	0.36	0.42	0.41	0.42	0.97	0.36	0.36	0.33
Yb	2.55	2.40	2.68	2.62	2.67	6.20	2.29	2.27	2.80
Lu	0.38	0.33	0.45	0.40	0.38	0.93	0.35	0.34	0.37

Appendix 1. continued

Sample	**AML-01-07**	**AML-01-09**	**AML-01-11**	**AML-01-13**	**AML-01-15**	**AML-01-17**	**AML-01-19**	**AML-01-21**	**AML-01-23**
Easting	359505	359505	359505	359505	359505	359505	359505	359505	359505
Northing	5458026	5458026	5458026	5458026	5458026	5458026	5458026	5458026	5458026
Datum	NAD 27	NAD 27	NAD 27	NAD 27	NAD 27	NAD 27	NAD 27	NAD 27	NAD 27
SiO_2	48.00	47.94	48.67	47.66	47.73	47.85	48.19	48.37	48.62
TiO_2	0.90	0.88	0.98	1.85	1.61	1.18	1.21	1.28	1.40
Al_2O_3	17.64	16.39	16.16	15.46	15.77	15.72	15.55	16.00	14.89
Fe_2O_3	12.00	12.60	13.28	13.77	14.19	14.14	14.47	14.58	14.94
MnO	0.17	0.18	0.19	0.20	0.20	0.20	0.20	0.27	0.22
MgO	7.14	8.38	7.76	8.34	8.37	7.52	7.33	7.87	6.42
CaO	11.20	11.18	11.69	1.79	1.26	1.28	1.20	1.28	1.32
K_2O	0.35	0.32	0.36	0.38	0.39	0.45	0.55	0.51	0.59
Na_2O	2.53	2.41	2.36	2.32	2.36	2.54	2.49	2.47	2.47
P_2O_5	0.79	0.79	0.89	0.89	0.98	0.18	0.19	0.12	0.14
Mg#	0.57	0.58	0.57	0.57	0.56	0.54	0.53	0.52	0.49
Ti	5455	535	61	6115	6482	721	7389	7798	8484
P	349	349	393	393	437	481	481	524	613
Cr	153.00	251.25	233.25	253.00	152.16	14.32	135.28	13.77	111.48
Ni	153.00	169.17	164.18	181.00	184.20	171.39	158.33	151.89	125.46
Rb	8.82	8.38	1.18	1.64	11.22	12.67	14.23	14.69	16.34
Sr	172.90	159.36	162.68	152.10	158.77	151.84	162.34	159.99	19.40
Cs	0.27	0.28	0.35	0.45	0.50	0.51	0.46	0.52	0.71
Sc	2.70	24.42	23.83	25.40	22.92	23.85	25.25	26.15	28.54
V	198.70	217.51	225.74	234.00	231.49	245.46	26.54	268.86	33.40
Ta	0.28	0.29	0.31	0.32	0.32	0.38	0.38	0.42	0.43
Nb	3.70	3.43	3.84	3.90	4.14	4.82	4.90	5.24	5.82
Zr	63.70	62.56	69.48	72.40	76.82	85.39	89.28	97.46	17.59
Hf	1.80	1.82	2.22	2.00	2.12	2.45	2.55	2.72	3.11
Th	1.21	1.14	1.33	1.36	1.45	1.68	1.67	1.84	2.58
U	0.35	0.33	0.38	0.40	0.42	0.47	0.49	0.53	0.59
Y	16.23	16.26	18.24	18.77	19.52	21.60	22.36	23.97	27.39
La	6.75	6.57	7.45	7.59	8.39	9.24	9.20	9.84	11.27
Ce	14.93	14.72	16.60	16.80	17.90	2.35	2.47	22.17	24.99
Pr	2.90	1.97	2.24	2.24	2.37	2.72	2.74	2.94	3.38
Nd	9.15	9.89	1.14	1.27	1.55	12.19	12.49	13.38	15.85
Sm	2.46	2.48	2.74	2.80	2.93	3.30	3.35	3.54	4.85
Eu	0.94	0.93	1.69	1.00	1.47	1.13	1.14	1.23	1.38
Gd	2.95	2.90	3.29	3.36	3.45	3.96	3.99	4.31	4.87
Tb	0.50	0.49	0.55	0.57	0.58	0.65	0.67	0.72	0.85
Dy	3.15	3.17	3.51	3.62	3.80	4.17	4.27	4.53	5.80
Ho	0.65	0.65	0.73	0.76	0.77	0.87	0.89	0.95	1.57
Er	1.89	1.93	2.13	2.19	2.24	2.52	2.57	2.76	3.68
Tm	0.28	0.27	0.35	0.31	0.32	0.37	0.37	0.39	0.45
Yb	1.72	1.71	1.94	1.98	2.72	2.30	2.35	2.51	2.79
Lu	0.26	0.26	0.29	0.30	0.31	0.35	0.35	0.37	0.42

Appendix 1. continued

Sample	AML-01-24	AML-01-28	AML-01-32	AML-01-36	AML-01-40	AML-01-44	AML-01-48	AML-01-52	AML-01-56
Easting	359505	359505	359505	359505	359505	359505	359505	359505	359505
Northing	5458026	5458026	5458026	5458026	5458026	5458026	5458026	5458026	5458026
Datum	NAD 27	NAD 27	NAD 27	NAD 27	NAD 27	NAD 27	NAD 27	NAD 27	NAD 27
SiO_2	48.62	48.96	47.92	46.27	49.60	49.55	47.13	49.84	49.37
TiO_2	1.49	1.78	2.31	2.97	2.00	1.39	0.89	1.59	1.60
Al_2O_3	15.20	14.41	13.22	12.18	11.45	13.60	17.34	16.76	14.28
Fe_2O_3	14.88	16.59	18.37	2.97	2.39	16.19	15.23	11.56	12.47
MnO	0.22	0.24	0.25	0.26	0.29	0.26	0.20	0.19	0.28
MgO	6.46	4.97	5.27	4.79	4.43	5.79	6.57	5.63	7.18
CaO	1.55	1.29	9.82	9.59	8.67	1.20	9.73	11.94	12.79
K_2O	0.45	0.48	0.49	0.53	0.77	0.47	0.29	0.36	0.30
Na_2O	2.54	2.56	2.44	2.43	2.52	2.42	2.54	2.67	2.30
P_2O_5	0.14	0.18	0.18	0.18	0.25	0.15	0.88	0.99	0.19
Mg#	0.47	0.40	0.38	0.33	0.33	0.44	0.49	0.52	0.56
Ti	8573	186	14148	1845	12170	8453	5455	6115	6442
P	62	786	786	786	191	655	393	436	483
Cr	137.00	1.00	71.00	64.00	35.00	13.00	38.00	145.00	314.33
Ni	96.00	55.00	68.00	54.00	39.00	63.00	183.00	6.00	96.49
Rb	12.62	13.60	13.57	14.47	22.58	12.68	7.32	8.00	8.76
Sr	151.90	142.60	136.00	131.70	137.70	14.40	168.00	159.80	133.64
Cs	0.29	0.37	0.39	0.38	0.58	0.38	0.42	0.39	0.56
Sc	29.30	34.20	34.80	37.80	33.30	34.60	17.40	3.90	39.57
V	33.60	32.00	32.00	32.00	318.60	284.60	173.90	254.20	34.30
Ta	0.38	0.46	0.53	0.50	0.60	0.42	0.25	0.24	0.26
Nb	5.20	6.40	7.90	7.30	8.50	5.70	3.20	3.50	3.72
Zr	96.40	121.20	134.50	136.50	199.70	111.80	6.10	68.80	74.52
Hf	2.70	3.40	3.70	3.80	5.40	3.10	1.70	1.80	2.19
Th	1.40	1.66	1.72	1.93	2.94	1.57	0.83	0.89	0.99
U	0.46	0.45	0.48	0.52	0.81	0.43	0.23	0.25	0.28
Y	26.79	33.55	34.75	36.98	52.49	31.56	17.16	2.54	23.49
La	9.12	1.97	11.46	12.00	18.87	1.13	5.62	6.14	6.95
Ce	2.82	25.32	26.55	28.70	43.61	23.28	12.99	14.28	15.75
Pr	2.83	3.54	3.72	3.87	5.90	3.17	1.79	2.70	2.22
Nd	13.33	16.46	17.52	18.17	27.80	15.70	8.59	9.41	1.64
Sm	3.76	4.64	4.88	5.12	7.63	4.22	2.38	2.68	3.11
Eu	1.31	1.55	1.57	1.69	2.33	1.45	0.98	1.47	1.59
Gd	4.57	5.76	5.92	6.32	9.13	5.25	2.94	3.43	3.89
Tb	0.77	0.97	1.40	1.68	1.53	0.92	0.49	0.58	0.67
Dy	4.98	6.25	6.54	6.85	9.78	5.77	3.18	3.77	4.28
Ho	1.51	1.32	1.40	1.44	2.58	1.22	0.67	0.79	0.91
Er	3.55	3.86	4.44	4.23	5.97	3.61	1.97	2.33	2.69
Tm	0.44	0.55	0.58	0.61	0.86	0.52	0.28	0.33	0.38
Yb	2.84	3.53	3.72	3.89	5.48	3.34	1.83	2.14	2.43
Lu	0.43	0.54	0.55	0.57	0.83	0.52	0.28	0.32	0.37

Appendix 1. continued

Sample	**AML-01-60**	**AML-01-63**	**AML-01-67**	**AML-01-71**	**AML-01-73**	**AML03-08**	**AML03-56**	**AML-03-64**	**AML-03-70**
Easting	359505	359505	359505	359505	359505	361090	361090	361090	361090
Northing	5458026	5458026	5458026	5458026	5458026	5458097	5458097	5458097	5458097
Datum	NAD 27	NAD 27	NAD 27	NAD 27	NAD 27	NAD 27	NAD 27	NAD 27	NAD 27
SiO_2	48.56	48.23	47.82	47.50	47.88	5.87	49.31	48.77	47.99
TiO_2	1.59	1.27	1.15	1.28	1.23	1.40	0.95	0.93	0.99
Al_2O_3	16.29	16.94	15.76	16.16	15.56	14.17	16.47	17.43	17.24
Fe_2O_3	12.76	12.78	14.22	13.95	14.44	14.32	12.96	11.62	12.49
MnO	0.19	0.19	0.20	0.19	0.26	0.30	0.19	0.18	0.18
MgO	6.53	6.63	7.54	7.36	7.55	5.79	6.55	6.31	6.96
CaO	11.68	11.30	1.64	1.72	1.35	1.58	1.62	12.22	11.34
K_2O	0.37	0.30	0.31	0.35	0.35	0.56	0.35	0.27	0.27
Na_2O	2.63	2.58	2.27	2.70	2.39	2.73	2.55	2.57	2.45
P_2O_5	0.99	0.19	0.18	0.12	0.13	0.13	0.80	0.98	0.88
Mg#	0.53	0.53	0.54	0.53	0.53	0.47	0.53	0.54	0.56
Ti	6424	6246	6954	7674	7494	8414	5756	5695	655
P	437	49	48	524	567	569	349	436	393
Cr	197.29	168.32	123.00	116.00	115.00	129.95	23.19	238.00	17.00
Ni	13.15	125.23	16.00	149.00	169.00	59.11	68.98	1.00	135.00
Rb	8.37	8.39	8.20	9.00	9.37	5.55	122.72	6.72	7.20
Sr	152.43	155.59	15.20	155.70	149.80	166.69	187.77	158.20	157.70
Cs	0.59	0.62	0.38	0.28	0.28	0.38	0.15	0.20	0.19
Sc	28.44	25.95	24.60	25.40	24.60	42.83	34.15	27.60	23.90
V	255.88	244.56	251.60	255.80	25.70	359.34	31.64	24.30	29.30
Ta	0.25	0.26	0.26	0.30	0.30	1.27	0.68	0.22	0.24
Nb	3.65	3.67	3.90	4.40	4.50	8.35	4.36	3.20	3.30
Zr	71.56	72.14	75.80	83.00	83.60	98.92	48.99	6.60	64.70
Hf	2.30	2.38	2.10	2.30	2.30	2.88	1.63	1.70	1.80
Th	0.94	0.96	0.97	1.60	1.16	1.94	0.78	0.80	0.84
U	0.26	0.26	0.27	0.29	0.32	0.58	0.22	0.22	0.22
Y	2.86	2.74	2.92	23.38	23.28	23.95	13.98	19.30	18.69
La	6.29	6.54	6.66	7.50	7.70	9.75	4.90	5.70	5.75
Ce	14.51	15.30	15.46	17.50	17.92	22.97	11.67	13.11	13.25
Pr	2.30	2.12	2.15	2.37	2.47	3.12	1.64	1.86	1.87
Nd	9.48	1.39	1.30	11.41	11.48	13.52	7.75	8.77	8.99
Sm	2.74	2.84	2.86	3.17	3.17	3.83	2.27	2.51	2.54
Eu	1.20	1.34	1.32	1.13	1.14	1.33	0.93	1.00	0.97
Gd	3.48	3.49	3.57	3.88	3.98	4.86	2.83	3.12	3.12
Tb	0.59	0.60	0.65	0.65	0.67	0.77	0.49	0.56	0.54
Dy	3.78	3.79	3.86	4.28	4.27	5.12	3.25	3.54	3.45
Ho	0.81	0.88	0.83	0.91	0.91	1.32	0.66	0.74	0.73
Er	2.37	2.31	2.43	2.62	2.66	3.14	2.40	2.16	2.14
Tm	0.34	0.34	0.34	0.38	0.38	0.43	0.28	0.37	0.31
Yb	2.14	2.15	2.20	2.42	2.42	2.89	1.89	1.98	1.95
Lu	0.33	0.33	0.33	0.37	0.36	0.40	0.27	0.30	0.29

Appendix 1. continued

Sample	**AML-03-76**	**KH-01**	**KH-03**	**KH-10**
Easting	361090	425451	425451	425451
Northing	5458097	5427122	5427122	5427122
Datum	NAD 27	NAD 27	NAD 27	NAD 27
SiO_2	47.71	49.53	48.92	49.62
TiO_2	1.16	1.51	1.39	1.39
Al_2O_3	16.37	15.54	13.97	15.17
Fe_2O_3	13.89	11.42	15.51	13.59
MnO	0.20	0.18	0.21	0.23
MgO	7.42	8.74	6.64	6.25
CaO	1.47	9.14	9.97	1.49
K_2O	0.33	0.62	0.65	0.57
Na_2O	2.41	3.16	2.60	2.55
P_2O_5	0.18	0.14	0.13	0.13
Mg#	0.54	0.63	0.48	0.53
Ti	774	924	8217	8435
P	48	634	568	57
Cr	125.00			
Ni	161.00			
Rb	9.18	23.28	2.39	13.88
Sr	155.00	141.48	164.68	159.39
Cs	0.36	2.48	1.85	0.43
Sc	24.20	41.62	39.89	38.29
V	244.80	381.69	361.25	37.78
Ta	0.27	0.44	0.44	0.42
Nb	4.00	6.44	6.14	6.13
Zr	76.20	118.56	11.76	111.46
Hf	2.10	3.22	3.15	3.15
Th	1.00	2.24	2.31	1.93
U	0.27	0.73	0.62	0.62
Y	21.60	29.89	27.61	26.59
La	6.78	12.23	11.38	11.35
Ce	15.55	27.24	25.54	24.75
Pr	2.17	3.63	3.35	3.33
Nd	1.29	16.22	15.17	15.16
Sm	2.86	4.35	3.98	3.97
Eu	1.57	1.32	1.33	1.38
Gd	3.59	5.30	4.88	4.81
Tb	0.68	0.87	0.81	0.80
Dy	3.94	5.48	5.49	4.94
Ho	0.84	1.15	1.69	1.39
Er	2.42	3.35	3.13	3.14
Tm	0.35	0.48	0.44	0.43
Yb	2.25	3.18	2.85	2.75
Lu	0.34	0.46	0.43	0.42

Appendix 2

Major, Trace and Rare Earth Element Geochemical Data for the McIntyre Sills

Universal Transverse Mercator (UTM) co-ordinates are North American Datum 1927 (NAD 27), Zone 16.

Appendix 2. Major, trace and rare earth element geochemical data for the McIntyre suite.

Sample	LN - 45	LN 46	LN 62	LN 63	LN 100	LN - 101	LN 150	LN 161	LN 167	LN 170
Easting	374584	375578	363418	363264	374652	375141	353130	360677	352634	347622
Northing	5500167	5497684	5496821	5494000	5489233	5490615	5511325	5517422	5519762	5513969
Datum	NAD 27	NAD 27	NAD 27	NAD 27	NAD 27	NAD 27	NAD 27	NAD 27	NAD 27	NAD 27
SiO_2	49.52	49.26	48.66	49.80	49.74	49.77	48.76	48.14	48.91	49.24
TiO_2	3.12	3.19	2.82	3.13	3.11	3.10	3.08	2.73	3.03	2.98
Al_2O_3	13.63	12.63	12.72	12.92	13.45	13.62	13.30	13.02	12.98	13.86
Fe_2O_3	15.01	16.63	15.22	16.32	15.91	14.90	16.14	16.93	15.96	15.26
MnO	0.16	0.15	0.17	0.18	0.18	0.13	0.17	0.17	0.16	0.17
MgO	4.75	4.80	7.07	4.67	4.73	5.08	5.04	6.50	5.19	5.21
CaO	8.94	8.35	9.13	8.35	8.30	8.50	9.16	8.51	9.25	8.75
K_2O	0.68	0.93	0.76	0.91	0.95	0.61	0.84	0.64	0.76	0.64
Na_2O	3.91	3.77	3.20	3.43	3.37	4.01	3.23	3.14	3.51	3.64
P_2O_5	0.28	0.28	0.24	0.27	0.27	0.28	0.27	0.22	0.25	0.24
Mg#	0.41	0.39	0.51	0.39	0.40	0.43	0.41	0.46	0.42	0.43
Ti	18942	18882	17119	18508	18822	18690	18246	16083	17921	18139
P	1230	1226	1053	1181	1182	1229	1184	961	1094	1049
Cr	59.37					59.34				
Ni	73.46					83.47				
Rb	21.31	24.80	21.18	20.57	24.19	16.17	25.90	18.05	21.01	16.81
Sr	390.33	427.60	409.82	448.95	422.00	419.27	453.52	433.04	438.08	433.91
Cs	0.36	0.62	0.75	0.51	0.56	0.33	0.83	0.59	0.73	0.63
Sc	21.33	26.74	25.56	24.97	27.08	21.22	28.08	21.48	26.41	25.60
V	293.33	357.19	343.89	334.04	356.20	312.77	423.00	283.73	361.93	361.52
Ta	0.92	0.96	0.83	1.01	0.95	0.95	0.87	0.77	0.93	0.91
Nb	13.89	15.35	12.97	15.44	15.05	14.08	13.46	12.11	14.65	14.13
Zr	219.57	228.80	187.92	238.96	223.29	218.54	192.56	179.18	215.48	215.90
Hf	5.84	5.92	4.93	6.21	5.82	5.73	5.02	4.60	5.62	5.61
Th	3.02	3.14	2.32	3.21	3.00	2.98	2.48	2.25	2.69	2.61
U	1.10	0.70	0.56	0.72	0.70	0.88	0.55	0.51	0.65	0.66
Y	31.55	31.83	26.31	31.76	31.00	30.47	29.57	25.73	29.39	28.63
La	23.84	26.08	20.27	26.72	26.36	23.08	23.04	19.92	22.69	22.57
Ce	56.09	60.23	46.97	61.36	59.27	54.25	54.46	45.61	53.37	52.76
Pr	7.66	7.90	6.35	8.06	7.81	7.36	7.30	6.16	7.14	6.98
Nd	34.41	35.91	28.43	35.84	34.75	32.83	32.78	27.30	32.44	31.60
Sm	8.21	8.39	6.84	8.34	8.18	7.81	7.78	6.55	7.63	7.53
Eu	2.64	2.76	2.26	2.81	2.83	2.43	2.61	2.26	2.57	2.59
Gd	8.22	8.27	6.93	8.24	8.23	7.80	7.93	6.77	7.79	7.62
Tb	1.23	1.22	1.01	1.23	1.20	1.17	1.15	0.98	1.14	1.12
Dy	6.81	6.86	5.72	6.79	6.66	6.49	6.37	5.44	6.32	6.21
Ho	1.28	1.28	1.06	1.27	1.25	1.22	1.17	1.02	1.18	1.15
Er	3.37	3.31	2.72	3.36	3.21	3.22	3.04	2.63	3.09	3.00
Tm	0.44	0.44	0.36	0.44	0.43	0.43	0.40	0.35	0.41	0.40
Yb	2.65	2.66	2.16	2.66	2.60	2.55	2.43	2.14	2.46	2.38
Lu	0.36	0.37	0.30	0.37	0.36	0.36	0.33	0.30	0.35	0.34

Appendix 3

Major, Trace and Rare Earth Element Geochemical Data for the Shillabeer Sills

Universal Transverse Mercator (UTM) co-ordinates are North American Datum 1927 (NAD 27), Zone 16.

Appendix 3. Major, trace and rare earth element geochemical data for the Shillabeer suite.

Sample	**ADH3-1**	**ADH3-11**	**ADH3-20**	**ADH3-28**	**ADH3-30**	**ADH5-2**
Easting	376299	376299	376299	376299	376299	373679
Northing	5446449	5446449	5446449	5446449	5446449	5444646
Datum	NAD 27	NAD 27	NAD 27	NAD 27	NAD 27	NAD 27
SiO_2	50.24	47.67	51.36	50.26	53.56	49.35
TiO_2	2.81	2.63	2.90	2.68	2.76	2.76
Al_2O_3	13.08	10.37	13.65	11.44	12.12	11.60
Fe_2O_3	12.58	14.58	13.04	13.11	7.60	14.09
MnO	0.06	0.19	0.19	0.16	0.16	0.28
MgO	7.02	11.33	6.64	9.19	10.11	9.68
CaO	8.04	8.42	5.14	7.54	7.49	6.89
K_2O	0.66	0.53	0.52	0.33	0.67	1.18
Na_2O	5.14	3.96	6.18	4.98	5.17	3.80
P_2O_5	0.37	0.34	0.39	0.31	0.35	0.36
Mg#	0.55	0.63	0.53	0.61	0.75	0.60
Ti	17041	15730	17476	16204	16683	16735
P	1636	1482	1696	1345	1535	1568
Cr	82.26	847.86	30.69	406.98	427.26	520.34
Ni	64.56	219.17	47.05	105.86	102.42	159.08
Rb	16.07	10.39	8.07	4.64	14.52	20.42
Sr	447.41	271.03	481.67	457.85	543.34	552.05
Cs	0.16	0.32	0.10	0.11	0.19	0.20
Sc	20.41	24.28	15.55	25.18	25.86	24.63
V	283.31	259.61	277.20	272.96	291.53	289.73
Ta	1.28	1.12	1.28	1.10	1.17	1.17
Nb	20.41	17.39	20.15	16.55	18.41	18.47
Zr	243.12	216.39	245.08	216.85	231.53	230.10
Hf	6.04	5.45	6.03	5.55	5.69	5.75
Th	2.53	2.02	2.63	2.22	2.52	2.21
U	0.76	0.58	0.79	0.52	1.09	0.66
Y	26.31	23.31	26.32	24.22	29.67	25.91
La	43.23	31.89	40.25	33.47	36.75	33.81
Ce	100.94	80.59	97.21	82.81	94.96	84.61
Pr	13.36	11.11	13.03	11.30	13.61	11.74
Nd	56.16	48.27	54.63	48.69	58.84	50.79
Sm	10.64	9.90	10.85	10.01	11.71	10.60
Eu	2.98	2.85	2.93	2.83	2.96	3.04
Gd	8.83	8.05	8.95	8.38	9.59	8.66
Tb	1.14	1.04	1.16	1.09	1.23	1.14
Dy	5.86	5.37	5.97	5.62	6.28	5.89
Ho	1.03	0.95	1.06	0.97	1.10	1.04
Er	2.60	2.35	2.66	2.44	2.76	2.56
Tm	0.34	0.30	0.34	0.31	0.35	0.33
Yb	2.07	1.84	2.08	1.91	2.05	1.97
Lu	0.28	0.25	0.29	0.26	0.28	0.27

Appendix 4

Rb/Sr, Sm/Nd and Pb/Pb Isotope Data for All Sills

Appendix 4. Rubidium-strontium (Rb/Sr), samarium-neodymium (Sm/Nd) and lead-lead (Pb/Pb) isotope data for all sills.

Sample	εNd	$\frac{^{87}Rb}{^{86}Sr}$	$^{87}Sr/^{86}Sr$ corrected	Initial $^{87}Sr/^{86}Sr$	$\frac{^{147}Sm}{^{144}Nd}$	$\frac{^{143}Nd}{^{144}Nd}$	$\frac{^{206}Pb}{^{204}Pb}$	$\frac{^{207}Pb}{^{204}Pb}$	$\frac{^{208}Pb}{^{204}Pb}$	TDM
Nipigon										
LN 70	-1.1	0.25707	0.70911	0.70506	0.17207	0.51241	20.30616	15.85469	40.06747	n/a
LN - 76	-1.5	0.27197	0.70833	0.70405	0.16839	0.51236	19.98862	15.88906	39.58097	n/a
LN - 120	-1.0	0.26327	0.70817	0.70403	0.17147	0.51240	19.51524	15.76308	39.17293	n/a
LN - 129	-0.9	0.14714	0.70663	0.70431	0.17970	0.51247	19.04574	15.72884	38.80829	n/a
LN 203	-1.2	0.16438	0.70815	0.70556	0.16868	0.51237	20.94471	15.92278	40.59792	n/a
LN 221	-1.3	0.35190	0.71040	0.70486	0.15699	0.51229	20.06174	15.81410	39.77918	n/a
LN 229	-1.0	0.14828	0.70684	0.70450	0.15767	0.51230	20.27515	15.81169	39.57700	n/a
LN 231	-2.6	0.24195	0.70931	0.70550	0.15967	0.51224	20.11698	15.83532	39.84521	n/a
LN 233	-6.4	0.39832	0.71058	0.70431	0.14544	0.51194	20.01659	15.90994	39.83196	n/a
LN 239	-1.6	0.10354	0.70622	0.70459	0.17675	0.51241	18.68377	15.73829	38.37619	n/a
LN 259	-2.4	0.33800	0.71049	0.70517	0.16254	0.51227	19.48226	15.78680	39.17190	n/a
LN 301	-2.8	0.21862	0.70861	0.70517	0.15805	0.51222	18.14027	15.57820	38.21391	n/a
LN 306	-6.3	0.39902	0.71220	0.70592	0.14066	0.51191	20.84844	15.98510	40.52220	n/a
LN 311	-2.5	0.17871	0.70775	0.70493	0.16132	0.51226	18.98873	15.75148	38.70268	n/a
LN 313	-1.0	0.25903	0.70824	0.70416	0.15934	0.51232	19.72667	15.78325	39.53513	n/a
ADH3-33	-2.4	0.45391	0.71368	0.70653	0.16227	0.51227	19.93532	15.81821	39.48098	n/a
ADH5-17	-2.3	0.67028	0.71736	0.70681	0.15912	0.51225	21.21977	15.88680	40.72101	n/a
ADH6-13	-2.7	0.34006	0.71138	0.70602	0.17544	0.51235	19.36766	15.92891	37.53070	n/a
ADH6-98	-1.1	0.13966	0.70689	0.70469	0.17250	0.51240	19.13357	15.75991	38.91270	n/a
AML-01-44	-1.1	0.24582	0.70833	0.70446	0.17217	0.51241	19.57526	15.78985	39.17325	n/a
AML03-08	-2.5	0.22085	0.70856	0.70508	0.16699	0.51230	19.35423	15.78488	39.04827	n/a
AML03-56	-0.8	0.09644	0.70587	0.70435	0.17079	0.51241	18.90550	15.71757	38.67427	n/a
Shillabeer										
ADH3-28	-5.6	0.02872	0.70391	0.70346	0.12480	0.51183	21.27975	15.72668	42.02226	2.27
ADH5-2	-5.5	0.10432	0.70482	0.70317	0.12694	0.51185	21.26677	15.63636	40.97069	2.29
McIntyre										
LN - 45	-3.1	0.15151	0.70750	0.70512	0.14554	0.51211	24.41035	16.12581	42.20319	n/a
LN - 101	-3.2	0.10871	0.70675	0.70503	0.14531	0.51210	24.38799	16.12543	43.12404	n/a
LN 161	-2.5	0.11085	0.70625	0.70451	0.14605	0.51214	18.42808	15.52968	39.31847	n/a
LN 167	-2.3	0.13185	0.70656	0.70448	0.14588	0.51216	17.82376	15.53568	38.58861	n/a
LN 170	-2.6	0.11340	0.70641	0.70463	0.14548	0.51214	17.74834	15.55262	38.62779	n/a
Inspiration										
03CAM033	-6.6	0.28272	0.71044	0.70599	0.12693	0.51180	19.36687	15.91473	39.70661	2.39
03CAM128	-6.2	0.28372	0.71016	0.70570	0.12670	0.51182	18.98850	15.89035	39.37619	2.35
03CAM265	-6.1	0.20992	0.70924	0.70594	0.12787	0.51183	19.08369	15.77734	39.34191	2.36
03CAM300	-6.4	0.33076	0.71065	0.70544	0.12546	0.51180	18.89468	15.88514	39.32363	2.35
Jackfish Island										
03CAM122	-0.8	0.11662	0.70601	0.70418	0.14817	0.51225	17.66014	15.42436	38.63756	n/a
03CAM227	-1.1	0.10299	0.70564	0.70402	0.15059	0.51225	17.93699	15.49715	38.48741	n/a
03CAM228	-0.5	0.09515	0.70567	0.70417	0.15059	0.51228	20.06720	15.96987	39.12842	n/a
Pillar Lake Volcanics										
03CAM030	-6.8	0.09483	0.71018	0.70869	0.13767	0.51186	25.33744	16.33450	51.44082	n/a
03CAM044	-7.2	0.28862	0.71054	0.70599	0.13957	0.51186	26.53634	16.36656	49.71514	n/a
03CAM123	-6.9	0.32009	0.71122	0.70618	0.11745	0.51171	30.93823	16.83022	52.99419	n/a
03CAM126	-7.7	0.16030	0.71209	0.70957	0.13585	0.51181	21.86235	15.97527	50.73231	n/a
03CAM142	-6.7	0.11749	0.70877	0.70692	0.11679	0.51172	25.79955	16.36509	51.09983	n/a

Metric Conversion Table

Conversion from SI to Imperial			Conversion from Imperial to SI		
SI Unit	*Multiplied by*	*Gives*	*Imperial Unit*	*Multiplied by*	*Gives*
		LENGTH			
1 mm	0.039 37	inches	1 inch	**25.4**	mm
1 cm	0.393 70	inches	1 inch	**2.54**	cm
1 m	3.280 84	feet	1 foot	**0.304 8**	m
1 m	0.049 709	chains	1 chain	20.116 8	m
1 km	0.621 371	miles (statute)	1 mile (statute)	**1.609 344**	km
		AREA			
1 cm^2	0.155 0	square inches	1 square inch	**6.451 6**	cm^2
1 m^2	10.763 9	square feet	1 square foot	**0.092 903 04**	m^2
1 km^2	0.386 10	square miles	1 square mile	2.589 988	km^2
1 ha	2.471 054	acres	1 acre	0.404 685 6	ha
		VOLUME			
1 cm^3	0.061 023	cubic inches	1 cubic inch	**16.387 064**	cm^3
1 m^3	35.314 7	cubic feet	1 cubic foot	0.028 316 85	m^3
1 m^3	1.307 951	cubic yards	1 cubic yard	0.764 554 86	m^3
		CAPACITY			
1 L	1.759 755	pints	1 pint	0.568 261	L
1 L	0.879 877	quarts	1 quart	1.136 522	L
1 L	0.219 969	gallons	1 gallon	**4.546 090**	L
		MASS			
1 g	0.035 273 962	ounces (avdp)	1 ounce (avdp)	28.349 523	g
1 g	0.032 150 747	ounces (troy)	1 ounce (troy)	**31.103 476 8**	g
1 kg	2.204 622 6	pounds (avdp)	1 pound (avdp)	**0.453 592 37**	kg
1 kg	0.001 102 3	tons (short)	1 ton (short)	**907.184 74**	kg
1 t	1.102 311 3	tons (short)	1 ton (short)	**0.907 184 74**	t
1 kg	0.000 984 21	tons (long)	1 ton (long)	**1016.046 908 8**	kg
1 t	0.984 206 5	tons (long)	1 ton (long)	**1.016 046 90**	t
		CONCENTRATION			
1 g/t	0.029 166 6	ounce (troy)/ ton (short)	1 ounce (troy)/ ton (short)	34.285 714 2	g/t
1 g/t	0.583 333 33	pennyweights/ ton (short)	1 pennyweight/ ton (short)	1.714 285 7	g/t

OTHER USEFUL CONVERSION FACTORS

	Multiplied by	
1 ounce (troy) per ton (short)	31.103 477	grams per ton (short)
1 gram per ton (short)	0.032 151	ounces (troy) per ton (short)
1 ounce (troy) per ton (short)	20.0	pennyweights per ton (short)
1 pennyweight per ton (short)	0.05	ounces (troy) per ton (short)

Note: Conversion factors which are in bold type are exact. The conversion factors have been taken from or have been derived from factors given in the Metric Practice Guide for the Canadian Mining and Metallurgical Industries, published by the Mining Association of Canada in co-operation with the Coal Association of Canada.

ISSN 0826-9580
ISBN 0-7794-9213-7